ECMWF COPERNICUS REPORT

Copernicus Atmosphere Monitoring Service

Validation report for the CAMS global reanalyses of aerosols and reactive trace gases, year 2003

Issued by: KNMI

Date: 29/09/2017

Ref: CAMS84_2015SC2_D84.7.1.2_Y1_v1, Final

IMPLEMENTED BY ECMWF

Validation report for the CAMS global reanalyses of aerosols and reactive trace gases, year 2003

EDITORS:
H.J. ESKES (KNMI), H. CLARK (CNRS-LA), M. SCHULZ (METNO),
Y. CHRISTOPHE (BIRA-IASB), M. RAMONET (LSCE)

AUTHORS:
S. BASART (BSC), A. BENEDICTOW (METNO), A.-M. BLECHSCHMIDT (IUP-UB),
S. CHABRILLAT (BIRA-IASB), E. CUEVAS (AEMET), H. FLENTJE (DWD),
K. M. HANSEN (AU), U. IM (AU), O. JOSSOUD (LSCA), J. KAPSOMENAKIS (AA),
B. LANGEROCK (BIRA-IASB), K. PETERSEN (MPG), A. RICHTER (IUP-UB),
N. SUDARCHIKOVA (MPG), V. THOURET (CNRS-LA), A. WAGNER (MPG),
T. WARNEKE (UBC), C. ZEREFOS (AA)

REPORT OF THE COPERNICUS ATMOSPHERE MONITORING SERVICE, VALIDATION SUBPROJECT.

AVAILABLE AT:
HTTP://ATMOSPHERE.COPERNICUS.EU/

CITATION:
VALIDATION REPORT OF THE CAMS GLOBAL REANALYSIS, YEAR 2003.
H.J. ESKES, H. CLARK, M. SCHULZ, Y. CHRISTOPHE, M. RAMONET, S. BASART, A. BENEDICTOW, A.-M. BLECHSCHMIDT, S. CHABRILLAT, E. CUEVAS, H. FLENTJE, K.M. HANSEN, U. IM, O. JOSSOUD, J. KAPSOMENAKIS, B. LANGEROCK, K. PETERSEN, A. RICHTER, N. SUDARCHIKOVA, V. THOURET, A. WAGNER, T. WARNEKE, C. ZEREFOS, COPERNICUS ATMOSPHERE MONITORING SERVICE (CAMS) REPORT, CAMS84_2015SC2_D84.7.1.1_Y1_v1.pdf, MAY 2017.

STATUS:
VERSION 1, FINAL

DATE:
29/09/2017

Summary

The Copernicus Atmosphere Monitoring Service (http://atmosphere.copernicus.eu, CAMS) is a component of the European Earth Observation programme Copernicus. As one of the service products, CAMS is currently producing a global reanalysis of reactive trace gases, greenhouse gases and aerosol concentrations. The production of the reanalysis has started early 2017, and will be completed in 2018. The CAMS reanalysis will cover the period 2003-2017.

This document presents the validation results for the first year of the reanalysis run, 2003, focussing on aerosols and reactive gases. Updates of this document will appear during the production of the reanalysis: after reaching year 5 (2007), year 10 (2012) and year 15 (2017). The evaluation of the greenhouse gas reanalysis (CO_2, CH_4) will be discussed in the next update.

This summary is split according to service themes as introduced on the CAMS website: air quality & atmospheric composition, climate forcing, ozone layer and UV. Specific attention is given to the ability of the CAMS system to capture events. We furthermore assess the impact of the assimilation of the composition observations by comparing the validation results from the reanalysis to a 'control' configuration without assimilation. The CAMS reanalysis is also compared to the previous MACC reanalysis, available for the period 2003-2012.

Air quality and atmospheric composition

Global Aerosol

The first year of the CAMS reanalysis has been evaluated along with the CAMS control experiment for the year 2003. Detailed results are displayed on a subsection of the AeroCom/CAMS website. Taking the old MACC reanalysis as reference, the following changes with respect to aerosol optical depth (AOD) can be found in the CAMS reanalysis: Aerosol optical depth (AOD) reductions (-25%) are seen both in Northern hemisphere pollution regions, sea salt and dust regions. Quite a big change in composition is found such as a +90% increase in organic aerosol along with a -36% decrease in sulphate. The sum of sulphate and organic AOD is increased by 5% in CAMS, but the decrease in sea salt (-42%) and dust (-68%) is contributing to the overall reduction in AOD.

Despite the composition change the overall RMS error against daily Aeronet in 2003 is similar in the CAMS and MACC reanalysis for 2003. However, the regional RMS is reduced in regions such as East Asia, North Africa, India. Some simulated outliers e.g. due to volcanic plumes deteriorate global average RMS performance. The spatial distribution of AOD bias has become more evenly distributed with few spots sticking out. Volcanic aerosol hot spots near Hawaii seem to be responsible for high model outliers. The fraction of dust AOD appears too small, showing up as a high bias of the Ångström coefficient in cases of low Ångström coefficient (near deserts). On average 84% of the Ångström coefficient values are within a factor of two from observations.

The quality of the CAMS reanalysis (quantified with RMS, correlation and MNMB for the AOD) is similar as in the previous MACC reanalysis, this despite or because of the significant shift in the aerosol composition. Globally, no major issues have been found.

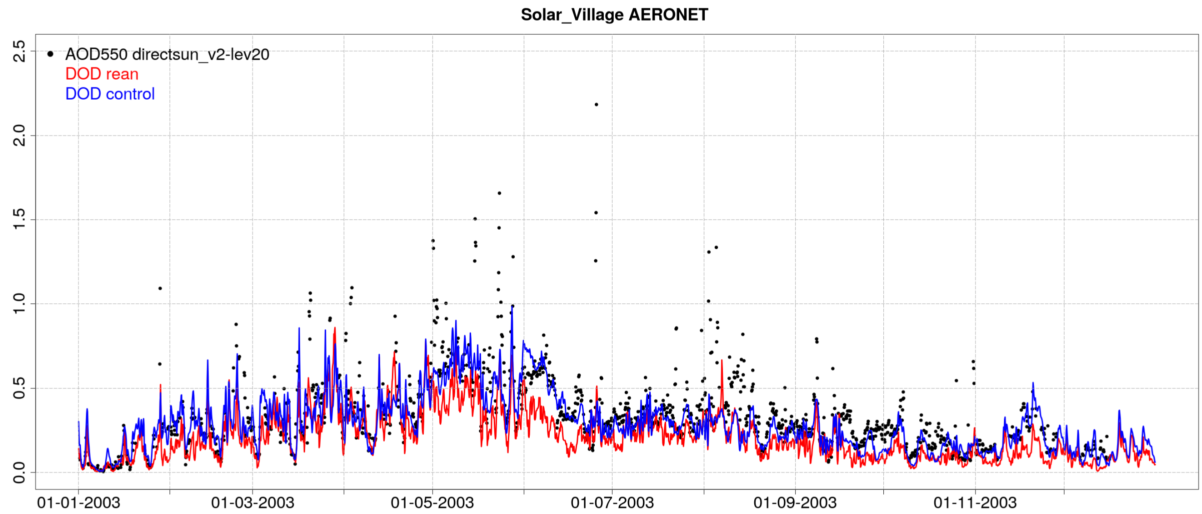

Figure S.1. Three-hourly AOD Version 2 direct-sun quality-assured AERONET observations (black dots), as well as the CAMS reanalysis dust optical depth (DOD) for 2003 (red) and control (blue) over Solar Village (Middle East).

Dust

The seasonal dust optical depth (DOD) fields from the CAMS reanalysis show a distinct seasonal pattern linked to the spatial distribution of dust emissions and transport throughout the year 2003, in good qualitative agreement with ground-based and satellite (MODIS and MISR) aerosol observations. However, DOD appears underestimated. The DOD comparison with dust-filtered AERONET observations shows that the reanalysis reproduces the annual variability showing seasonal correlation coefficients between 0.78 (in autumn) and 0.91 (in summer) in average for all the AERONET sites over Northern Africa, the Middle East and Europe but the dust aerosol content appears underestimated with seasonal MB between -0.14 (in winter) and -0.05 (in summer).

Differences between AOD and DOD observed over North Africa and the Middle East (causing strong DOD underestimations, see Figure S.1) are associated to the assimilation process. The presence of organic matter (OM) from biomass burning during wintertime, and the overestimation of secondary organics over heavily populated areas during summertime over desert dust sources, together with low aerosol concentrations in the control run, make OM a bit too preponderant through the assimilation step.

Tropospheric ozone (O_3)

In the free troposphere sonde and MOZAIC-IAGOS observations show that the reanalysis has a mean bias close to zero at midlatitudes, independent of the season. However, a positive bias in ozone of 10-20% is observed in the tropics, and a similar negative bias at high latitudes. On average the bias against GAW stations is small, but the variation between stations is considerable, with time correlations ranging between 0.3 and 0.9. The reanalysis compares well with IAGOS ozone observations in the surface layer and boundary layer. During the period of the 2003 heat wave, the model shows clear enhancements in ozone with a good timing, improved compared to the MACC reanalysis, but the highest ozone values are somewhat underestimated (Fig. S.2).

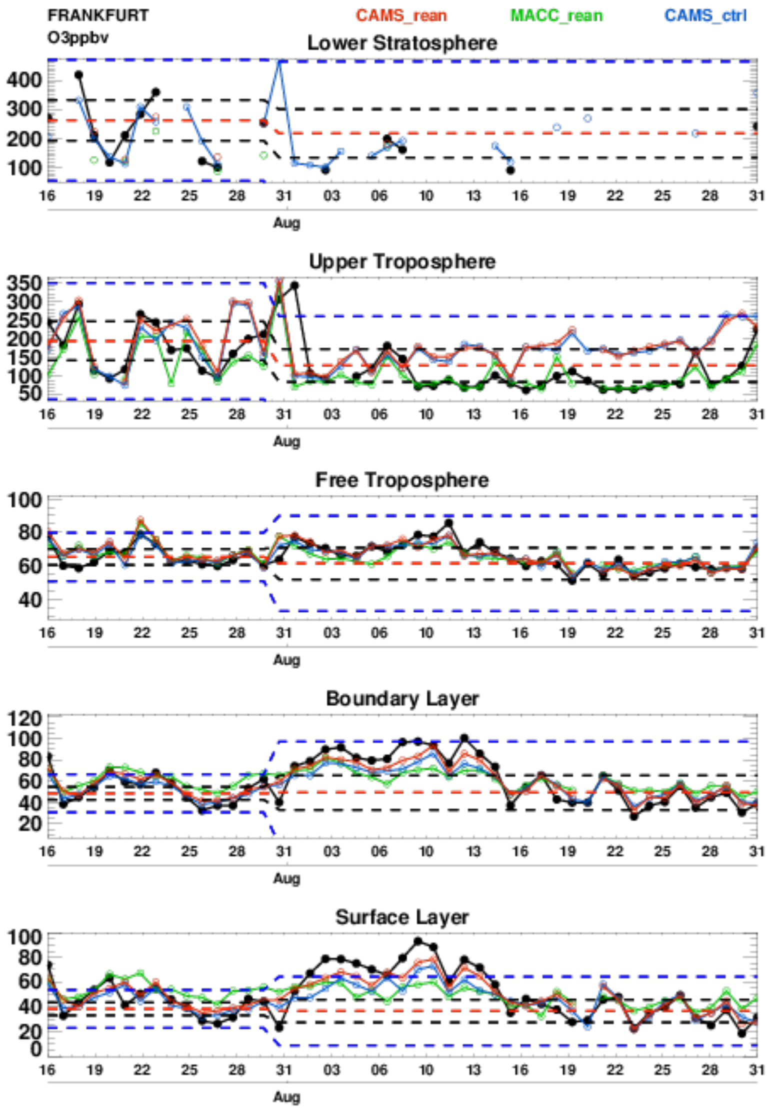

Figure S.2. Time series of ozone over Frankfurt for the period of the intense heat wave over Europe, 16 July-31 August. Observations are in black, the CAMS reanalysis is in red, the CAMS control in blue and the MACC reanalysis in green. The red dashed line is the mean of the observations from 2003-2012 the black dashed line is 1 sigma from the mean, and the blue dashed line is 3 sigma from the mean. The description of the high ozone peaks during the heat wave have clearly improved compared to the MACC reanalysis.

In the upper troposphere the models overestimate the amount of ozone, with the control generally performing better. Therefore this may be related to details in the assimilation of satellite ozone observations. The description of ozone in winter-spring over (Northern) Europe has improved considerably compared with the MACC reanalysis (Fig. S.3).

Tropospheric Carbon Monoxide (CO)

The CO total column seasonality for different regions is in general well reproduced by the reanalysis model in comparison with MOPITT satellite observations, with the exception of May and July 2003 in the Siberian fire region, where the CAMS reanalysis is first overestimating (May) the satellite observations by ~15% and then in July underestimating the observed CO total columns by ~15%. At the three FTIR measurements sites, Kiruna (68°N), Zugspitze (47°N) and Izaña (28°N), CO is

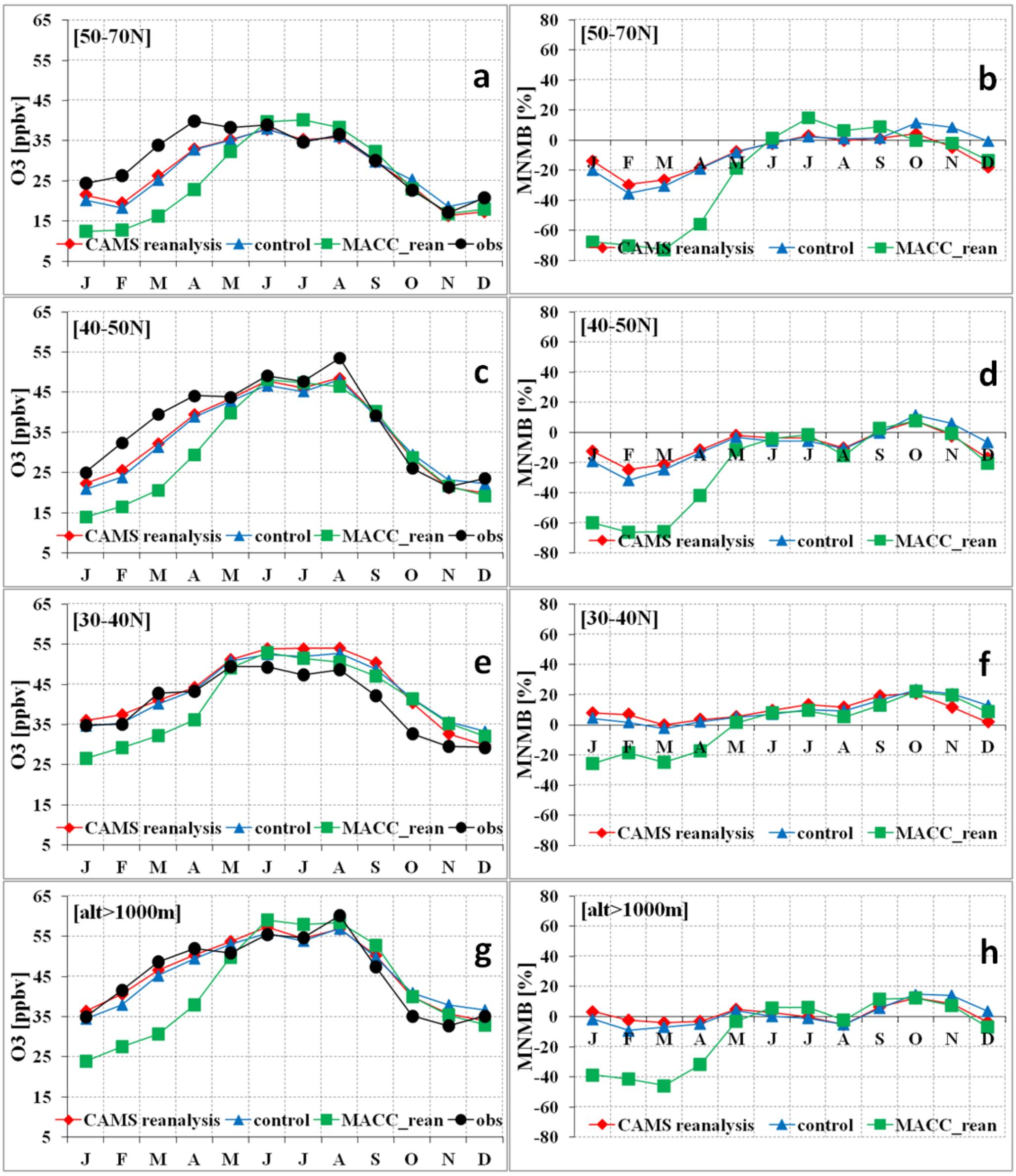

Figure S.3. Mean monthly ozone variability for the year 2003 (left) and the MNMBs (right) of the new CAMS reanalysis (red), the control experiment (blue), the MACC reanalysis (green), and the EMEP observations (black) over Northern Europe (1st row, a and b), Central Europe (2nd row, c and d), Southern Europe (3rd row, e and f) as well as for stations with altitude greater than 1000m a.s.l. (4rd row, g and h). Winter-spring ozone values have clearly improved compared to the MACC reanalysis.

generally underestimated, with values between -5% and -10%, which is slightly larger than the reported measurement uncertainty range (6%). Surface CO for GAW stations is mostly slightly underestimated (with MNMBs between -30% and +12%) by the reanalysis. Similarly, IAGOS data also shows that the models underestimate CO in the surface layer, boundary layer and free troposphere.

The CAMS reanalysis appears to be better than the MACC reanalysis at capturing the high concentrations of CO in the surface layer over European airports (Frankfurt, Paris, Vienna, Munich) during winter 2003.

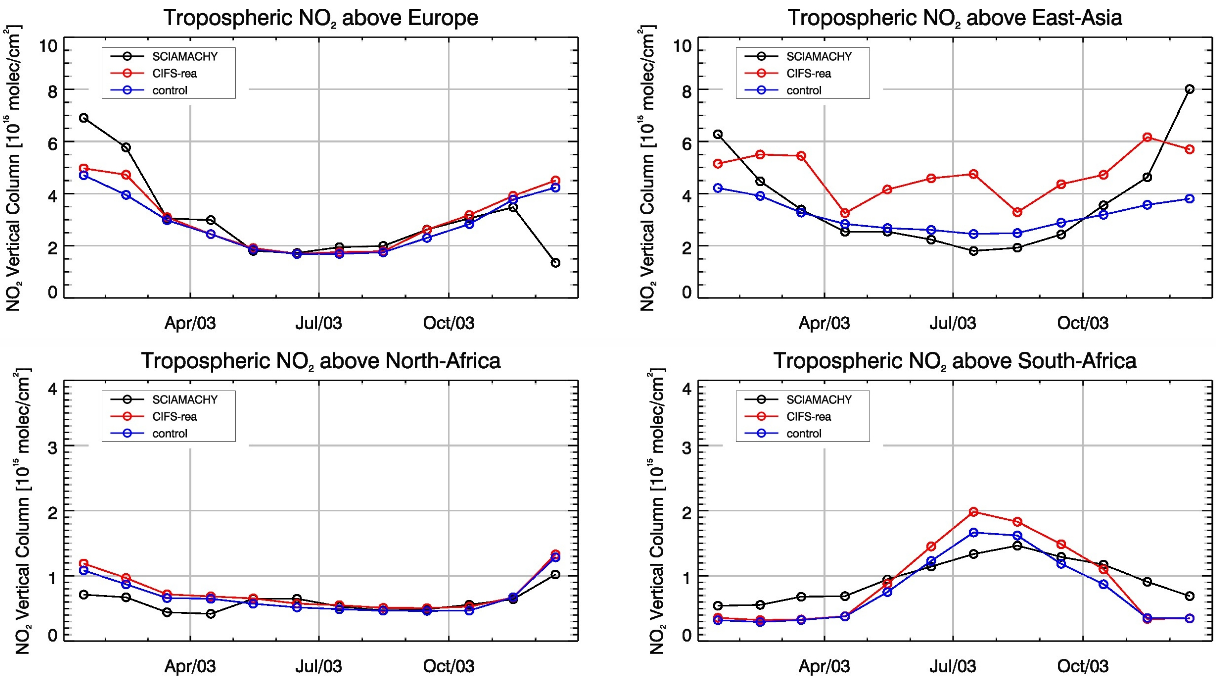

Figure S.4. Comparison of time series of tropospheric NO_2 columns from SCIAMACHY to reanalysis (green) and control (red) results over selected regions. Upper panels represent regions dominated by anthropogenic emissions; lower panels represent those dominated by biomass burning.

Tropospheric Nitrogen dioxide (NO_2)

The CAMS reanalysis performs reasonably well regarding magnitude and seasonality, with the exception of East-Asia, where the reanalysis fails to reproduce observed seasonality and the control compares better (Fig. S.4). Apart from this, we see similar features as for the CAMS operational forecast service, i.e. stronger shipping signals and overestimation of boreal forest fire emissions (the latter is also the case for tropospheric HCHO for some cases, but not in general, indicating a different performance probably related to fire emission factors depending on the trace gas, region and season), overestimation of values over the Red Sea and Persian Gulf and a tendency to underestimate values over Central European pollution hotspots around the Benelux countries, while other distinct hotspots are overestimated (e.g. Moscow).

Formaldehyde

HCHO concentrations over East Asia and Eastern-US show a good agreement with SCIAMACHY satellite observations. Values over North Africa and Indonesia are overestimated by a factor of about 2.

System performance in the Arctic

The simulated surface O_3 mixing ratios in the Arctic are on average in good agreement with the observations apart from spring ozone depletion events related to halogen chemistry reactions that are not represented in the model simulations. This results in an overestimation during spring while the model tends to underestimate O_3 during fall and winter. The reanalysis shows good correlation during the winter period, whereas the correlation is low during spring and summer. The overall

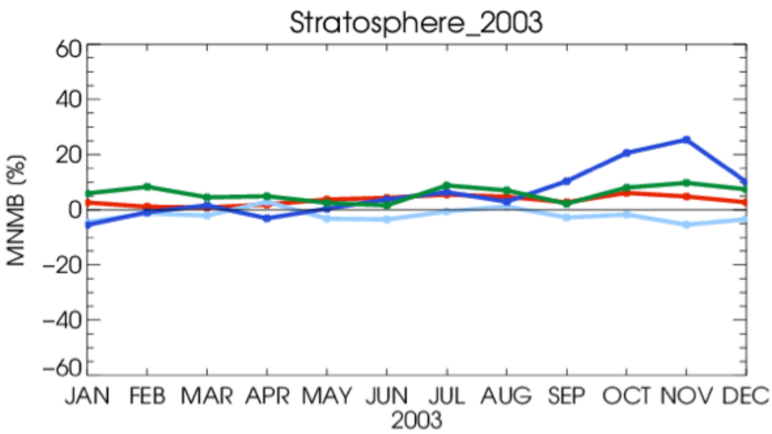

Fig. S.5: Normalised bias of the reanalysis versus ozone sondes, for 4 regions in the stratosphere (dark blue: Antarctic, light blue: Arctic, red: Northern midlatitudes, green: Tropics). The biases are averaged between 90 and 10hPa in the extra-tropics and between 60 and 10hPa in the Tropics.

correlation is relatively low (between 0.16 and 0.69) due to the pronounced ozone depletion events. The reanalysis and the control simulations are very similar.

Ozone sondes from the free troposphere in the Arctic shows a negative bias between -2% and -24% with lower MNMBs for the assimilated run except for between September and December 2003, where the control run shows lower MNMBs. In the UTLS O_3 concentrations are underestimated with between -4% and -14%.

At Alert, the surface CO concentrations are underestimated by about -10%. The temporal variability is well captured at the site by the assimilated run with correlation coefficient of 0.75, while the control run shows a lower correlation of r = 0.45.

System performance in the Mediterranean

Aerosol over the Mediterranean

Over the Mediterranean, the AOD AERONET comparison shows how the CAMS reanalysis can reproduce the Saharan long-range transport with seasonal correlation coefficients between 0.47 (in spring in Western Mediterranean) and 0.81 (in spring in Central Mediterranean) and seasonal MB between -0.07 (in spring in Western Mediterranean) and 0.04 (in winter in Eastern Mediterranean). The model tends to underestimate the AOD observations in Northern Mediterranean sites and overestimate AOD in the Southern sites. These overestimations are not observed in the control run and they are mainly linked to sulphates and OM contributions. Surface PM10 Airbase observations highlight the ability of the global reanalysis to detect the impact of desert dust long-range transport at ground level. Underestimations in PM10 are found in Western Mediterranean during summertime.

The seasonality of ozone in the Mediterranean (30-40N) has improved in comparison to the MACC reanalysis, with little bias in winter, and a positive bias of 10-20% in summer.

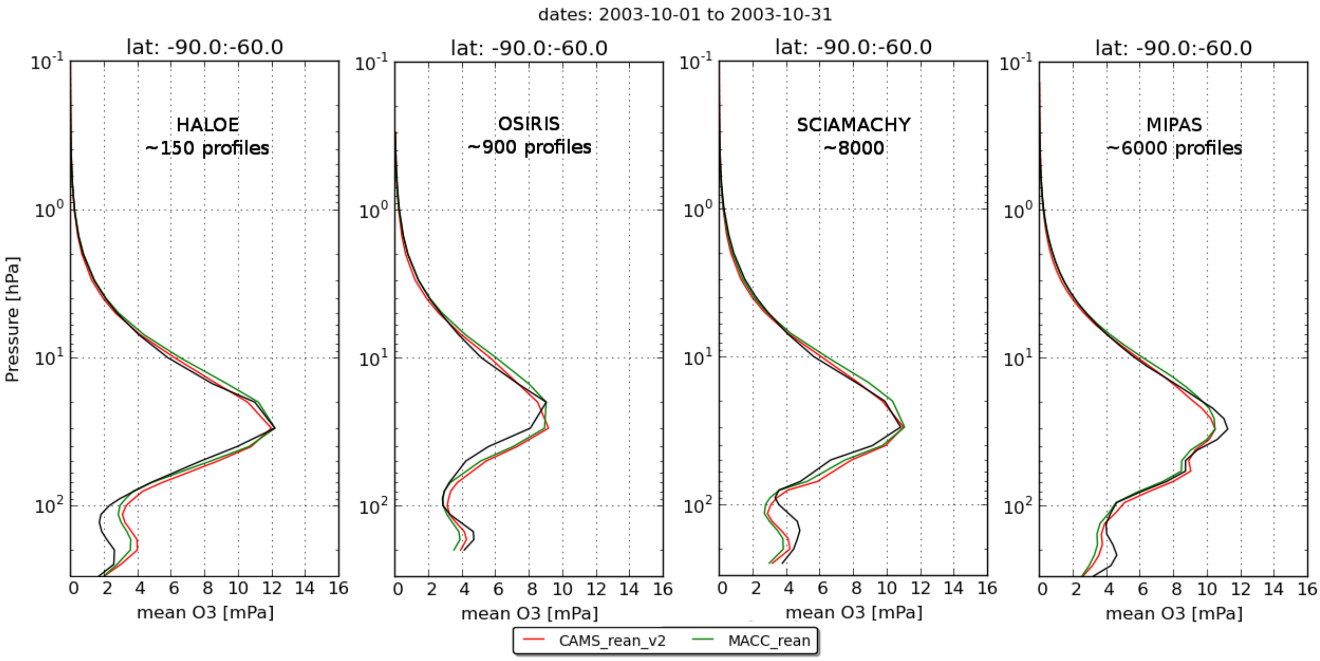

Figure S.6: Mean profiles for October 2003 over the South Pole latitude band (90°S-60°S): CAMS (red) and MACC reanalysis (green) versus satellite observations (black) using, from left to right: HALOE, OSIRIS, SCIAMACHY and MIPAS.

Ozone layer and UV

Ozone partial columns and vertical profiles

Ozone columns and profiles have been compared with the following observations: vertical profiles from balloon-borne ozone sondes; ground-based remote-sensing observations from the NDACC (Network for the Detection of Atmospheric Composition Change, http://www.ndacc.org); and satellite observations by several limb-profiling instruments. Furthermore, the reanalyses are compared with the MACC reanalysis of global atmospheric composition.

Compared to ozone sondes the model O_3 partial pressures are within 10% for the whole year, except in the Antarctic during the ozone hole period: in the layer between 90 and 10 hPa during the month of October, ozone is overestimated by 25% on average, see Fig. S.5.

Apart from the ozone hole period, the comparison with independent satellite observations yields a good agreement, with differences smaller than the spread between the independent datasets, see Fig. S.6.

Other stratospheric trace gases

Due to the lack of stratospheric chemistry in the IFS-CB05 scheme, the only useful product in the stratosphere is ozone. Other species, like NO_2, have also been evaluated but the results are only indicative.

Table of Contents

1. Introduction

The Copernicus Atmosphere Monitoring Service (CAMS, http://atmosphere.copernicus.eu/) is a component of the European Earth Observation programme Copernicus. The CAMS global near-real time (NRT) service provides daily analyses and forecasts of trace gas and aerosol concentrations. Apart from these daily analyses, CAMS will produce a global reanalysis covering 15 years (2003-2017). The CAMS system was originally developed by a series of MACC research projects (MACC I-II-III) until it became operational in 2015, and in this report we show comparisons between the CAMS reanalysis and the MACC reanalysis. The CAMS near-real time and reanalysis services consist of daily analysis and forecasts with the ECMWF IFS system with modelling and data assimilation of trace gas concentrations and aerosol properties. A second component of CAMS consists of the provision of air-quality forecasts and reanalyses over Europe, based on an ensemble of European air quality models.

This document presents the validation of the global CAMS reanalysis during production (2017-2018). The validation methodology and measurement datasets are discussed in Eskes et al. (2015). In this report the performance of the system is assessed in two ways: both the longer-term mean performance (seasonality) as well as its ability to capture events are documented. Table 1.1 provides an overview of the trace gas species and aerosol aspects discussed in this CAMS reanalysis validation report. The reanalysis results are compared with results for a free model run without assimilation, to document the improvements by using the (satellite) observations.

Key CAMS products and their users are: Boundary conditions for regional air quality models (e.g. AQMEII, air quality models not participating in CAMS); Long range transport of air pollution (e.g. LRTAP); Stratospheric ozone column and UV (e.g. WMO, DWD); 3D ozone fields (e.g. SPARC).

As outlined in the MACC-II Atmospheric Service Validation Protocol (2013) and MACC O-INT document (2011), relevant user requirements are quick looks of validation scores, and quality flags and uncertainty information along with the actual data. This is further stimulated by QA4EO (Quality Assurance Framework for Earth Observation, http://www.qa4eo.org) who write that "all earth observation data and derived products is associated with it a documented and fully traceable quality indicator (QI)". It is our long-term aim to provide such background information. The user is seen as the driver for any specific quality requirements and should assess if any supplied information, as characterised by its associated QI, are "fit for purpose" (QA4EO task team, 2010).

CAMS data are made available to users as data products (grib or netcdf files) and graphical products from ECMWF, http://atmosphere.copernicus.eu/. The stratospheric ozone service is provided by BIRA-IASB at http://copernicus-stratosphere.eu.

A summary of the reanalysis system is given in section 2. Section 3 gives an overview of the performance of the system for various species. Section 4 describes the performance of the system concerning greenhouse gases, and section 5 describes several events. Extended validation for the CAMS forecasts and reanalysis fields can be found online via regularly updated verification pages, http://atmosphere.copernicus.eu/user-support/validation/verification-global-services.
Table 1.2 lists all specific validation websites that can also be found through this link.

Table 1.1: Overview of the trace gas species and aerosol aspects discussed in the CAMS reanalysis validation reports. Shown are the datasets assimilated in the CAMS reanalysis (second column) and the datasets used for validation, as shown in this report (third column). Green colours indicate that substantial data is available to either constrain the species in the analysis, or substantial data is available to assess the quality of the analysis. Yellow boxes indicate that measurements are available, but that the impact on the analysis is not very strong or indirect (second column), or that only certain aspects are validated (third column). Note that not all the observations listed in the assimilation and validation column are available during 2003 (see e.g. Table 2.2).

Species, vertical range	Assimilation	Validation
Aerosol, optical properties	MODIS Aqua/Terra AOD, AATSR	AOD, Ångström: AERONET, GAW, Skynet, MISR, OMI, lidar, ceilometer
Aerosol mass (PM10, PM2.5)	-	European AirBase stations
O_3, stratosphere	MIPAS, MLS, SCIAMACHY, GOME-2A, GOME-2B, OMI, SBUV-2	Sonde, lidar, MWR, FTIR, HALOE, GOMOS, OSIRIS, SCIAMACHY
O_3, UT/LS	Indirectly constrained by limb and nadir sounders	MOZAIC, IAGOS, ozone sonde
O_3, free troposphere	Indirectly constrained by limb and nadir sounders	MOZAIC, IAGOS, ozone sonde
O_3, PBL / surface	-	Surface ozone: WMO/GAW, NOAA/ESRL-GMD, AIRBASE, EMEP
CO, UT/LS	-	MOZAIC, IAGOS
CO, free troposphere	MOPITT	MOZAIC, IAGOS, MOPITT, IASI, TCCON
CO, PBL / surface	Indirectly constrained by satellite IR sounders	Surface CO: WMO/GAW, NOAA/ESRL
NO_2, troposphere	SCIAMACHY, OMI, GOME-2A, GOME-2B	SCIAMACHY, GOME-2, MAX-DOAS
HCHO	-	SCIAMACHY, GOME-2, MAX-DOAS
Stratosphere, other than O_3	-	SCIAMACHY, GOME-2 (NO_2 column)
CO_2, surface, PBL		ICOS
CO_2, column	SCIAMACHY, IASI, TANSO	TCCON
CH_4, surface, PBL		ICOS
CH_4, column	SCIAMACHY, IASI, TANSO	TCCON

Table 1.2: Overview of quick-look validation websites of the CAMS system.

Reactive gases – Troposphere
GAW surface ozone and carbon monoxide: **http://macc.copernicus-atmosphere.eu/d/services/gac/verif/grg/gaw/gaw_station_ts/** IAGOS tropospheric ozone and carbon monoxide: **http://www.iagos.fr/cams/** Surface ozone from EMEP (Europe) and NOAA-ESRL (USA): **http://www.academyofathens.gr/cams** Tropospheric nitrogen dioxide and formaldehyde columns against satellite retrievals: **http://www.doas-bremen.de/macc/macc_veri_iup_home.html** Tropospheric CO columns against satellite retrievals: **http://cams.mpimet.mpg.de**
Reactive gases - Stratosphere
Stratospheric composition: **http://www.copernicus-stratosphere.eu** NDACC evaluation in stratosphere and troposphere (the NORS server) **http://nors-server.aeronomie.be**
Aerosol
Evaluation against selection of Aeronet stations: **http://www.copernicus-atmosphere.eu/d/services/gac/verif/aer/nrt/** Aerocom evaluation: **http://aerocom.met.no/cgi-bin/aerocom/surfobs_annualrs.pl?PROJECT=MACC&MODELLIST=MACC-VALreports&** WMO Sand and Dust Storm Warning Advisory and Assessment System (SDS-WAS) model intercomparison and evaluation: **http://sds-was.aemet.es/forecast-products/models**
Satellite data monitoring
Monitoring of satellite data usage in the Reanalysis and Near-Real-Time production: **http://copernicus-atmosphere.eu/d/services/gac/monitor/**

The CAMS validation reports are accompanied by the "Observations characterization and validation methods" report, Eskes et al. (2016), which describes the observations used in the comparisons, and the validation methodology. This report can also be found on the global validation page, http://atmosphere.copernicus.eu/user-support/validation/verification-global-services.

2. System summary and model background information

The specifics of the CAMS reanalysis model versions are given (section 2.1). An overview of products derived from this system is given in section 2.3. Several external products used for validation and intercomparison are listed in section 2.4. Timeliness and availability of the CAMS products is given in section 2.5.

2.1 System based on the ECMWF IFS model

Key model information is given on the CAMS reanalysis data-assimilation and its control experiment. Further details on the different model runs and their data usage can be found at http://atmosphere.copernicus.eu/documentation-global-systems and http://atmosphere.copernicus.eu/user-support/operational-info

2.1.1 CAMS reanalysis system

The reanalysis system consists of the IFS-CB05 chemistry combined with the CAMS bulk aerosol model. The chemistry is described in Flemming et al. (2015) and Flemming et al. (2017), aerosol is described by Morcrette et al. (2009). The data is stored under experiment IDs "**gqm5**" (until 30-6-2003) and "**gq7s**" (from 1-7-2003). For the greenhouse gases the experiment ID is "**gqk1**". In the end, the entire reanalysis will be provided to users with one uniform access mechanism, and users do not have to worry about the underlying experiments. The model resolution is T255 with 60 vertical layers. Here a summary of the main specifications of the CAMS reanalysis system is given.

- The meteorological model is based on IFS version cy42r1, with interactive ozone and aerosol in radiation scheme, see also http://www.ecmwf.int/en/forecasts/documentation-and-support/changes-ecmwf-model; the model resolution is T255L60.
- The modified CB05 tropospheric chemistry is used (Williams et al., 2013), originally taken from the TM5 chemistry transport model (Huijnen et al., 2010)
- Stratospheric ozone during the forecast is computed from the Cariolle scheme (Cariolle and Teyssèdre, 2007) as already available in IFS, while stratospheric NOx is constrained through a climatological ratio of HNO_3/O_3 at 10 hPa.
- Monthly mean dry deposition velocities are based on the SUMO model provided by the MOCAGE team.
- Data assimilation is described in Inness et al. (2015) and Benedetti et al. (2009) for chemical trace gases and aerosol, respectively.
- Anthropogenic reactive gas emissions are based on MACCity (Granier et al., 2011), where wintertime CO emissions have been scaled up over Europe and US (Stein et al., 2014). Hourly biogenic emissions are from MEGAN-MERRA (Sindelarova et al., 2014).
- CO_2 emission are from EDGAR v4.2 (anthropogenic), CHTESSEL (ecosystem), ACCMIP/EDGAR (aviation), Takahashi 2009 (ocean). CH_4 emissions are from LPJ-HYMN (wetland, natural), Bergamaschi 2013 (chemical sinks) and EDGAR v4.2 (anthropogenic).
- NRT fire emissions are taken from GFASv1.2 (Kaiser et al. 2012).

Figure 2.1: Satellite observation usage in the reanalysis, from Oct. 2002 onwards. The three green rows correspond to SCIAMACHY NO2, SCIAMACHY CO2 and CH4, MOPITT CO, and are assimilated using the averaging kernels in the retrieval product.

The following updates were applied to the chemistry:

- Update of heterogeneous rate coefficients for N2O5 and HO2 based on clouds and aerosol.
- Modification of photolysis rates by aerosol.
- Dynamic tropopause definition based on T profile for coupling to stratosphere and tropospheric mass diagnostics.
- Monthly mean VOC emissions calculated by the MEGAN model for all VOCs and for whole period 2003-2015 period.
- Bug fixes, in particular for diurnal cycle of dry deposition whose correction has decreased ozone dry deposition (about 15-20%).

The model configuration for GHG is based on the specification of the following components documented in the listed papers below:

- Emissions for CO2 are documented in Agusti-Panareda et al. (2014), Massart et al. (2016).
- Bias correction for CO2 ecosystem fluxes based on the Biogenic Flux Adjustment Scheme is documented by Agusti-Panareda et al. (2016).
- Emissions and loss rate for CH4 is documented in Massart et al. (2014).
- Mass fixer configuration for CO2 and CH4 is documented by Agusti-Panareda et al. (2017).

The aerosol model includes 12 prognostic variables, which are 3 bins for sea salt and desert dust, hydrophobic and hydrophilic organic matter and black carbon, sulphate aerosols and its precursor trace gas SO_2 (Morcrette et al., 2009). Aerosol total mass is constrained by the assimilation of MODIS AOD (Benedetti et al. 2009) and AATSR AOD. A variational bias correction for the MODIS AOD is in place based on the approach used also elsewhere in the IFS (Dee and Uppala, 2009).

Table 2.2: Satellite retrievals of reactive gases, greenhouse gases and aerosol optical depth that are actively assimilated in the reanalysis. The table only contains datasets used for the year 2003.

Variable	Instrument	Satellite	Product	Period	AK
O3	SCIAMACHY	Envisat	TC	CCI	no
O3	MIPAS	Envisat	PROF	ESA NRT: 20030127- 20030720 MARS ESA NRT: 20030721-20040326 CCI: 20050127-20120331	no
O3	SBUV/2	NOAA-16	PC 13L	V8.6	no
O3	SBUV/2	NOAA-17	PC 13L	v8.6	no
CO	MOPITT	Terra	TC	V6	yes
NO2	SCIAMACHY	Envisat	TRC	v1p	yes
AOD	AATSR	Envisat	TC	CCI	no
AOD	MODIS	Terra	TC	COL6	no
AOD	MODIS	Aqua	TC	COL6	no
CO2	SCIAMACHY	Envisat	TC	CCI, Bremen	yes
CH4	SCIAMACHY	Envisat	TC	CCI, SRON, V7.0	yes

2.1.2 Control

The control run (experiment "**gqk3**") applies the same settings as the reanalysis, based on the IFS-CB05 system with CAMS aerosol for cy42r1, except that data assimilation is not switched on. It consists of 24h cycling forecasts.

2.2 Other systems

2.2.1 The MACC reanalysis and CAMS forecasts

The previous reanalysis was produced during the MACC project. This reanalysis is available through the CAMS website, or ECMWF archive with EXP='rean', CLASS='mc'.

In a few places the performance of the reanalysis is compared with the CAMS operational forecasts/analyses. This system is sometimes referred to as CAMS "o-suite".

2.2.2 BASCOE

The NRT analyses and forecasts of ozone and related species for the stratosphere, as delivered by the Belgian Assimilation System for Chemical ObsErvations (BASCOE) of BIRA-IASB (Lefever et al., 2014; Errera et al., 2008), are used as an independent model evaluation of the CAMS products. The NRT BASCOE product is the ozone analysis of Aura/MLS-SCI level 2 standard products, run in the following configuration (version 05.07):

- The following species are assimilated: O_3, H_2O, HNO_3, HCl, HOCl, N_2O and ClO.
- It lags by typically 4 days, due to latency time of 4 days for arrival of non-ozone data from Aura/MLS-SCI (i.e. the scientific offline Aura/MLS dataset).
- Global horizontal grid with a 3.75° longitude by 2.5° latitude resolution.
- Vertical grid is hybrid-pressure and consists in 86 levels extending from 0.01 hPa to the surface.

- Winds, temperature and surface pressure are interpolated in the ECMWF operational 6-hourly analyses.
- Time steps of 20 minutes, output every 3 hours

See the stratospheric ozone service at http://www.copernicus-stratosphere.eu/.
It delivers graphical products dedicated to stratospheric composition and allows easy comparison between the results of o-suite, BASCOE and TM3DAM. The BASCOE data products (HDF4 files) are also distributed from this webpage. Other details and bibliographic references on BASCOE can be found at http://bascoe.oma.be/. A detailed change log for BASCOE can be found at
http://www.copernicus-stratosphere.eu/4_NRT_products/3_Models_changelogs/BASCOE.php.

2.2.3 TM3DAM and the multi-sensor reanalysis

One of the MACC products was a 30-year reanalysis, near-real time analysis and 10-day forecast of ozone column amounts performed with the KNMI TM3DAM data assimilation system, the Multi-Sensor Reanalysis (MSR) system (van der A et al., 2010, 2015),
http://www.temis.nl/macc/index.php?link=o3_msr_intro.html.
The corresponding validation report can be found at
http://www.copernicus-atmosphere.eu/services/gac/global_verification/validation_reports/.

The NRT TM3DAM product used for the validation of the CAMS NRT streams is the ozone analysis of Envisat/SCIAMACHY (until April 2012), AURA/OMI, and MetOp-A/GOME-2, run in the following configuration:

- Total O_3 columns are assimilated.
- Global horizontal grid with a 3° longitude by 2° latitude resolution.
- Vertical grid is hybrid-pressure and consists in 44 levels extending from 0.1 hPa to 100 hPa.
- Dynamical fields from ECMWF operational 6-hourly analysis.

An update of the MSR (MSR-2) was presented in van der A et al. (2015), which extended the record to 43 years based on ERA-interim reanalysis meteo and with an improved resolution of 1x1 degree.

2.2.4 SDS-WAS multimodel ensemble

The World Meteorological Organization's Sand and Dust Storm Warning Advisory and Assessment System (WMO SDS-WAS) for Northern Africa, Middle East and Europe (NAMEE) Regional Center (http://sds-was.aemet.es/) started its activities in 2012. During this period, the Regional Center has established a protocol to routinely exchange products from dust forecast models and observations (i.e. ground-based and satellite aerosol products) as the basis for both near-real-time and delayed common model evaluation.

Global and regional dust models for international operational and research institutions are currently providing daily operational dust forecasts (i.e. dust optical depth, DOD, and dust surface concentration). Different multi-model products are generated from the different prediction models. Two products describing centrality (multi-model median and mean) and two products describing spread (standard deviation and range of variation) are daily computed. In order to generate them, the model outputs are bi-linearly interpolated to a common grid mesh of 0.5º x 0.5º. The SDS-WAS multi-model DOD (at 550 nm) Median from available dust prediction models participating in the SDS-WAS Regional Center is used for the validation of the CAMS NRT streams.

The current routine evaluation of dust predictions is focused on total-column dust optical depth (DOD) and uses remote-sensing retrievals from sun-photometric (AERONET) and satellite (MODIS) measurements.

The updated list of dust models participating in the model intercomparison can be found at https://sds-was.aemet.es/forecast-products/forecast-evaluation/model-inter-comparison-and-forecast-evaluation/

2.3 CAMS reanalysis product

The CAMS 3D reanalysis products are stored as 3-hourly fields and will update the MACC global reanalysis which is also available on the CAMS website, http://atmosphere.copernicus.eu/. The new reanalysis will also be made available through this CAMS website. The following fields are archived:

- Forecast fields: From 0z, 3-hourly, step=0,3,.., 48
- Analysis fields: Every 3 hours, e.g. 0z, 3z,...21z
- Surface forecast fields: From 0z, 1-hourly, step=0,1,2,...,48

3. Validation results for reactive gases and aerosol

This section describes the validation results of the CAMS global reanalysis for aerosols and reactive gases for the year 2003 (the first year of the CAMS reanalysis). Naming and color-coding conventions predominantly follow the scheme as given in Table 3.1.

Table 3.1 Naming and colour conventions.

Name in figs	Experiment	Colour
{obs name}	{obs}	black
CAMS reanalysis	gqm5, gq7s, gqk1	red
Control	gqk3	blue
MACC reanalysis	rean, class=mc	green

3.1 Aerosol

3.1.1 Global aerosol distribution

The global aerosol fields are analysed both for the reanalysis and a control simulation. For comparison the previous MACC reanalysis is used. More detailed results can be found on the AeroCom/CAMS website (http://aerocom.met.no/cgi-bin/aerocom/surfobs_annualrs.pl?PROJECT=CAMS&MODELLIST=CAMS-reanalysis) in the CAMS reanalysis section.

The evaluation in table 3.1.1.1 shows the average global AOD and speciated AOD for the three experiments in 2003 and illustrates a shift from MACC to CAMS in aerosol composition. The control experiment shows the lowest AOD, consistently with the current CAMS operational model version (o-suite), indicating a model version which is gaining aerosol mass and AOD through assimilation, not in balance with the emissions. Changes in total AOD are relatively smaller than the increase in organic AOD and the decrease in dust AOD. The decrease in total AOD is due to reductions in dust, sulphate and sea salt AOD. Figures 3.1.1.1 and 3.1.1.2 show where the changes occur. Volcanic eruptions add sulphate near Hawaii and Middle America, seen as little hot spots on the map. These high values in the CAMS reanalysis near Hawaii lead to some outliers in figure 3.1.1.3, where Aeronet measures much smaller values on average, indicating an overestimation of the volcanic derived sulphate. The scatterplots in figure 3.1.1.3 show all possible comparisons for 2003, as daily and monthly aggregates. CAMS AOD at Aeronet sites is larger than MACC, while it is smaller on global average. The aerosol dispersion is less pronounced in CAMS, which is also visible in smaller AOD at polar locations (figure 3.1.1.1) than in MACC. Overall performance of the CAMS and MACC reanalysis is very good and rather similar, despite significant changes in aerosol composition. Figure 3.1.1.4 shows the regional bias with reduced bias over North America. Figures 3.1.1.5 and 3.1.1.6 further illustrate a shift to finer particles, with more organic aerosol, less dust and sea salt, leading to similar total AOD distribution as in the MACC reanalysis.

Table 3.1.1.1: Mean annual, global total and speciated aerosol optical depth (AOD) in the CAMS reanalysis, the control experiment and MACC reanalysis experiment for year 2003.

	CAMS rean	Control	MACC rean
AOD@550	0.143	0.095	0.168
BC-OD@550	0.006	0.004	0.008
Dust-OD@550	0.018	0.022	0.036
OA-OD@550	0.052	0.018	0.024
SO4-OD@550	0.033	0.022	0.044
SS-OD@550	0.034	0.029	0.055

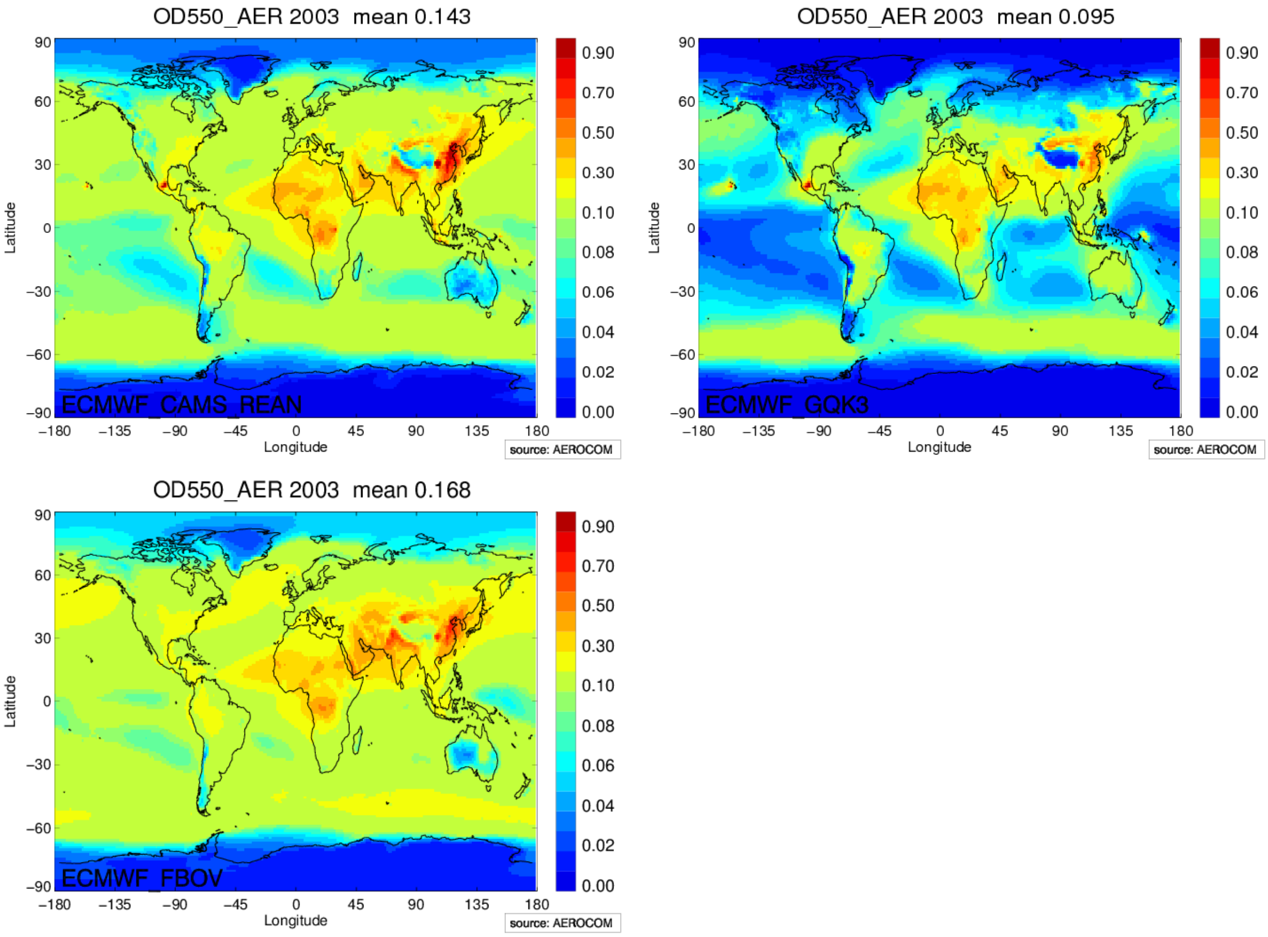

Figure 3.1.1.1: Averaged aerosol optical depth (AOD) from IFS experiments CAMS reanalysis (left), control (right) and MACC reanalysis (bottom) for the year 2003. Mean AOD is at 0.143, which is 16% less than what was in the earlier MACC reanalysis. Reductions are seen both in Northern hemisphere pollution regions and dust regions.

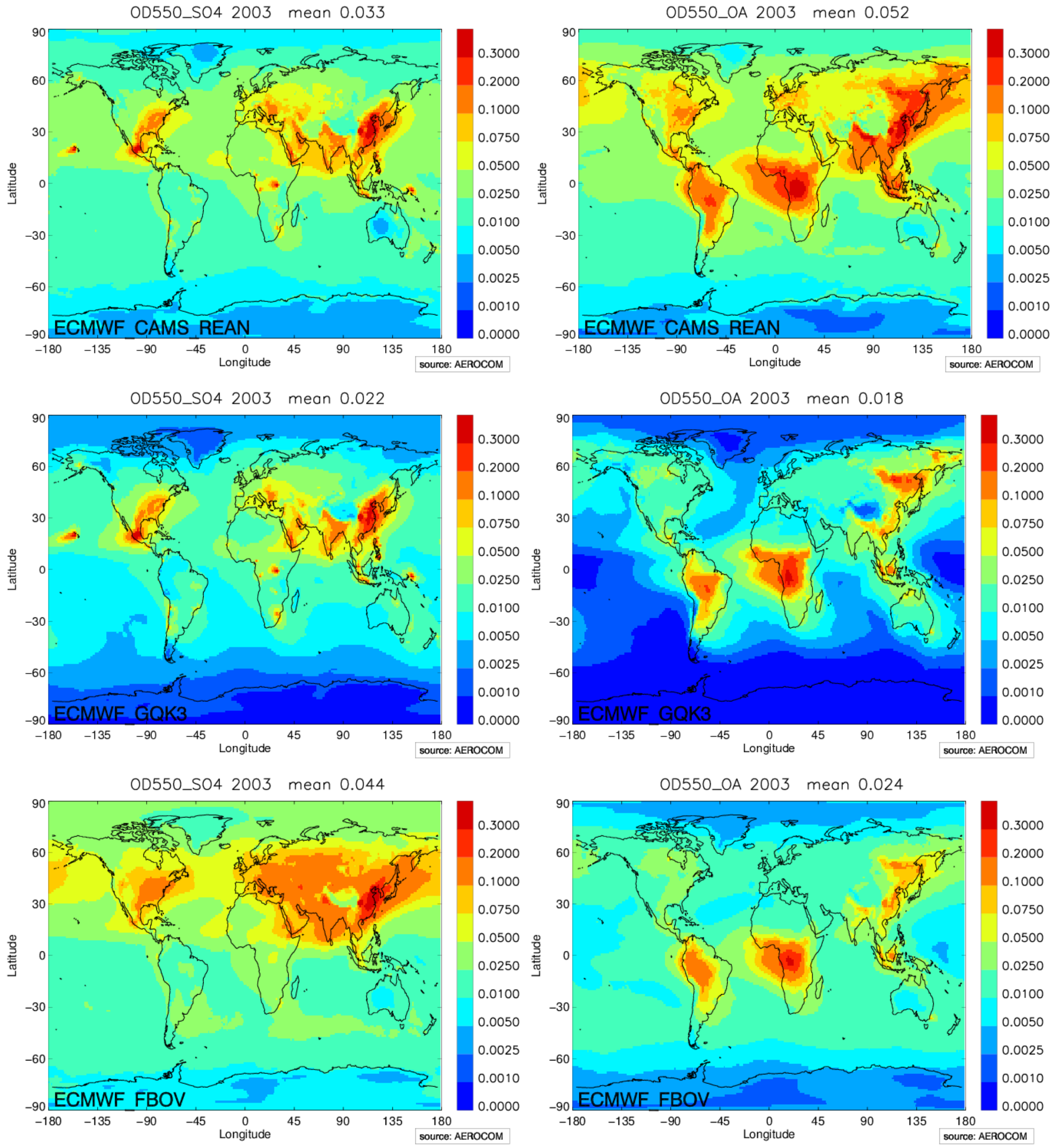

Figure 3.1.1.2: Averaged sulphate optical depth in left column (reanalysis (top), control run (middle) and MACC reanalysis (bottom)) and organic aerosol optical depth (right column), for the year 2003. While sulphate AOD was dominating over organic aerosol AOD in the MACC reanalysis, mean AODs of the two components are opposite in the reanalysis (sulphate AOD: 0.033, organic AOD: 0.052). An important shift in aerosol composition appears when comparing to the MACC reanalysis. The sum of sulphate and organic AOD has increased by 25% in the reanalysis, but a larger decrease in dust and sea salt is finally contributing to the overall decrease in AOD.

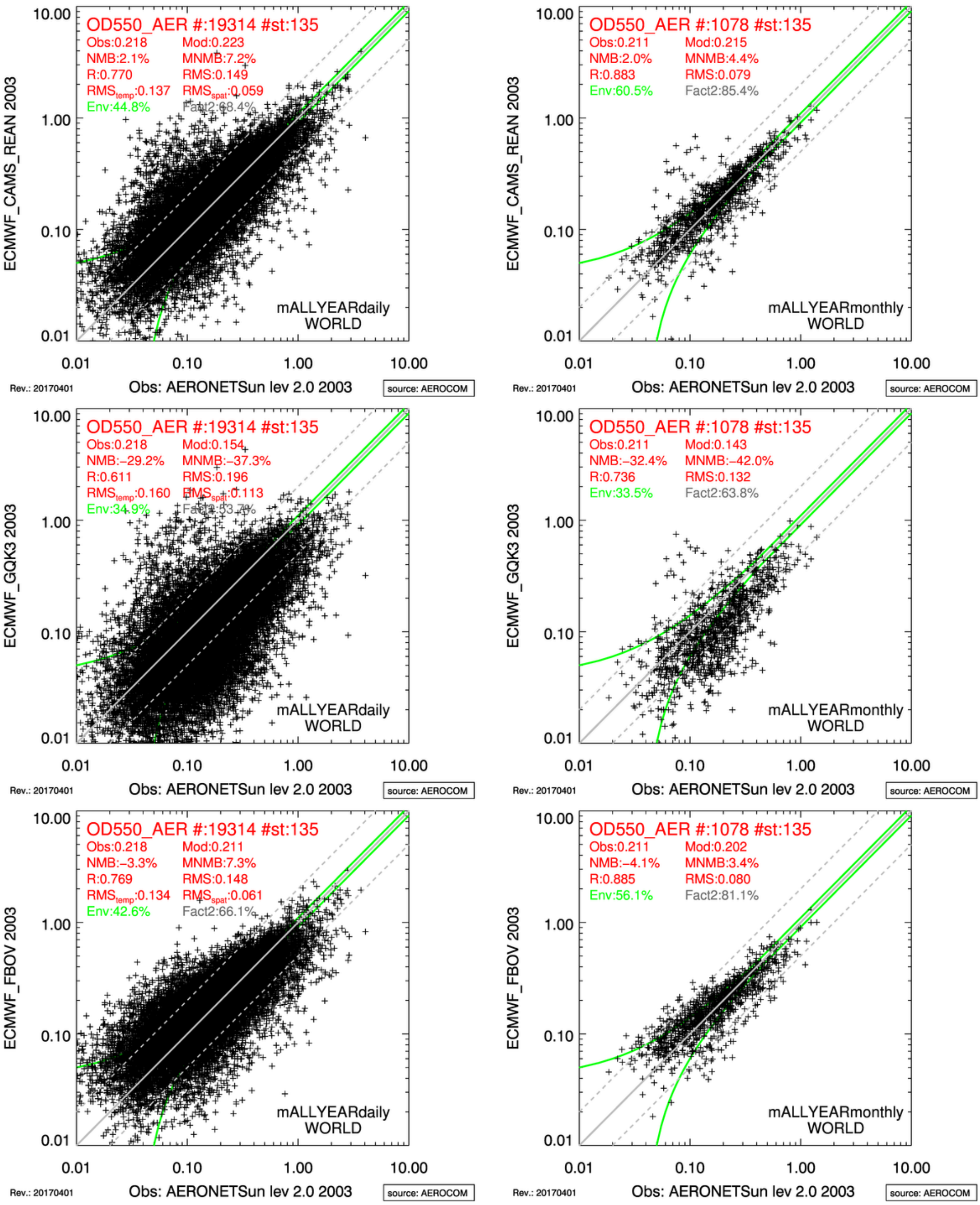

Figure 3.1.1.3: Evaluation of simulated daily (left column) and monthly (right column) AOD against Aeronet level 2.0 sun photometer measurements in the reanalysis (top), control run (middle) and MACC reanalysis (bottom) for the year 2003. Statistics shown in the figure show very similar results for MACC and CAMS, except a small negative bias in MACC, which has become a small positive bias in the CAMS reanalysis. The quality of the IFS reanalysis, despite or because of the significant shift in the aerosol composition is as good as MACC. The control run has lower bias and the temporal-spatial RMS errors are larger.

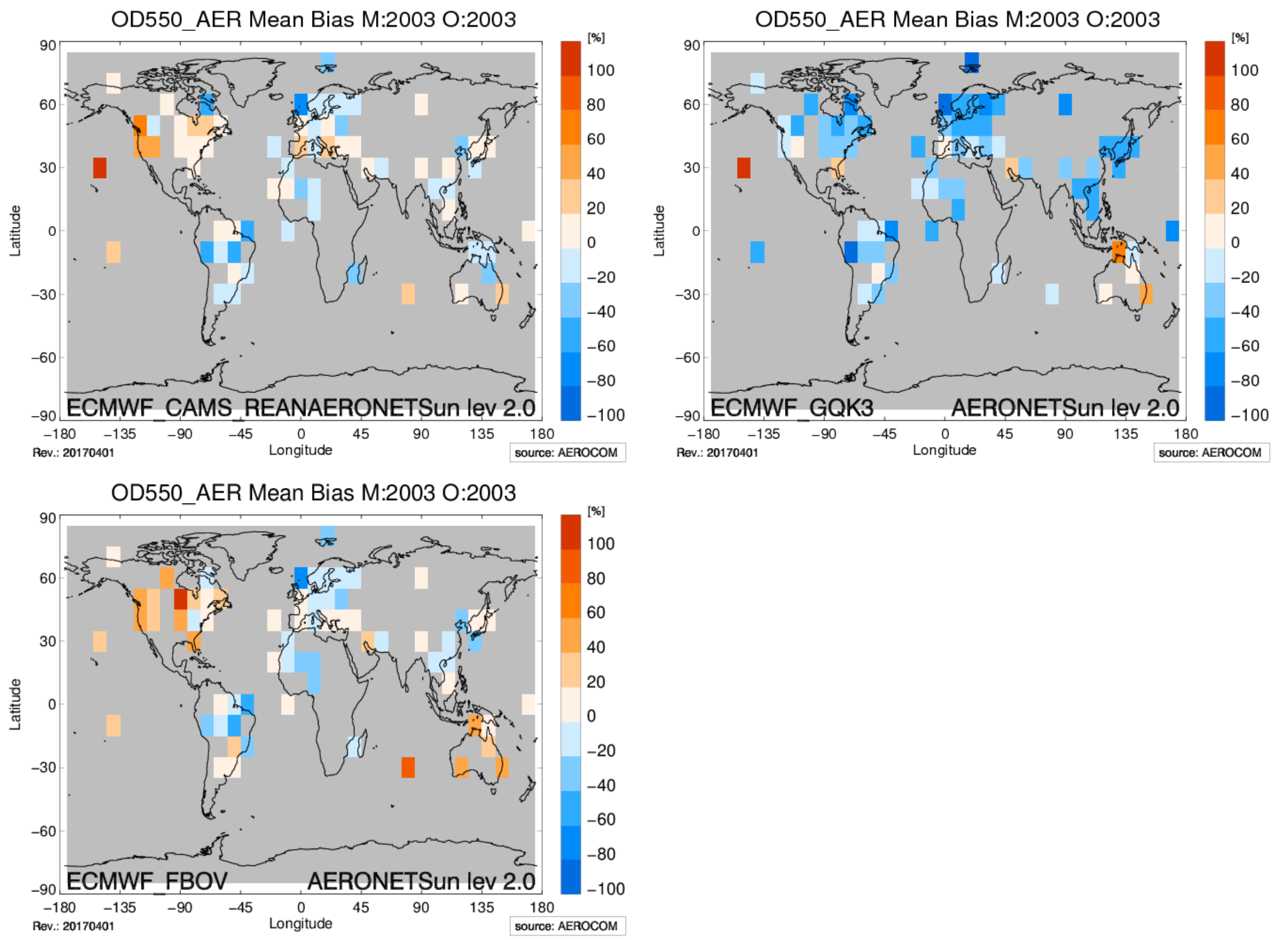

Figure 3.1.1.4: Regional relative mean bias of simulated daily AOD against Aeronet sun level 2.0 sun photometer measurements in the CAMS reanalysis (left), control run (right) and MACC reanalysis (bottom) for the year 2003. The regions with positive bias are reduced in the reanalysis and control experiments. More regions exhibit a bias of only +-20%, supporting that the reanalysis, despite or because of the significant shift in the aerosol composition, is better than both MACC and control.

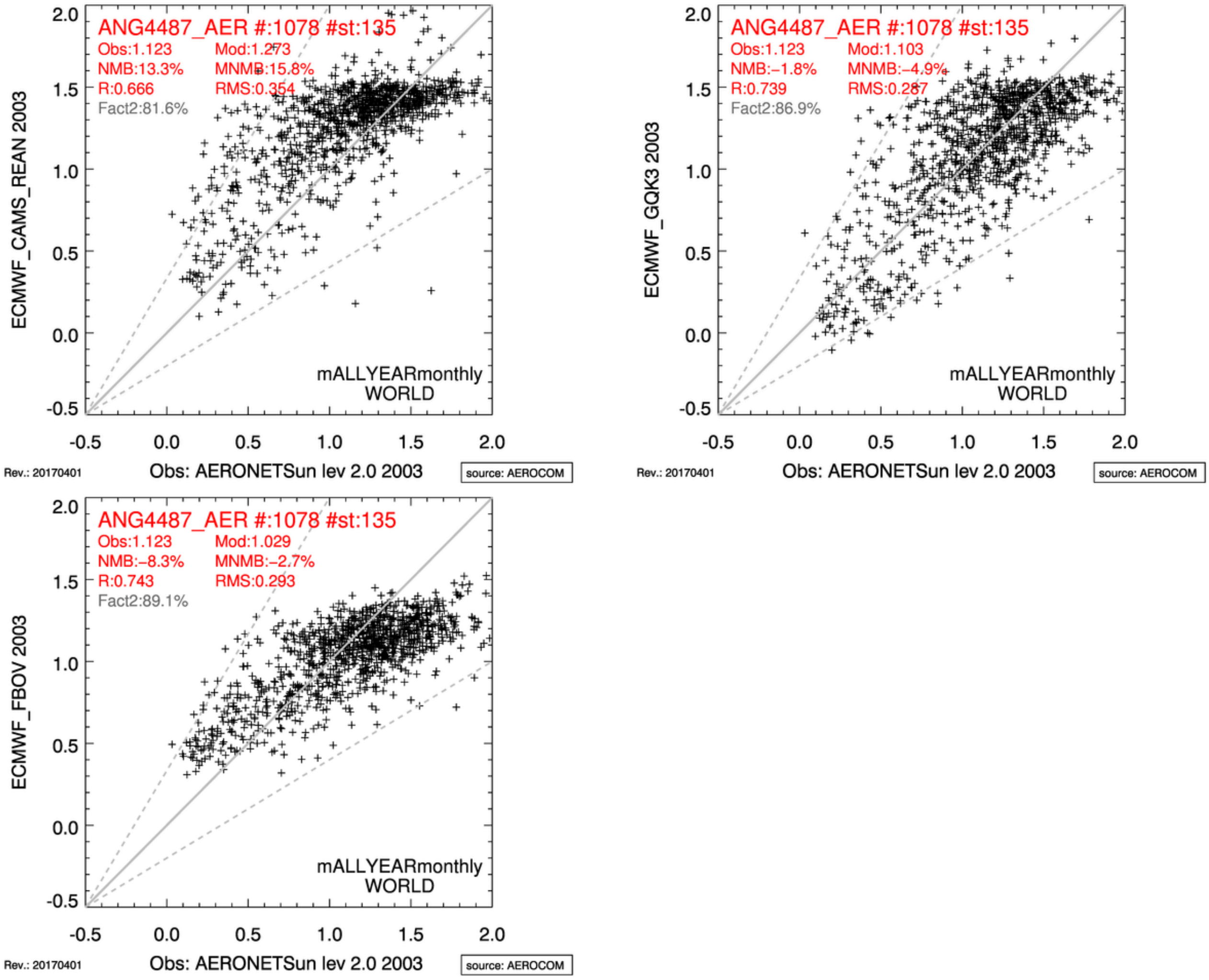

Figure 3.1.1.5: Evaluation of simulated daily Ångström Coefficient against Aeronet sun level 2.0 photometer measurements in the CAMS reanalysis (left), control run (right) and MACC reanalysis (bottom) for the year 2003. Statistics shown in the figure show a similar temporal-spatial RMS error reduction in both MACC and CAMS reanalyses. The MNMB-bias increased from -2.7% in MACC to +15.8% in CAMS.

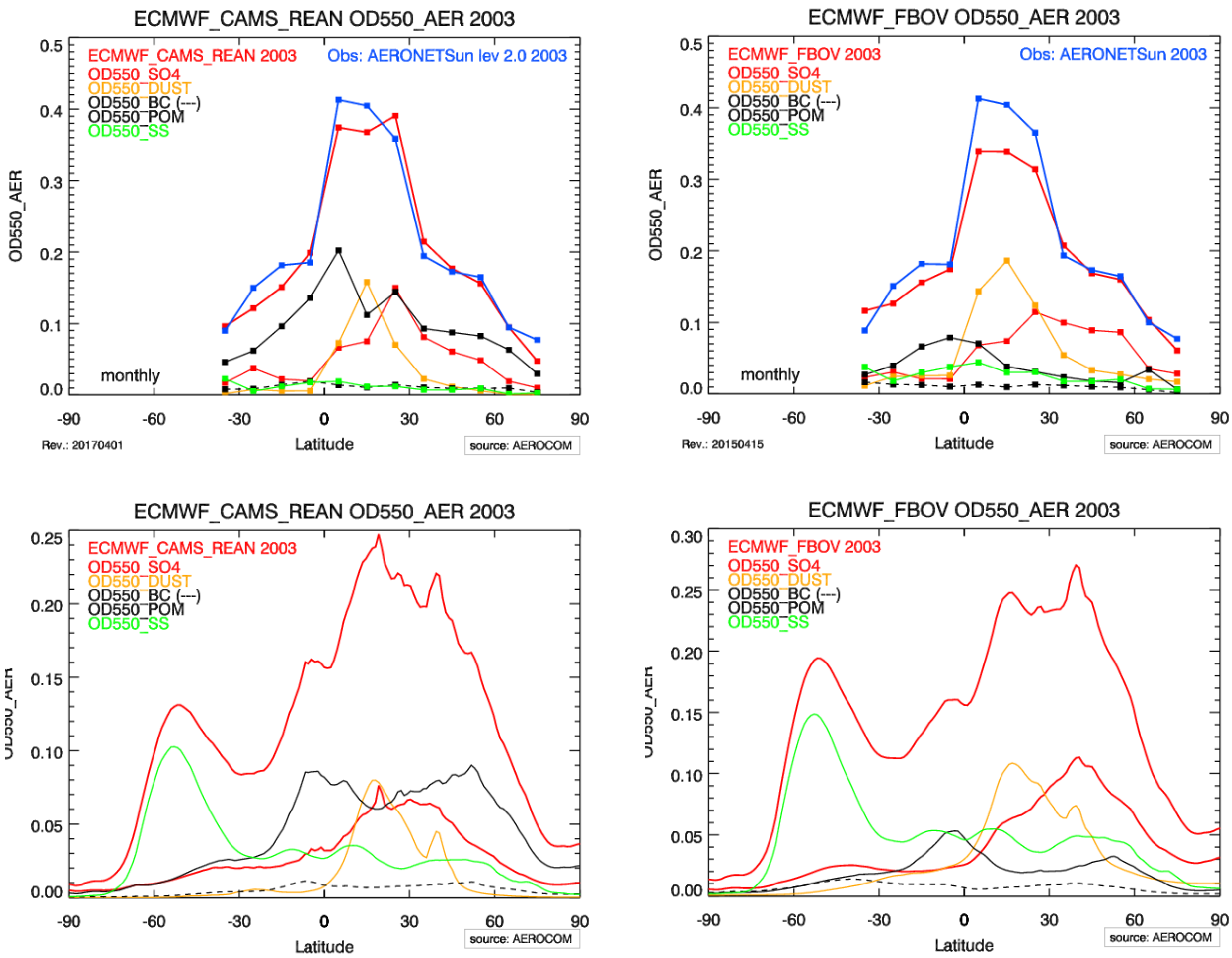

Figure 3.1.1.6: Upper row: Evaluation of latitudinal distribution of AOD in the CAMS reanalysis (left) and previous MACC reanalysis (right) for the year 2003. Total AOD from model (dark red upper curve) at Aeronet sites against total AOD from Aeronet (dark blue curve), aggregated as mean for 10 degree latitude bands, AOD speciation at Aeronet sites split in sulphate (red), dust (brown), black carbon (black dashed), organic (black) and sea salt (green); Lower row: Mean AOD in model against latitude. Total AOD (upper red curve), speciation as in upper row figures.

3.1.2 Dust model intercomparison over North Africa, Middle East and Europe

The seasonal DOD fields from the CAMS reanalysis show a distinct seasonal pattern linked to the spatial distribution of dust emissions and transport throughout the year 2003, in good qualitative agreement with both the MODIS Terra/Aqua and MISR AOD observations (Figure 3.1.2.1). The Bodéle, as well as the desert dust sources in Mauritania, Maghreb, Saudi Arabia and Oman, are systematically underestimated throughout the year. However, this new experiment also tends to underestimate AOD in comparison with observations, particularly over the subtropical and tropical North Atlantic (see Figure 3.1.2.2 and Capo Verde in Figure 3.1.2.4) as well as over the Red Sea, the Gulf of Oman and the Arabian Sea (see Figure 3.1.2.1). The most striking result is the big difference between AOD and DOD from CAMS precisely in desert areas (i.e. the Sahara and the Middle East) where mineral dust aerosol unambiguously dominates.

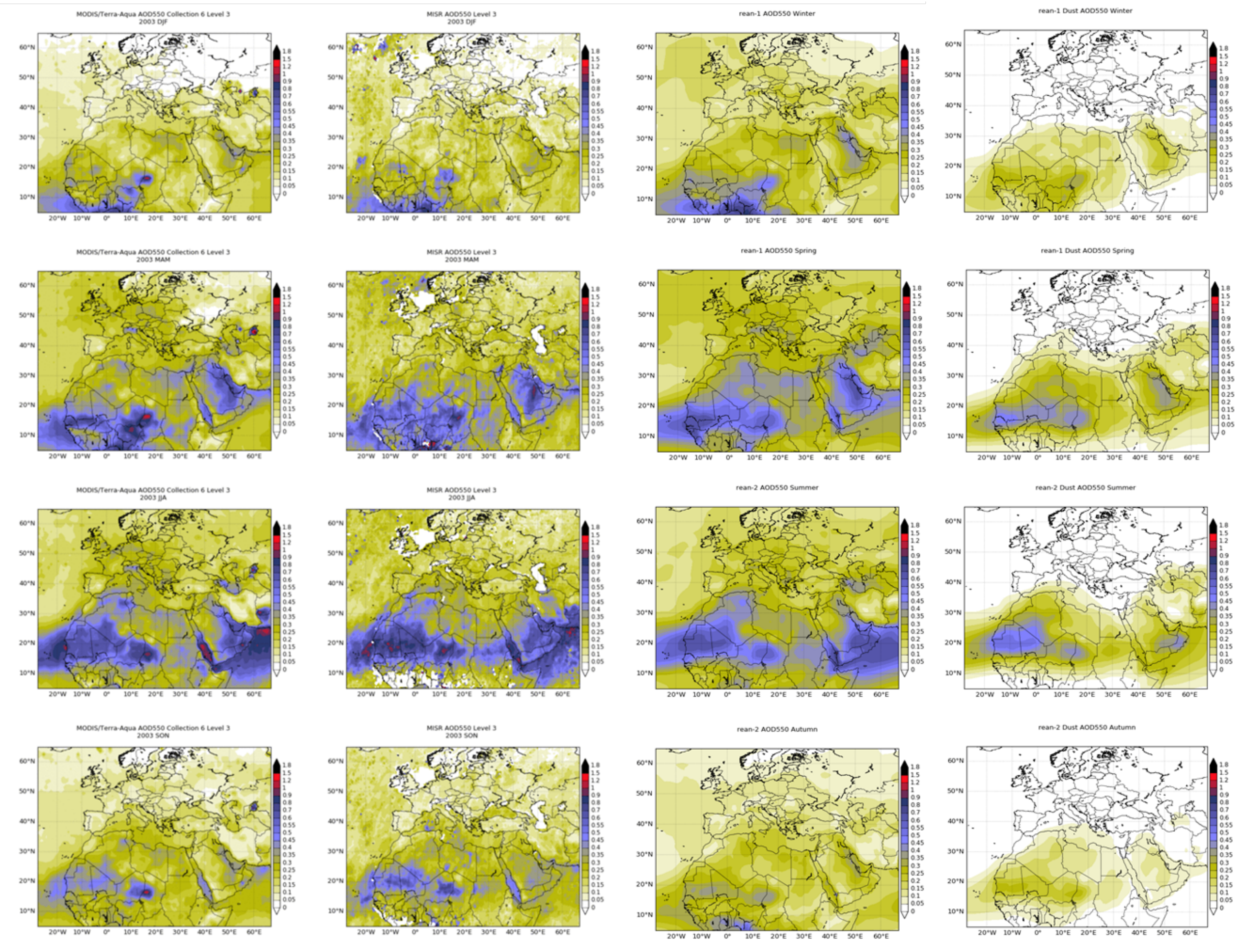

Figure 3.1.2.1: Seasonal averaged AOD from MODIS Collection 6 Terra/Aqua merged Dark target and Deep Blue Level 3 daily 1º x 1º global product (first column), MISR monthly Level 3 monthly 0.5º x 0.5º global product (second column) as well as AOD (third column) and DOD from CAMS reanalysis (merged gqm5 and gq7s experiments on 3-hourly basis; fourth column) for the year 2003. Winter (JFM), spring (AMJ), summer (JAS) and autumn (OND) from upper to lower rows.

The comparison with AERONET Version 2 direct-sun quality-assured observations also shows these differences between AOD and DOD over the North Africa and Middle East, which introduces strong DOD underestimations (see MB in Figure 3.1.2.2) with respect AOD (see MB in Figure 3.1.2.3). The comparison with AERONET DOD observations (i.e. dust-filtered AOD, on *3-hourly basis*, see selected available sites for 2003 in Figure 3.1.2.2) shows that the reanalysis reproduces rather well the annual variability showing seasonal correlation coefficients between 0.78 (in autumn) and 0.91 (in summer) in average for all the AERONET sites over Northern Africa, the Middle East and Europe but the dust aerosol content appears underestimated with seasonal MB between -0.14 (in winter) and -0.05 (in summer). The south-to-north gradient observed in the RMSE and FGE (see Figure 3.1.2.2) is associated with the lower DOD values towards northern latitudes. Meanwhile, the comparison with AERONET AOD observations shows seasonal MB between -0.05 (in winter) and 0 (in summer) and seasonal correlation coefficients between 0.73 (in autumn) and 0.84 (in winter) in average for all the AERONET sites (see Figure 3.1.2.3).

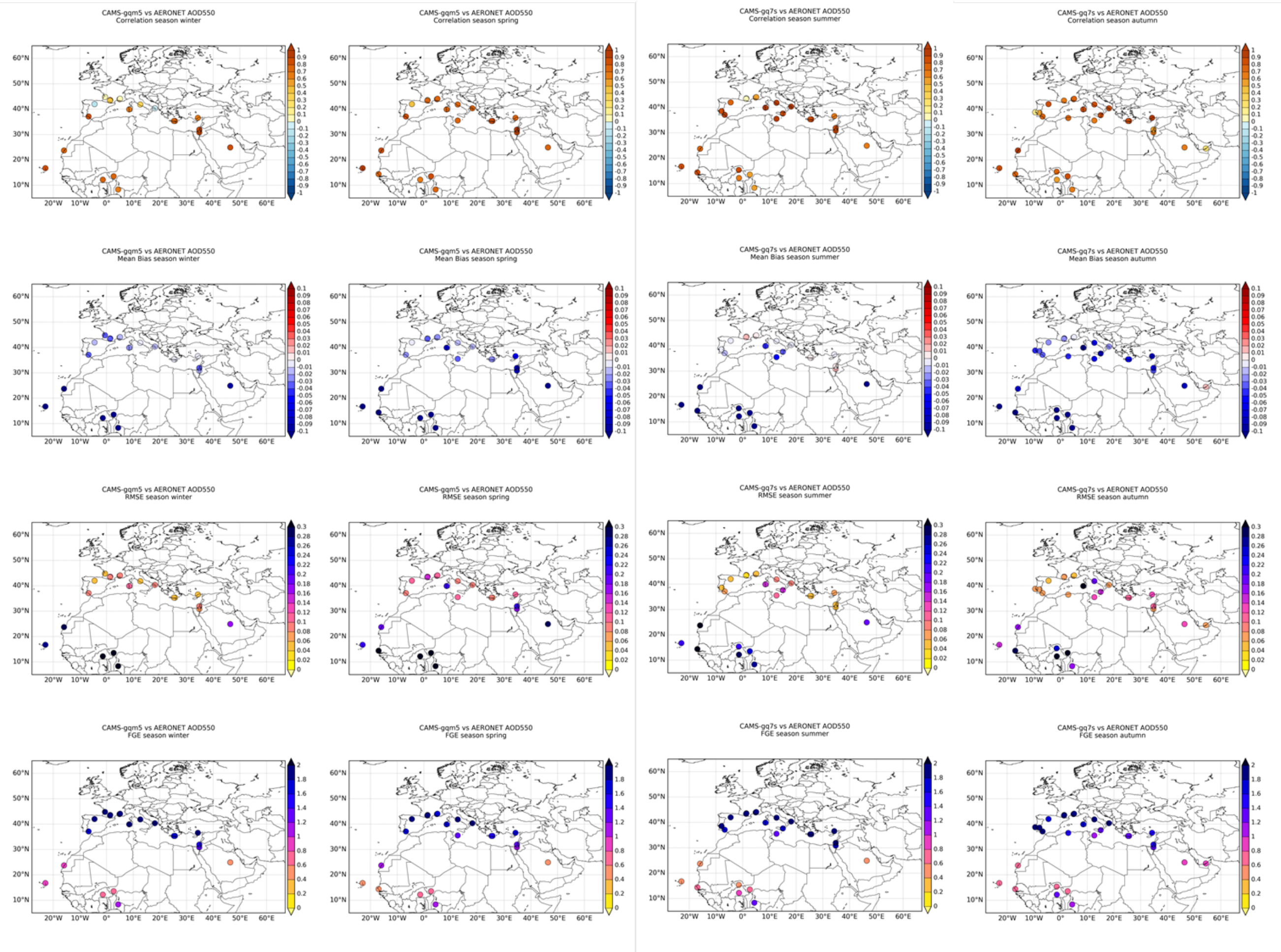

Figure 3.1.2.2: Seasonal skill scores (MB, FGE, RMSE and r) of DOD CAMS reanalysis for the year 2003. Dust-filtered AOD from AERONET Version 2 quality-assured filtered for dust is the reference. Calculations are done on 3-hourly basis. Winter (JFM), spring (AMJ), summer (JAS) and autumn (OND) from upper to lower rows.

The comparison with AERONET shows that differences between AOD and DOD observed over the North Africa and Middle East (causing strong DOD underestimations) are linked to the assimilation process as it is shown in Solar Village AERONET site (Figure 3.1.2.4). In this AERONET station, the DOD results of the CAMS reanalysis are lower than the control experiment. This is linked to an overestimation of organic matter (OM) from biomass burning during wintertime and also to overestimation of secondary organics over heavily populated areas during summertime. This, coupled with low AOD obtained in the control run (not shown here), makes OM a bit too preponderant through the assimilation step and hence, providing extremely low DOD values which are clearly underestimated.

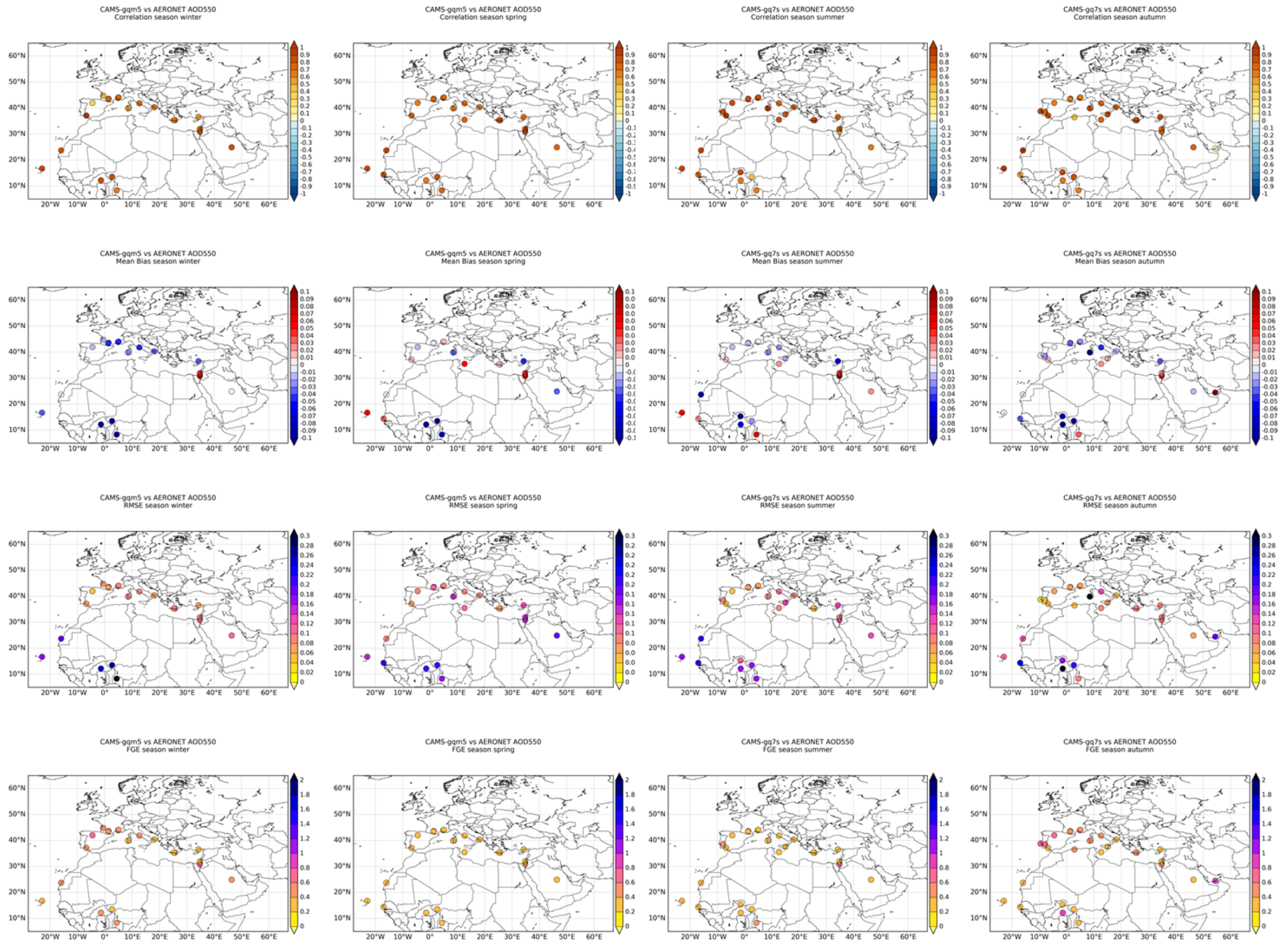

Figure 3.1.2.3: Seasonal skill scores (MB, FGE, RMSE and r) of AOD CAMS reanalysis for the year 2003. AOD from AERONET Version 2 quality-assured filtered for dust is the reference. Calculations are done on 3-hourly basis. Winter (JFM), spring (AMJ), summer (JAS) and autumn (OND) from upper to lower rows.

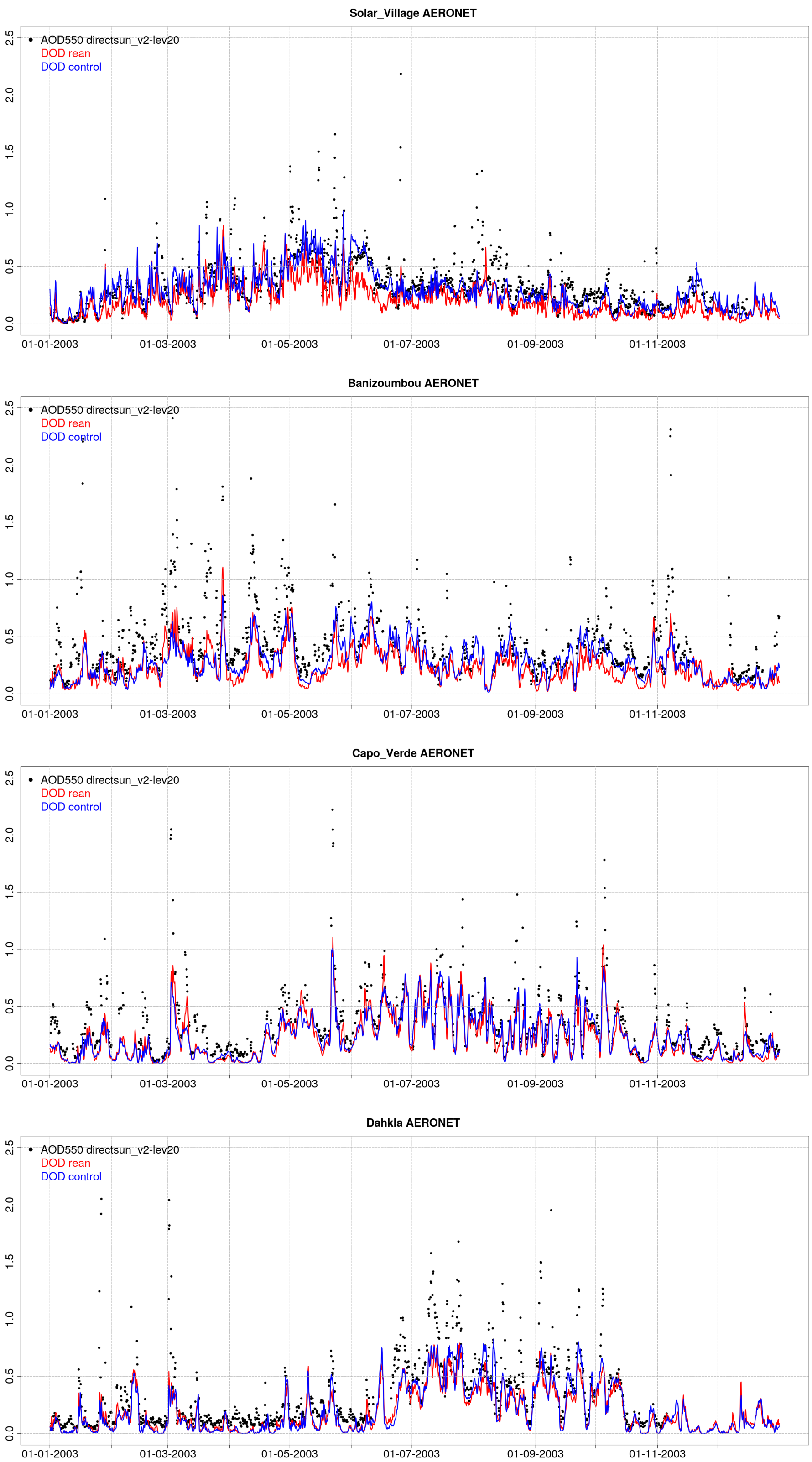

Figure 3.1.2.4: 3-houly AOD Level 2.0 AERONET observations (black dots), as well as the CAMS reanalysis (red) and control (blue) over Solar Village (Middle East), Banizoumbou (Sahel), Capo Verde (Tropical North Atlantic) and Dahkla (NW Maghreb).

3.1.3 Aerosol validation over the Mediterranean

Over the Mediterranean, CAMS reanalysis matches well the 3-hourly AOD variability of AERONET Version 2 direct-sun quality-assured observations (see Figure 3.1.2.3) with seasonal correlation coefficients between 0.47 (in spring in Western Mediterranean) and 0.81 (in spring in Central Mediterranean) and seasonal MB between -0.07 (in spring in Western Mediterranean) and 0.04 (in winter in Eastern Mediterranean). In general, the model reproduces the highest AOD peaks, which are associated with desert dust intrusions (see Figure 3.1.3.1) although it uses to underestimate their magnitude. Meanwhile the model tends to underestimate the AOD observations in Northern Mediterranean sites; it overestimates in Southern sites (see MB in Figure 3.1.2.3). Particularly in the Eastern Mediterranean (see Sede Boker in Figure 3.1.3.1). These AOD overestimations are mainly observed during summertime and they are linked to an enhanced of the OM contribution during the assimilation step. During summer, OM production of secondary organics over heavily populated areas during summertime when secondary processes are favoured.

The CAMS reanalysis is compared against 7 EIONET background-rural sites (on daily basis) provided within Openair project (www.openair-project.org/). The comparison is based on PM10 observations because no PM2.5 dataset is available for 2003. At surface level, CAMS reanalysis tends to underestimate the observations with seasonal MB between -9.42 $\mu g/m^3$ (in autumn) and 3.93 $\mu g/m^3$ (in winter) in average for all available sites. Negative MB values are observed over Majorca in the Balearic Islands (see Sa Pobla in Figure 3.1.3.2). Although these sites are categorized as background-rural sites, they are under the influence anthropogenic emissions. One of them is close to the city harbour, and the other two are quite near to urban areas. Despite of this, the comparison of the model with this set of sites shows higher underestimations during summertime (see Sa Pobla station in Figure 3.1.3.2) when secondary processes are favoured and the maritime traffic in the region enhanced. In Eastern Mediterranean, stronger underestimations are also observed during summertime, although CAMS reanalysis reproduces the maximum daily PM10 peaks of Airbase observations associated to desert dust outbreaks (see early-April of Ayia Marina site in Eastern Mediterranean in Figure 3.1.3.2). The comparison between CAMS reanalysis and control experiments highlights that the assimilation is able to enhance the background PM levels and reduce the magnitude of the most intense PM events.

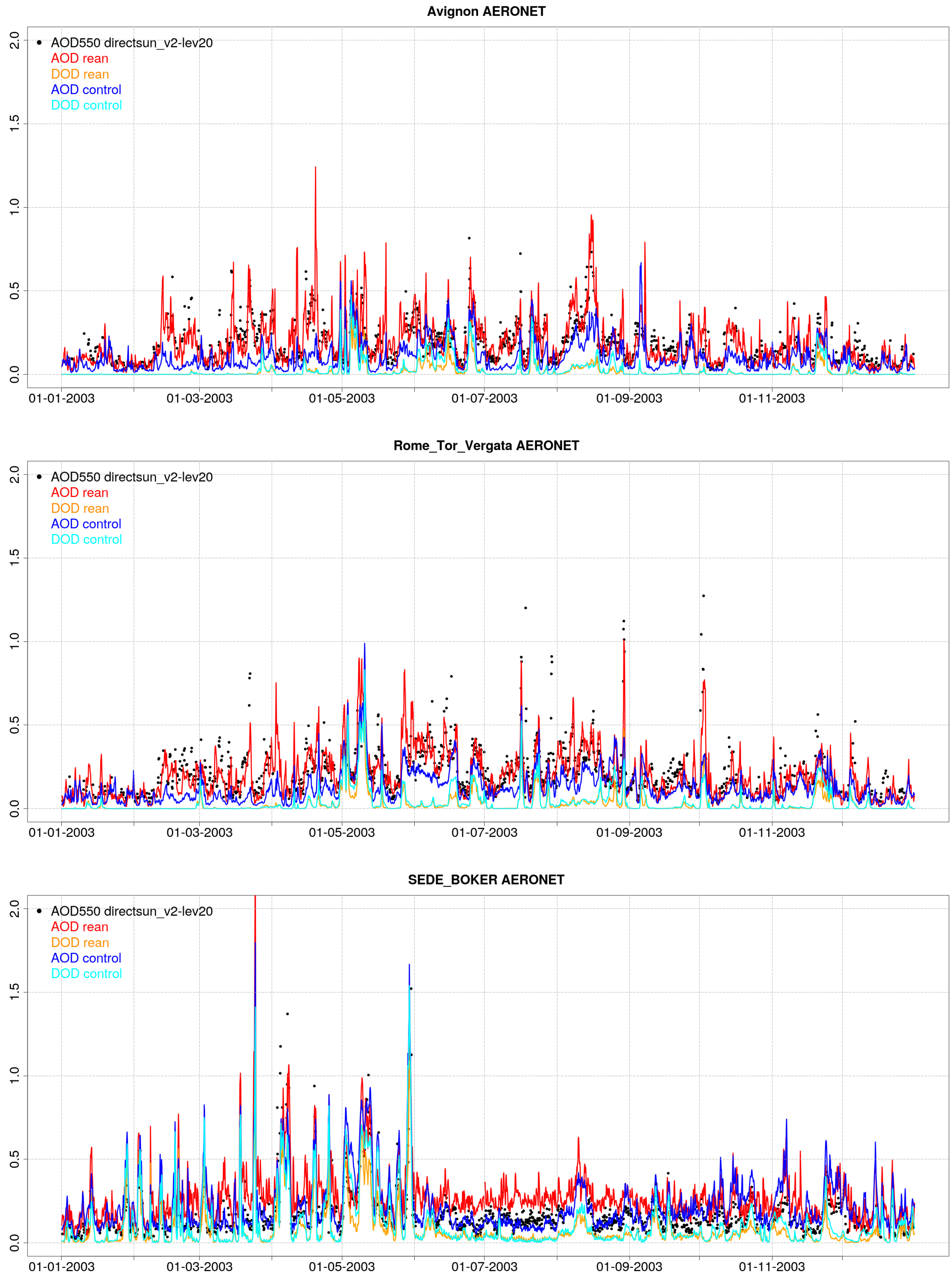

Figure 3.1.3.1: 3-houly AOD Version 2 Direct-Sun quality-assured AERONET observations (black dots), as well as CAMS AOD and DOD reanalysis (merged gqm5 and gq7s experiments) and control over Avignon (Western Mediterranean), Rome Tor Vergata (Central Mediterranean) and Forth Crete (Eastern Mediterranean).

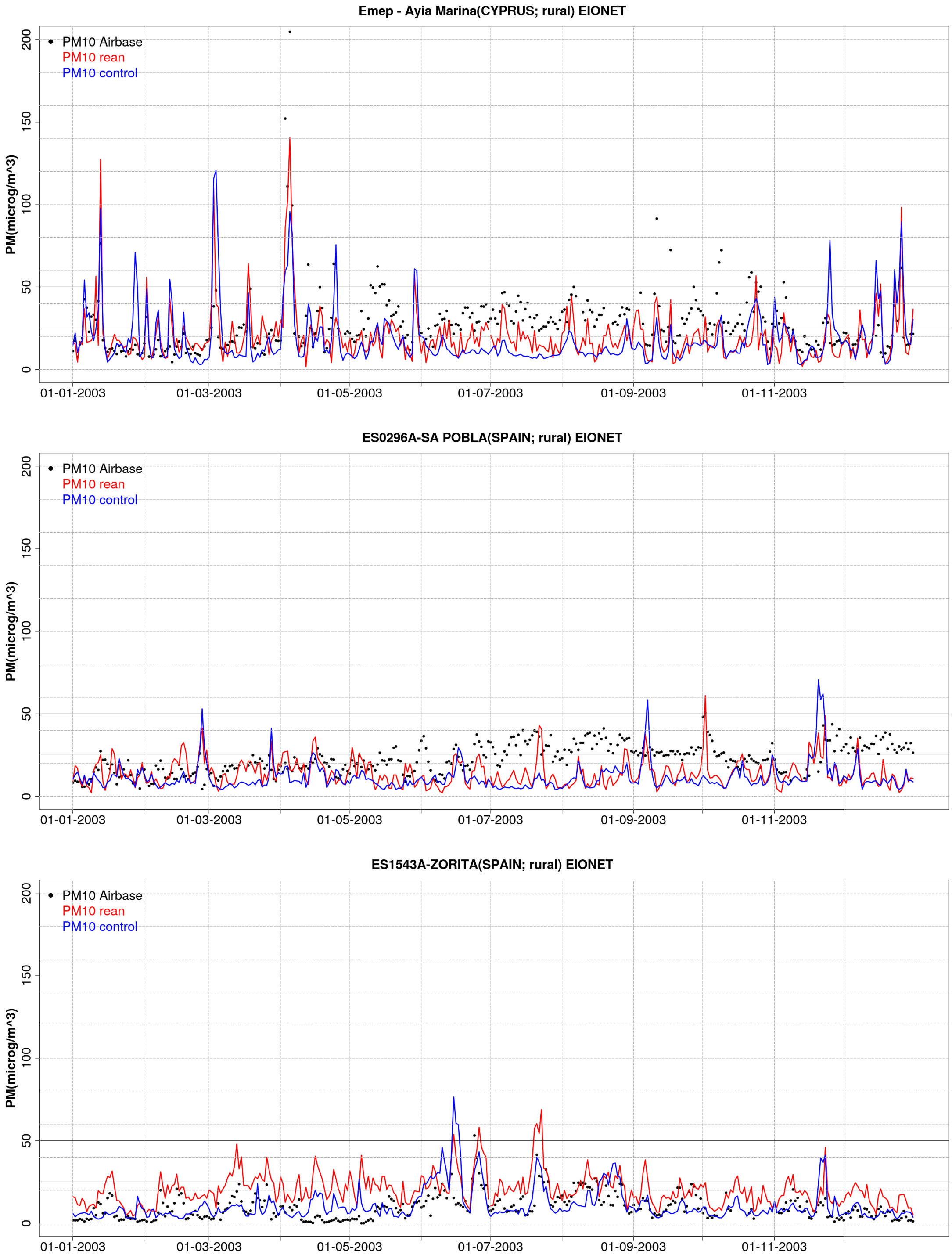

Figure 3.1.3.2: Daily PM10 EIONET observations (black dots, from Openair project), as well as CAMS reanalysis (merged experiments gqm5 and gq7s) and control experiments over Ayia Marina (Cyprus, Eastern Mediterranean), Sa Pobla (Mallorca, Balearic Islands) and Zorita (Eastern Iberian Peninsula) sites for the year 2003.

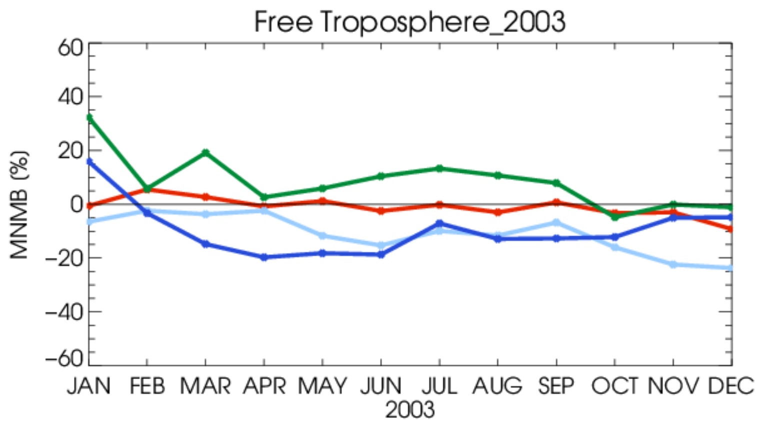

Fig 3.2.1.1: MNMBs of the reanalysis compared to ozone sondes for all 4 regions in the free troposphere (dark blue: Antarctica, light blue: Arctic, red: Northern midlatitudes, green: Tropics)

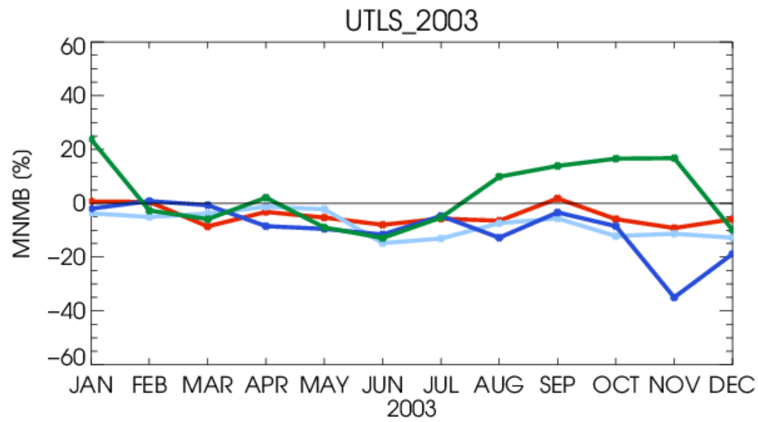

Fig 3.2.1.2: MNMBs of the reanalysis compared to ozone sondes for all 4 regions in the UTLS (dark blue: Antarctica, light blue: Arctic, red: Northern midlatitudes, green: Tropics)

3.2 Tropospheric Ozone

3.2.1 Validation with sonde data in the free troposphere

Model profiles of the CAMS reanalysis runs were compared to free tropospheric balloon sonde measurement data at 38 stations taken from the NDACC, WOUDC, NILU and SHADOZ databases for January to December 2003. Figure 3.2.1.3 contains the number of profiles in each month that are available for the evaluation. The methodology for model comparison against the observations is described in Eskes et al., 2016. The free troposphere is defined as the altitude range between 750 and 200 hPa in the tropics and between 750 and 350 hPa elsewhere, and the UTLS between 100 and 60 hPa in the tropics, and between 100 and 300 hPa elsewhere.

In the **free troposphere**, ozone mixing ratios are slightly underestimated over all regions except for the Tropics. MNMBs for the Northern midlatitudes range between 6 and -9% and for the Arctic between -2 and -24%. Over the Antarctic, MNMBs are between 16 and -22%. MNMBs for the Tropics are mostly within 20%, with exception of January 2003 where positive MNMBs range up to 32%, see Fig. 3.2.1.1. Data assimilation leads to lower MNMBs in all regions, except for the Arctic between September and December 2003, where the control run shows lower MNMBs, see Fig. 3.2.1.3.

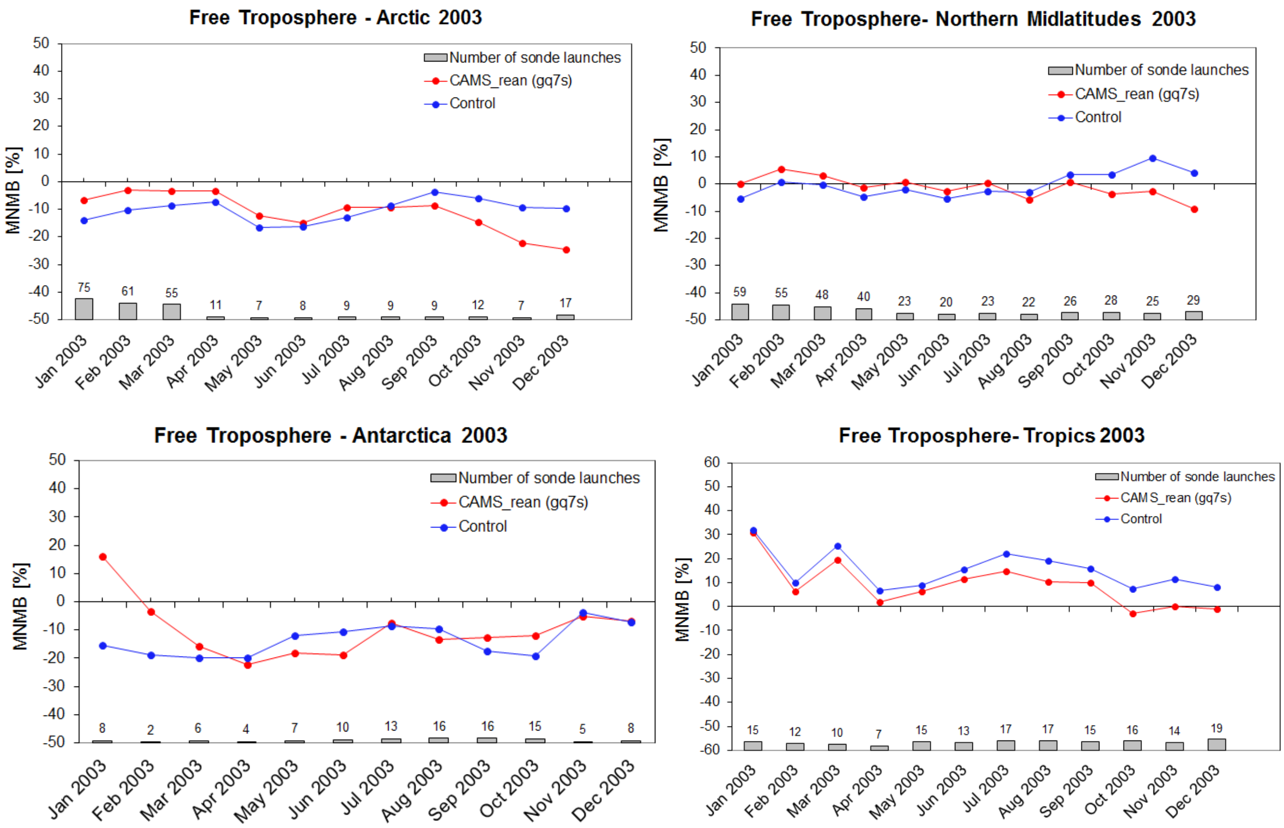

Fig 3.2.1.3: MNMBs for all 4 regions in the UTLS (dark blue: Antarctica, light blue: Arctic, red: Northern midlatitudes, green: Tropics).

In the **UTLS**, ozone mixing ratios are mostly underestimated. MNMBs range between -14 and 4% over the Arctic and between -9 and 3% over the Northern midlatitudes. For Antarctica, MNMBs are between 0 and -18%, except for in November 2003, where the MNMB drops to -35%. For the tropical UTLS, MNMBs are between -12 and 27%, see Fig. 3.2.1.2. Data assimilation improves the MNMBs for all regions, except for the Arctic between June and October 2003 and the Tropics between January and April, where the control run shows lower MNMBs.

3.2.2 Validation with GAW surface ozone observations

In the following, an evaluation of model performance for the reanalysis run and control has been carried out for the period January to December 2003. GAW hourly data from 42 stations from the World Data Centre for Greenhouse Gases (WDCGG) has been used for model verification, see Table 3.2.2.1.

The validation shows that the reanalysis can reproduce observed O_3 mixing values at the surface with MNMBs mostly within ±15%. The seasonal validation shows slightly negative MNMBs during the winter season and slightly positive MNMBs during the summer season see Fig 3.2.2.4.

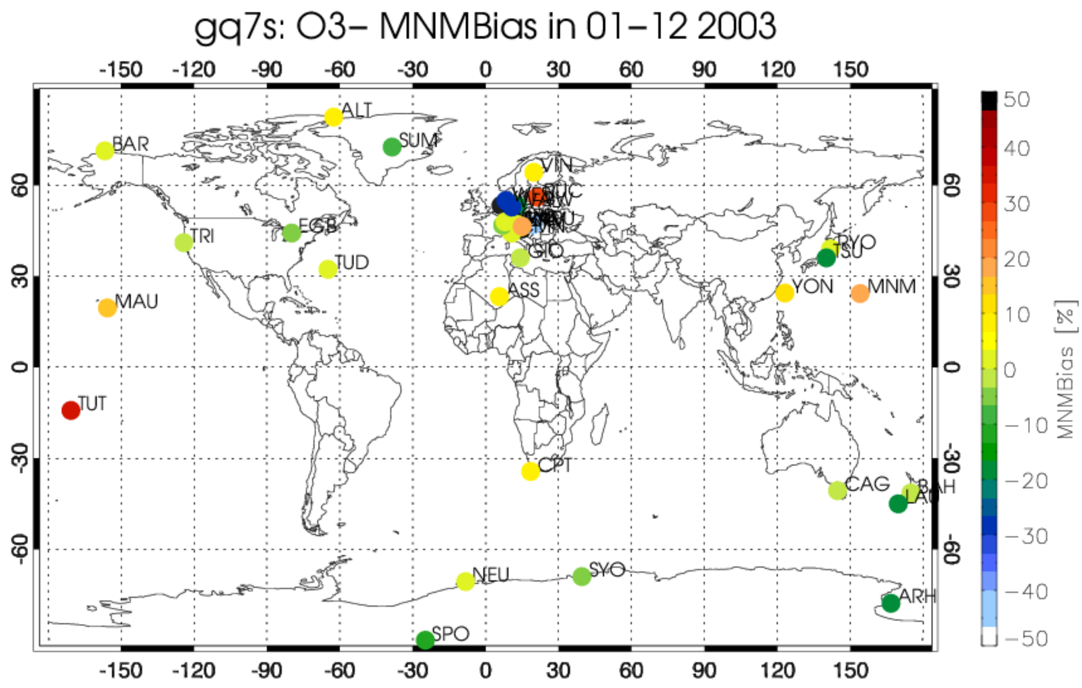

Fig 3.2.2.1: Map of MNMBs over the time period 01-12 2003

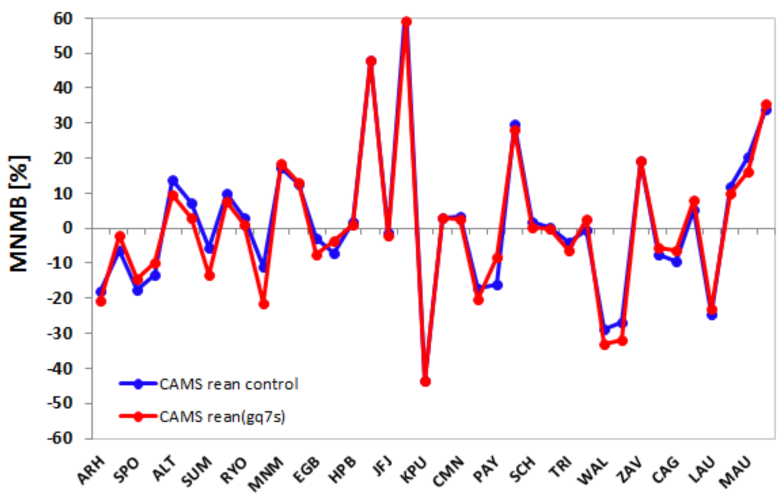

Fig 3.2.2.2: MNMBs for GAW stations calculated over the whole year 2003.

Correlation coefficients are mostly over 0.6 (see Figs. 3.2.2.3, 3.2.2.5 and 3.2.2.6), which shows a good linearity of the model and observations. The standard deviation close to the reference proves that the modelled variability of ozone is similar to the observed variability for most stations (Fig. 3.2.2.6). Results for the control run are generally very similar to the reanalysis (Figs. 3.2.2.2 and 3.2.2.3)

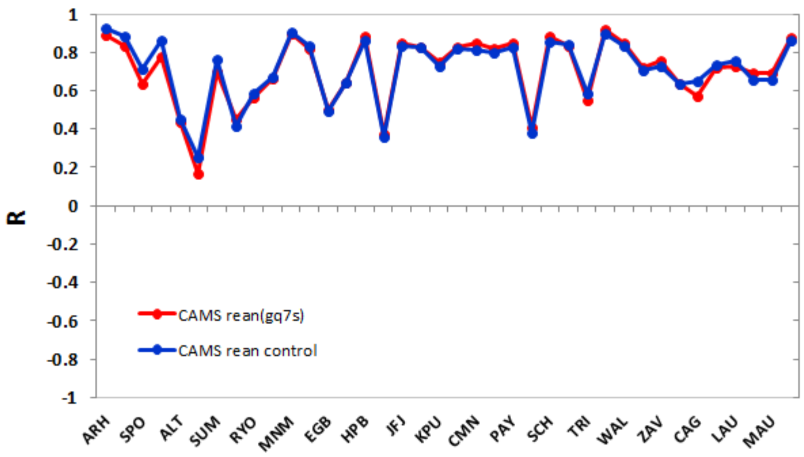

Fig 3.2.2.3: R for GAW stations calculated over the whole year 2003

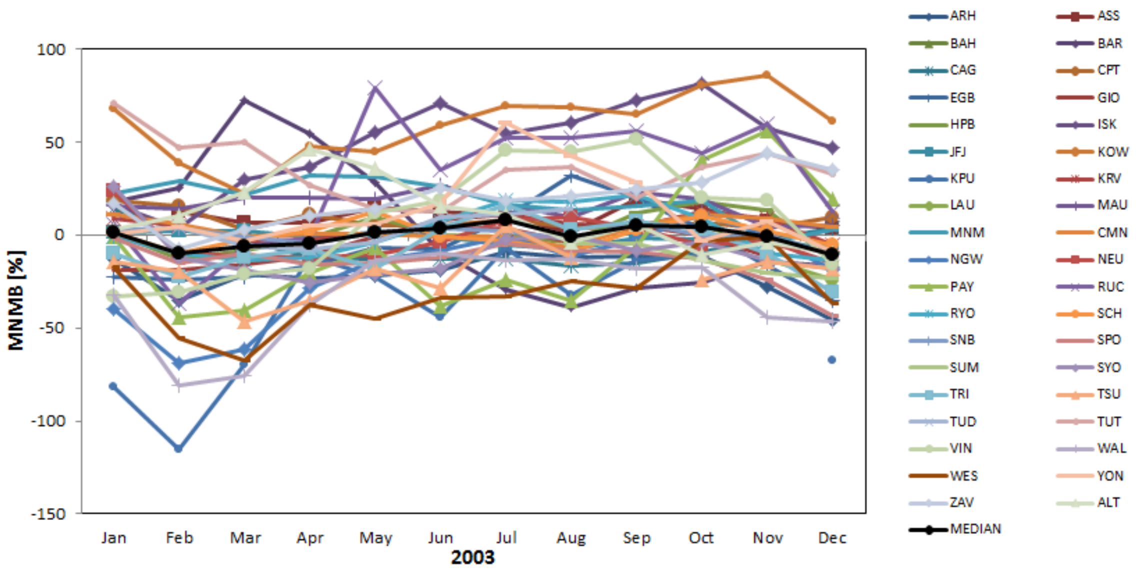

Fig 3.2.2.4: MNMBs for GAW stations calculated for each month in 2003

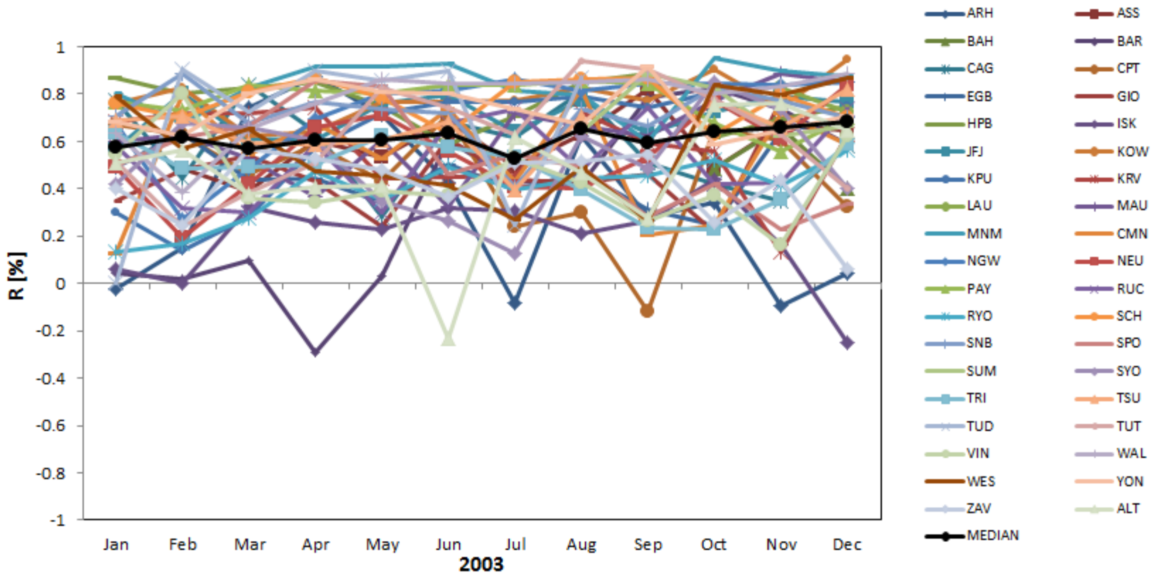

Fig 3.2.2.5: R for GAW stations calculated for each month and in 2003

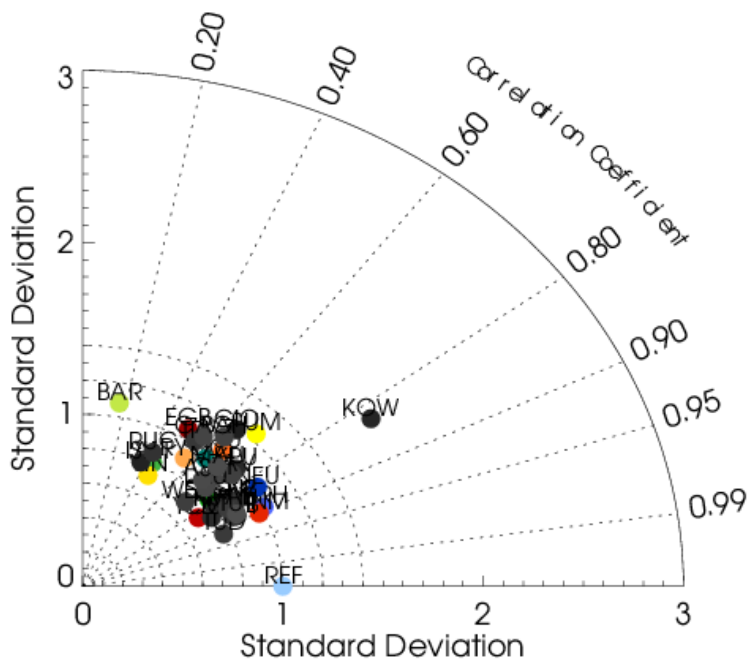

Fig 3.2.2.6: Taylor diagram with standard deviation and correlation for O3 over the period 01-12 2003

Table 3.2.2.1: GAW station data (O_3) used in the validation for 2003

Station	Name	Latitude	Longitude	Altitude
Alert	ALT	82.45	-62.52	210
Arrival Heights	ARH	-77.8	166.67	184
Assekrem	ASS	23.27	5.63	2710
Baring Head	BAH	-41.41	174.87	85
Barrow	BAR	71.32	-156.6	11
Cape Grim	CAG	-40.68	144.68	94
Monte Cimone	CMN	44.18	10.7	2165
Cape Point	CPT	-34.35	18.48	230
Egbert	EGB	44.23	-79.78	253
Giordan Lighthouse	GIO	36.07	14.22	167
Hohenpeissenberg	HPB	47.8	11.02	985
Iskrba	ISK	45.57	14.87	520
Izana	IZO	28.3	-16.5	2367
Jungfraujoch	JFJ	46.55	7.98	3578
Kollumerwaard	KOW	53.33	6.28	0
Kosetice	KOS	49.58	15.08	534
K-Puszta	KPU	46.97	19.55	125
Krvavec	KRV	46.3	14.53	1720
Lauder	LAU	-45.03	169.67	370
Mauna Loa	MAU	19.539	-155.578	3397
Minamitorishima	MNM	24.28	153.98	8
Neumayer	NEU	-70.65	-8.25	42
Neuglobsow	NGW	53.17	13.03	65
Payerne	PAY	46.82	6.95	490
Rigi	RIG	46.07	8.45	1031
Rucava	RUC	56.17	21.18	18
Ryori	RYO	39.03	141.82	260
Schauinsland	SCH	47.92	7.92	1205
Sonnblick	SNB	47.05	12.95	3106
South Pole	SPO	-89.98	-24.8	2810
Summit	SUM	72.58	-38.48	3238
Syowa Station	SYO	-69	39.58	2
Trinidad Head	TRI	41.05	-124.15	120
Tsukuba	TSU	36.05	140.13	25
Tudor Hill	TUD	32.27	-64.87	30
Tutuila	TUT	-14.24	-170.57	42
Vindeln	VIN	64.25	19.77	271
Waldhof	WAL	52.8	10.77	74
Westerland	WES	54.93	8.32	12
Yonagunijima	YON	24.47	123.02	30
Zavodnje	ZAV	46.43	15	770
Zingst	ZIN	54.43	12.73	1

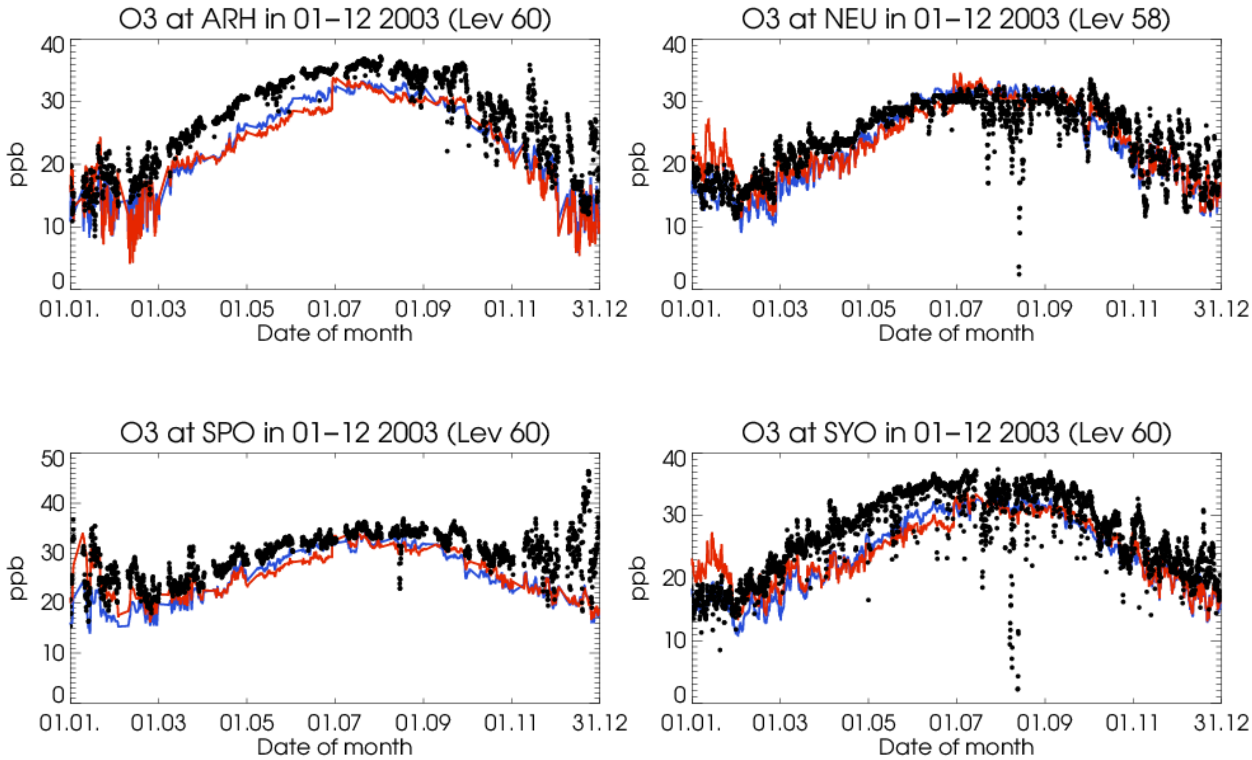

Fig 3.2.2.7: Time series for O3 in the period 01-12 2003 for GAW stations in Antarctica.

Antarctica

The reanalysis could reproduce O_3 for stations in Antarctica with MNMBs between -2 and -21% (control: -6 and -18%). Ozone is generally underestimated, except for January 2003 (first month). The underestimation increases during the Antarctic summer season. Monthly correlations are extremely low during ozone depletion events in Antarctic spring, which are not reproduced in the model, see Fig 3.2.2.7. Apart from that, the model shows good overall correlation with Rs between 0.63 and 0.89. A jump can be seen on 1 July, when the reanalysis changes from experiment gqm5 to gq7s.

Asia

For stations located in Asia (see Fig. 8), the model shows an underestimation of O_3 mixing ratios during winter and spring (around -10%) and an overestimation during summer (around 20%). Monthly correlation coefficients are generally high, but depend on the station. The overall MNMBs are between -21% and 1%. Overall correlation is between 0.56 and 0.90.

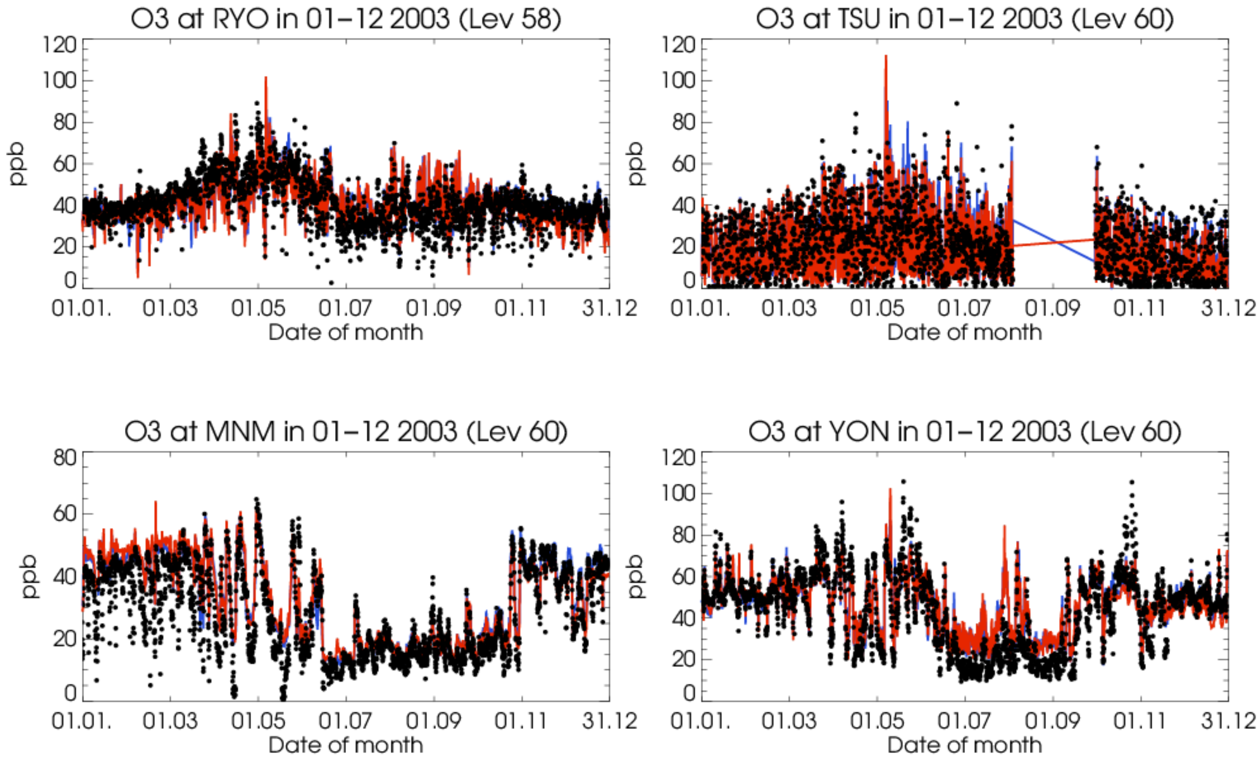

Fig 3.2.2.8: Time series for O_3 in the period 01-12 2003 for GAW stations in Asia.

<u>Europe</u>

Apart from single stations that show a strong overestimation of O_3 especially during summer and fall, most stations show an underestimation of O_3, for most of the year, with MNMBs ranging between -44 and 60%. The location of the stations plays an important role in the quality of the results: the more remote mountain stations (HPB, SNB, SCH, CMN, and JFJ) show very accurate results (see also map in Fig. 3.2.2.9) with low MNMBs (between -2 and 3%) and high correlation (>0.8) in contrast to the lower-altitude stations that may be more influenced by local pollution. Overall correlation coefficients are between 0.37 and 0.88.

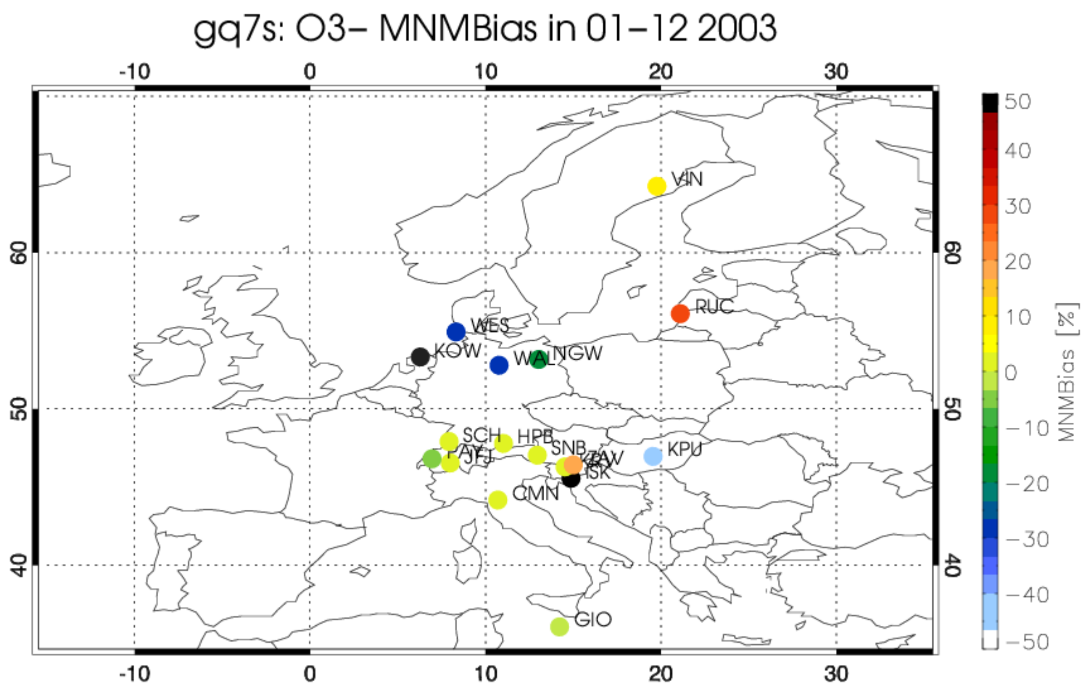

Fig 3.2.2.9: Map of MNMBs for European GAW stations over the time period 01-12 2003.

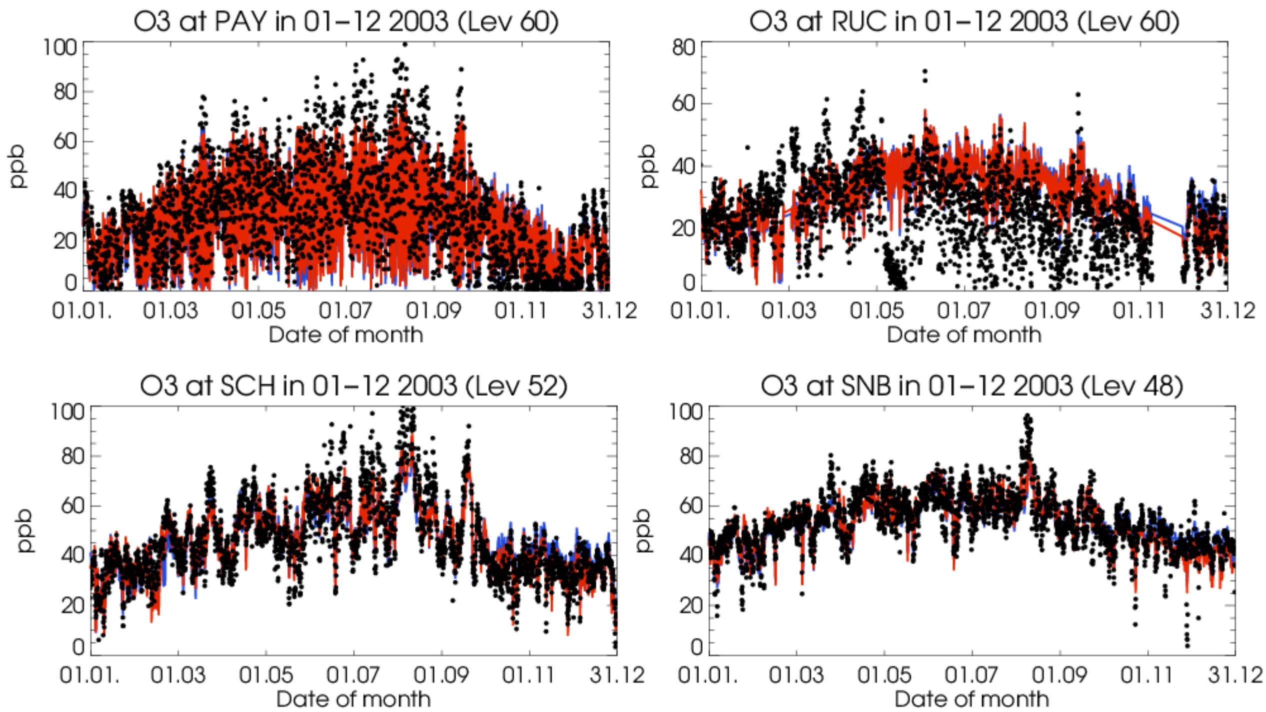

Fig 3.2.2.10: Time series for O_3 in the period 01-12 2003 for GAW stations in Europe.

Tropics

The model shows an overestimation for O_3 mixing ratios in the tropics with MNMBs between 10% and 36%. Correlation coefficients are between 0.6 and 0.87.

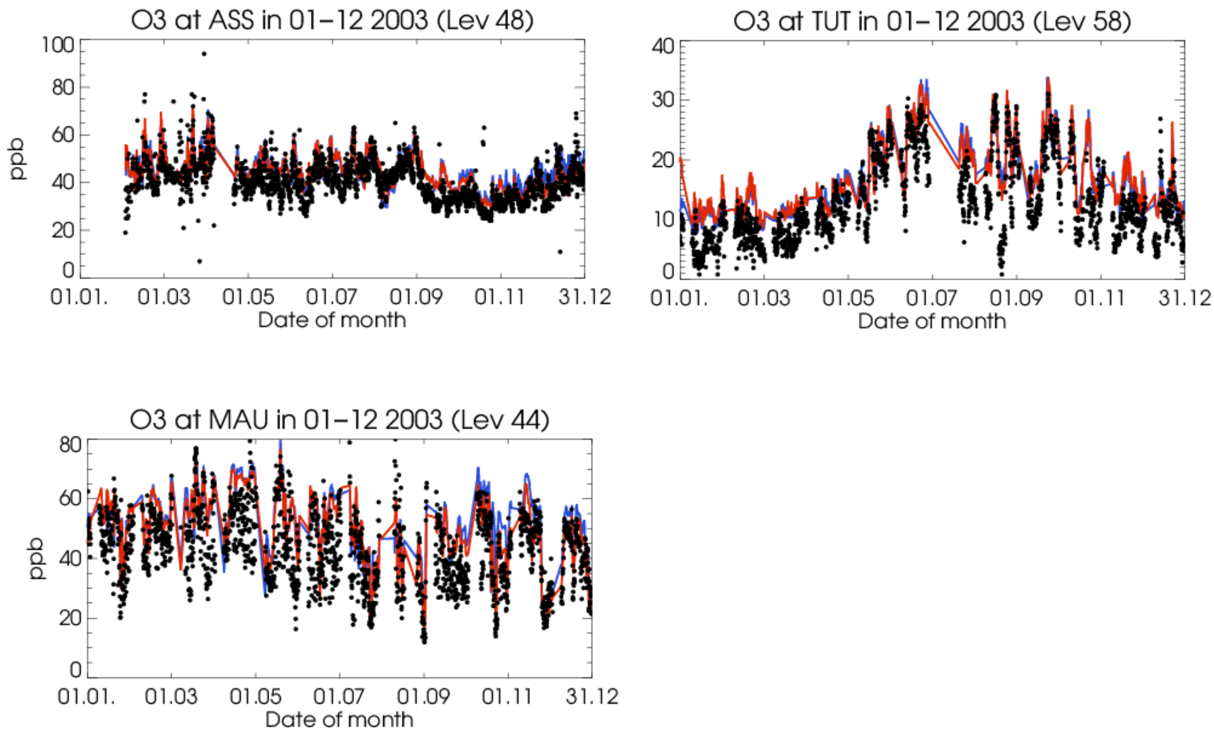

Fig 3.2.2.11: Time series for O_3 in the period 01-12 2003 for GAW stations in the Tropics

3.2.3 Verification with European EMEP surface ozone observations

The CAMS reanalysis as well as the CAMS control run and the MACC reanalysis were compared to the surface EMEP and Airbase background rural observations on a seasonal basis for the latitudinal zones of 30°N-40°N, 40°N-50°N and 50°N-70°N; these latitudinal zones denote the zonal monthly averages of surface ozone of the period 2003 over Southern, Central and Northern Europe respectively (Fig. 3.2.3.1).

Over Southern Europe, the CAMS reanalysis and control reproduce well the mean ozone concentrations during the first half of the year (MNMBs<5%) while systematically overestimating ozone mixing ratios during the second half of the year with the highest positive amplitudes being observed during autumn (MNMBs up to 20%). It should be noted that the strong negative offset (down to 50%) which appears in the MACC Reanalysis during the period January to April 2003 is corrected in the new reanalysis.

Over Central Europe the modelled surface ozone values in all three reanalysis experiments agree well with observations for the 2nd half of the year whilst during the 1st half of the year a large negative bias is observed (down to -8 ppbv, MNMBs≈-30% for the reanalysis, to -10 ppbv, MNMBs≈-35% for the control experiment and down to -15 ppbv, MNMBs≈-60% for the MACC reanalysis). Data assimilation seems to improve slightly the biases during the first 3 months of the year.

Lastly, over Northern Europe, the CAMS reanalysis underestimates O_3 levels during winter and spring seasons (MNMBs down to -40% during February), overestimates O_3 during autumn (MNMBs up to 20%) and reproduces well mean concentrations of ozone during summer season. It should be noted again that the negative offset during the cold part of the year is lower in the new reanalysis compared with the MACC reanalysis. It seems also that over Northern Europe the data assimilation reduces the biases during April and May. Surprisingly for December 2003 the reanalysis experiment show a larger negative offset (-20%) comparing with the control and the MACC reanalysis.

The same analysis was repeated for the high altitude stations (stations with altitude higher than 1000 m a.s.l.) and it was found that the CAMS reanalysis experiments underestimate slightly ozone mean concentrations during January to March 2003 (MNMBs down to -5%), overestimate it slightly during autumn (MNMBs up to 10%) and reproduces well O_3 levels during the rest of 2003. Again the CAMS reanalysis experiments performers better than the MACC reanalysis in terms of biases especially for the period January to April 2003. It seems also that again the data assimilation reduces the biases during January to April.

Similar results are found from Fig. 3.2.3.2 which shows the spatial distribution of the Modified Normalised Mean Biases (MNMBs) calculated for the CAMS Reanalysis experiment and the MACC Reanalysis over the 262 background rural European EMEP and AirBase stations in a seasonal base (winter months, spring, summer and autumn seasons).

Fig. 3.2.3.3 shows the spatial distribution of the temporal correlations between modelled and observed surface ozone values calculated for the CAMS Reanalysis experiment and the MACC Reanalysis over the 262 individual EMEP and AirBase stations in a seasonal base. Correlations between reanalysis ozone values and observations are highly significant for the majority of the stations and the higher correlations are observed during summer and autumn seasons ($0.5<r<0.9$); relatively lower correlations are observed during winter season particularly at the southern Europe stations ($0.0<r<0.4$ depending on the station) and during spring over stations northern the 60°N ($0.0<r<0.5$ depending on the station). It should be noted that the CAMS Reanalysis experiments performers better than the MACC reanalysis in terms of biases particularly during winter and spring 2003.

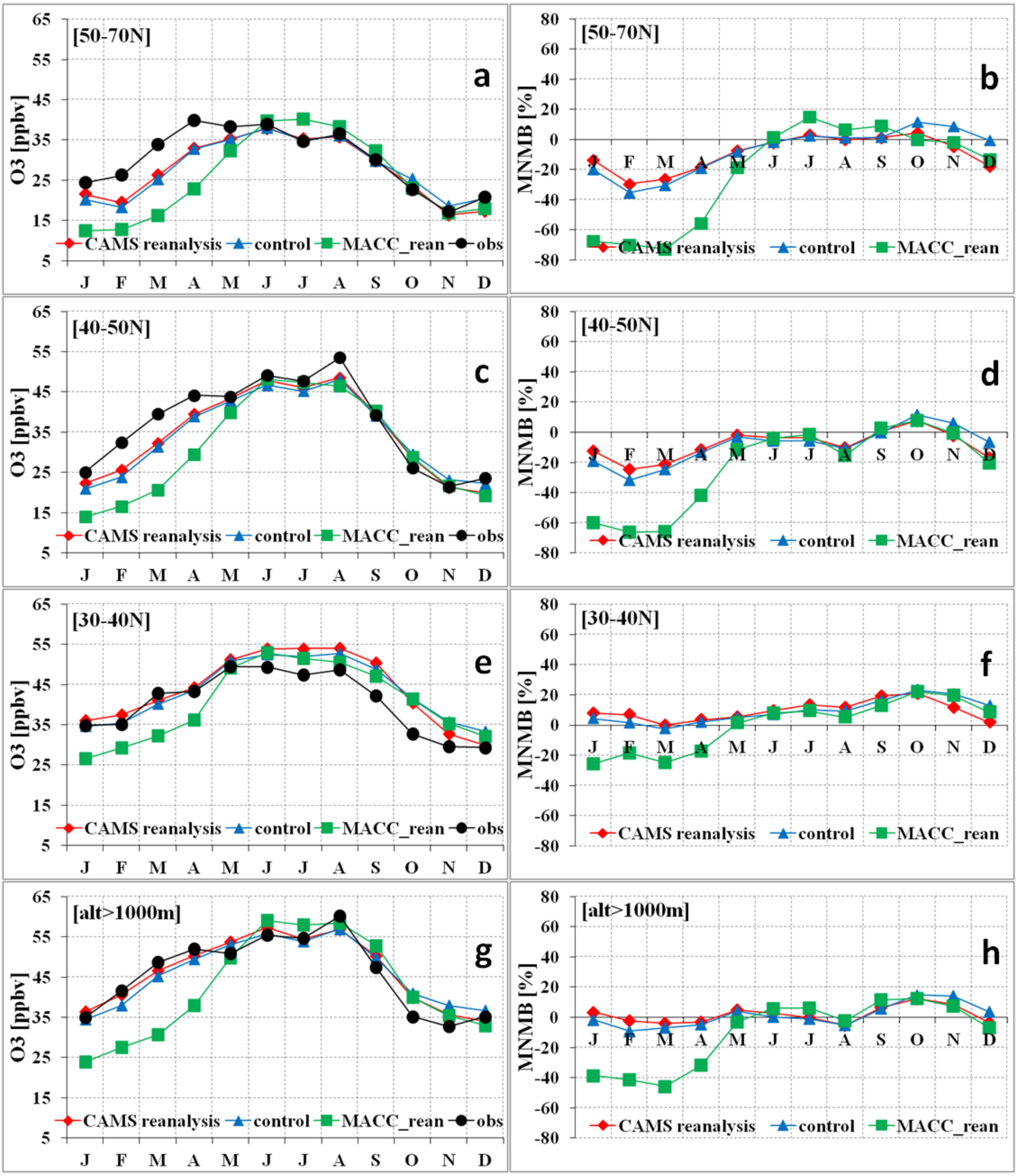

Figure 3.2.3.1. Mean monthly ozone variability for the year 2003 (left) and the MNMBs (right) of the Reanalysis experiment (red robs) the control experiment (blue triangles), the MACC reanalysis (green squares), and the EMEP observations (black circles) over Northern Europe (1st row, a and b), Central Europe (2nd row, c and d), Southern Europe (3rd row, e and f) as well as for stations with altitude greater than 1000m a.s.l. (4rd row, g and h).

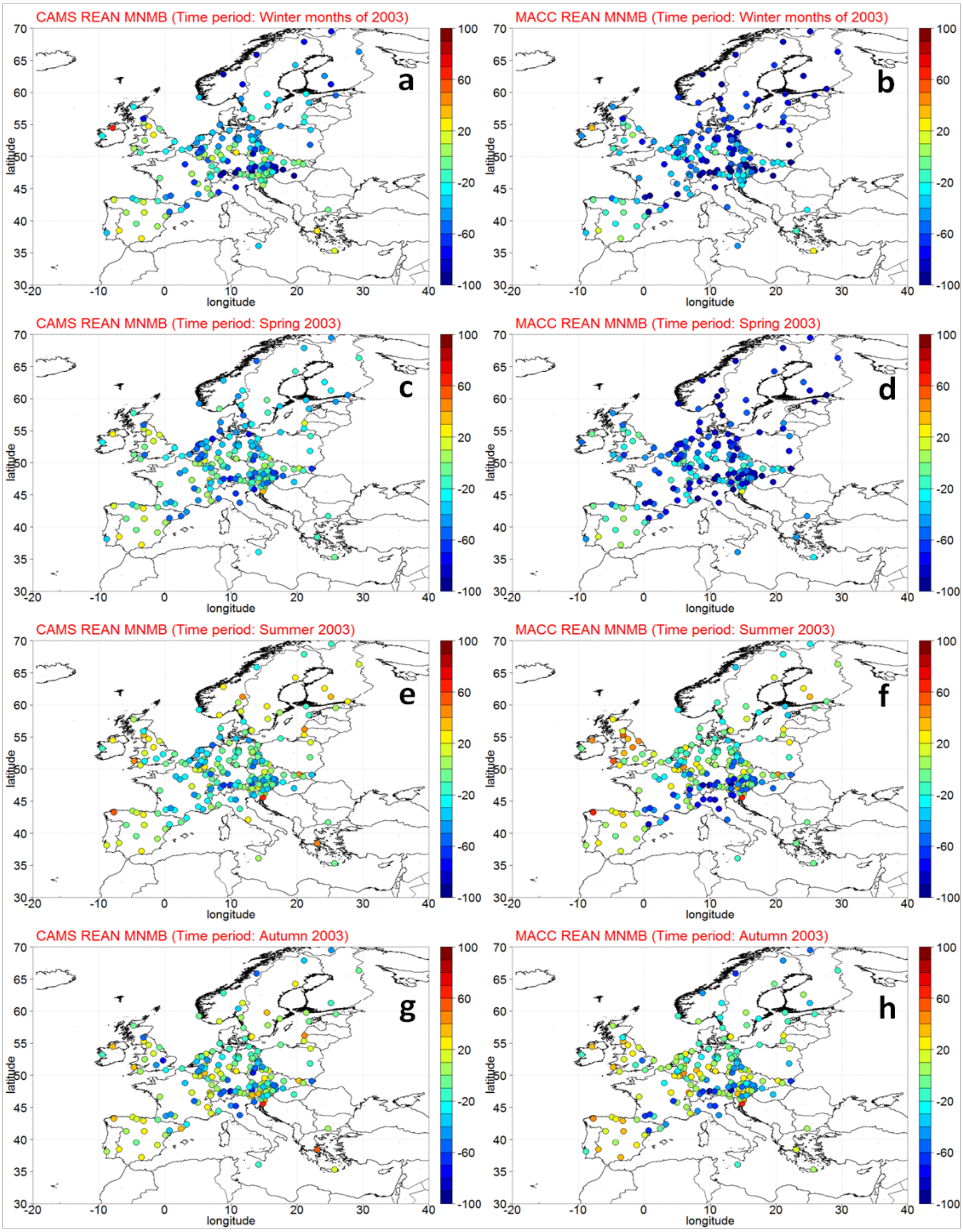

Figure 3.2.3.2. Modified Normalised Mean Biases (MNMBs) during Winter 2003 (1st row, a and b), Spring 2003 (2nd row, c and d), Summer 2003 (3rd row, e and f) and Autumn 2003 (4rd row, g and h) for the CAMS reanalysis experiment (left) and the MACC reanalysis (right).

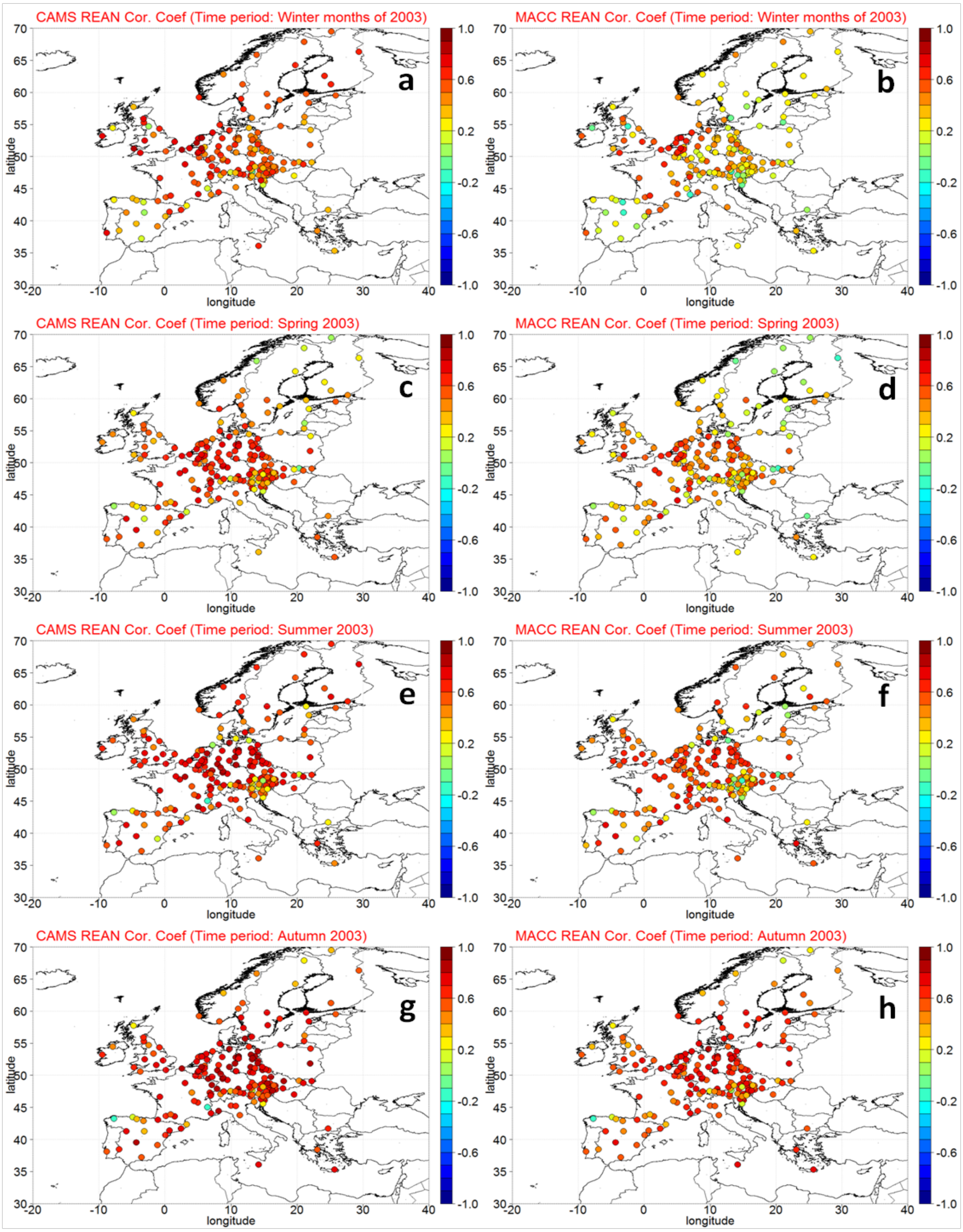

Figure 3.2.3.3. Correlation Coefficients (r) during Winter 2003 1st row, a and b), Spring 2003 (2nd row, c and d), Summer 2003 (3rd row, e and f) and Autumn 2003 (4th row, g and h) for the CAMS reanalysis experiment (left) and the MACC reanalysis (right).

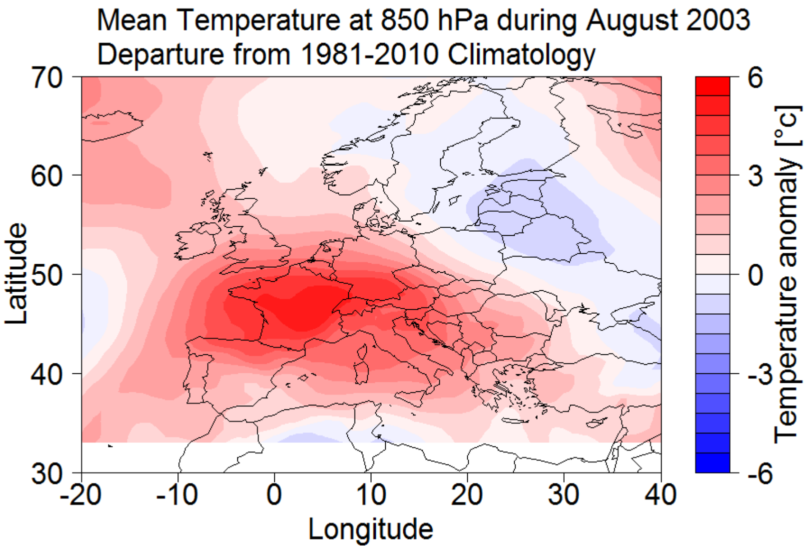

Figure 3.2.3.4. Spatial distribution of the Air temperature anomaly at 850 hPa in August 2003, compared to the 1981-2010 climatology.

Finally the reanalysis performance is validated for the major heat wave over central and northern Europe, during the 1st half of August 2003 (see Figure 3.2.3.4). Figure 3.2.3.5 shows surface ozone times series (observed and modelled) during August 2003 at four stations located in France, Germany and Switzerland where very high ozone concentrations (up to 120 ppb) was observed during 1-14 August. It is evident that although both CAMS reanalysis, CAMS control and MACC reanalysis underestimates ozone picks there is an improvement over the MACC reanalysis by both the CAMS control and the CAMS reanalysis in terms of both biases and correlations.

To summarize we conclude that, although the bias is improving, there is still a seasonal dependence of the bias and MNMB. The amplitude of the seasonality of MNMB is very much reduced in the latitudinal zones of 30°N-40°N as well as for the high altitude stations (stations with altitude higher than 1000 m a.s.l.).

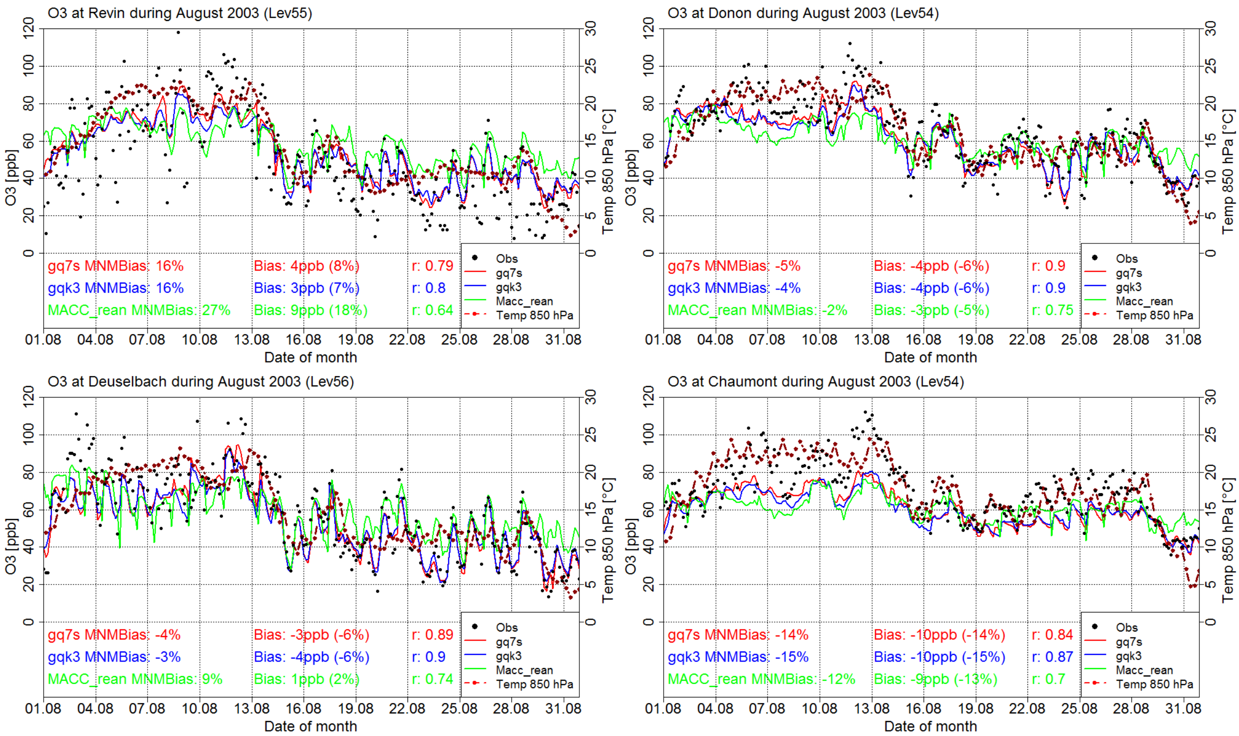

Figure 3.2.3.5. Time series of ozone over Revin, France (49.90°N, 4.63°E, top left), over Donon, France (48.50°N, 7.13°E, top right), over Deuselbach, Germany (49.76°N, 7.05°E, down left), over Chaumont, Switzerland (47.05°N, 6.98°E, down left) for the period of the intense heat wave over Europe 1 August - 31 August. Observations are in black, the CAMS reanalysis is in red, the CAMS control in blue and the MACC reanalysis in green.

3.2.4 Verification with IAGOS ozone observations

Figure 3.2.4.1 presents a time series of ozone from the reanalysis and the control for 2003 at Frankfurt airport where there are almost daily observations. The models compare well with the observations in the surface layer and boundary layer except during the period of the 2003 heat wave, which is discussed in more detail below. In the upper troposphere the models overestimate the amount of ozone, with the control generally performing better. This can be seen more clearly in the monthly averaged profile for February 2003 as shown in Figure 3.2.4.2. In figure 3.2.4.2, the models can be seen to underestimate ozone in the surface layer and boundary layer. Throughout the free troposphere, the reanalysis overestimates ozone, lying just outside the standard deviation of the measurements, whilst the control lies just within. In the upper troposphere the models also overestimate ozone, however here, the reanalysis lies within the standard deviation of the measurements.

In the upper troposphere the control run usually does better than the reanalysis as seen in Figure 3.2.4.3 showing Osaka and New York six months apart. During the winter months, when the tropopause mixing layer is lower, the models have difficulty in capturing the gradient of ozone. In the summer months, the mixing layer is encountered less frequently and hence the models do not need to reproduce the sharp gradient around the tropopause. The better behaviour by the control run over that with assimilation is a result also seen in the operational CAMS forecasts (o-suite), and has been described by Gaudel et al., (2015) in a study based on the MACC reanalysis.

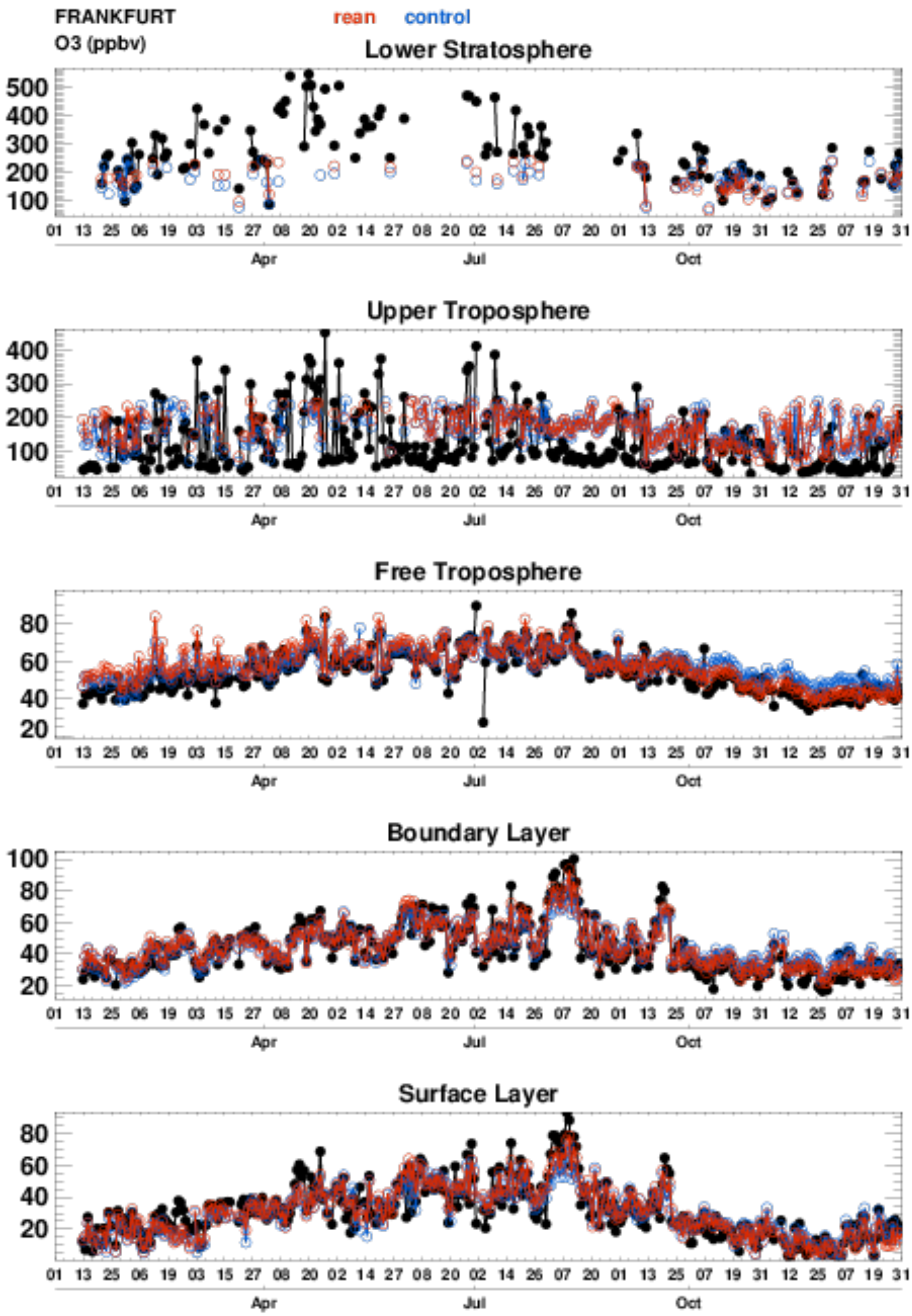

Figure 3.2.4.1. Time series for 2003 of ozone at Frankfurt from IAGOS (MOZAIC) observations in black and for the reanalysis in red and the control run (blue) and reanalysis (red). Units: ppbv.

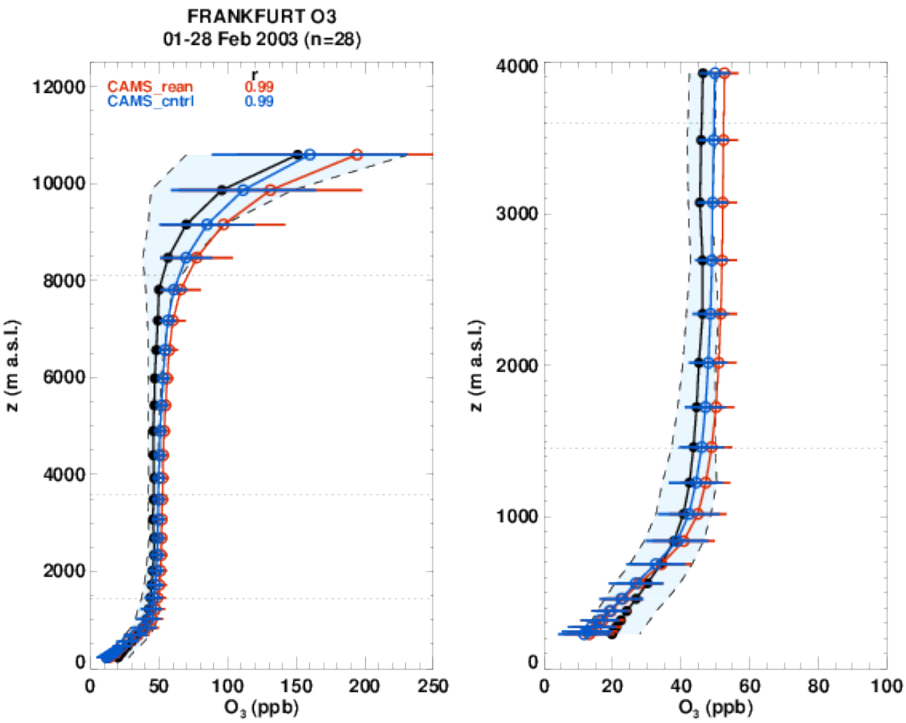

Figure 3.2.4.2. Monthly averaged ozone over Frankfurt for February 2003. The solid black line of the observations and the dashed black line show the standard deviation of the observations.

<u>Heat wave in summer 2003</u>

The main event of 2003 was the major heat wave over northern Europe, concerning particularly the period 2-14 August. The heat wave was studied with IAGOS (MOZAIC) measurements in detail by Tressol et al. (2008). In Figure 3.2.4.4 we show the monthly averaged profile for the period 16 July to 31 August over Frankfurt. All three runs perform similarly. The monthly averaged amount of ozone in the surface and boundary layers during the heat wave as seen by the IAGOS aircraft, is higher than usual, reaching 65 ppbv. The time series in Fig 3.2.4.5 shows that during the heat wave ozone is underestimated in the boundary layer but that there is an improvement over the MACC reanalysis by both the CAMS control and the CAMS reanalysis. In the free troposphere there is little difference among the runs. In the upper troposphere the CAMS reanalysis compares well with the observations until 7 August and thereafter shows an overestimation.

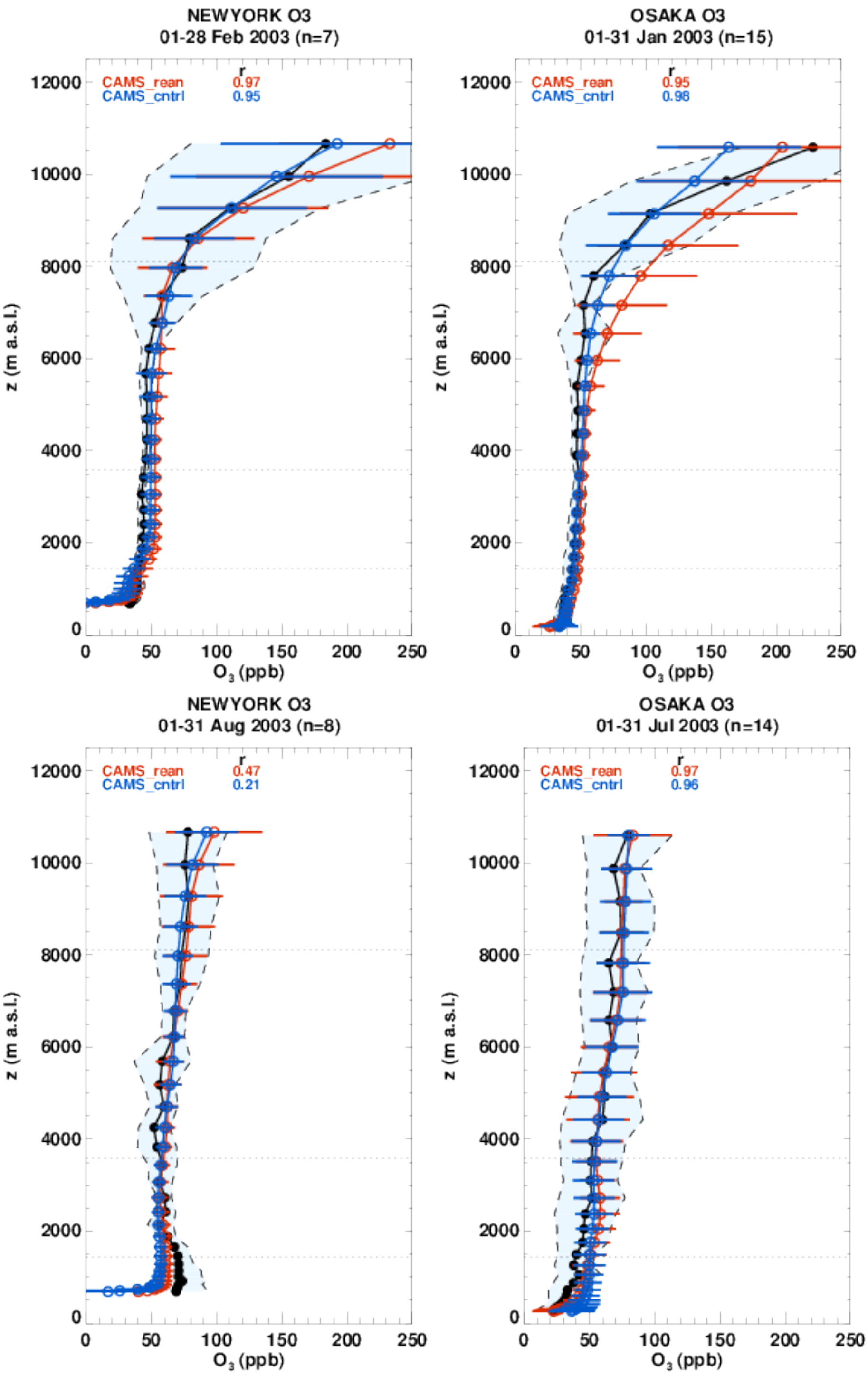

Figure 3.2.4.3. Monthly averaged ozone over Osaka for January and July, and for New York in February and August 2003. The solid black line if the observations and the dashed black line shows the standard deviation of the observations.

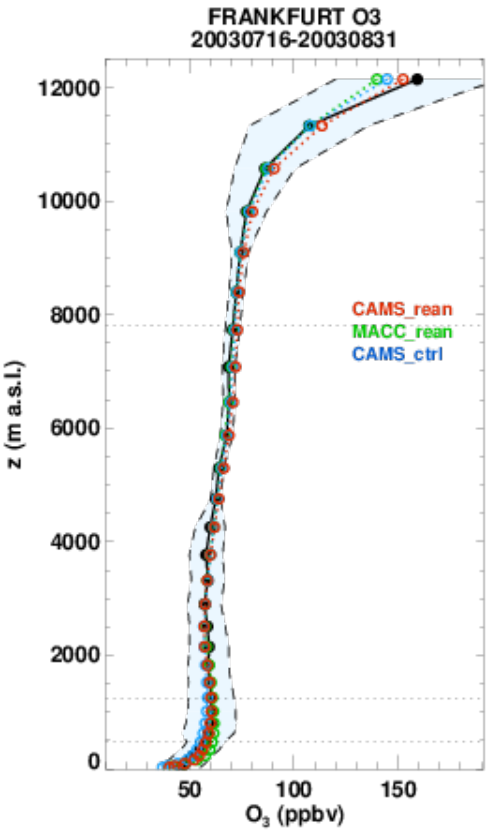

Figure 3.2.4.4. Ozone averaged of the period of the heat wave 16 July-30 August 2003. The CAMS reanalysis is in red, the MACC reanalysis in green and the CAMS control in orange. The solid black line is the observations and the dashed black line shows the standard deviation of the observations.

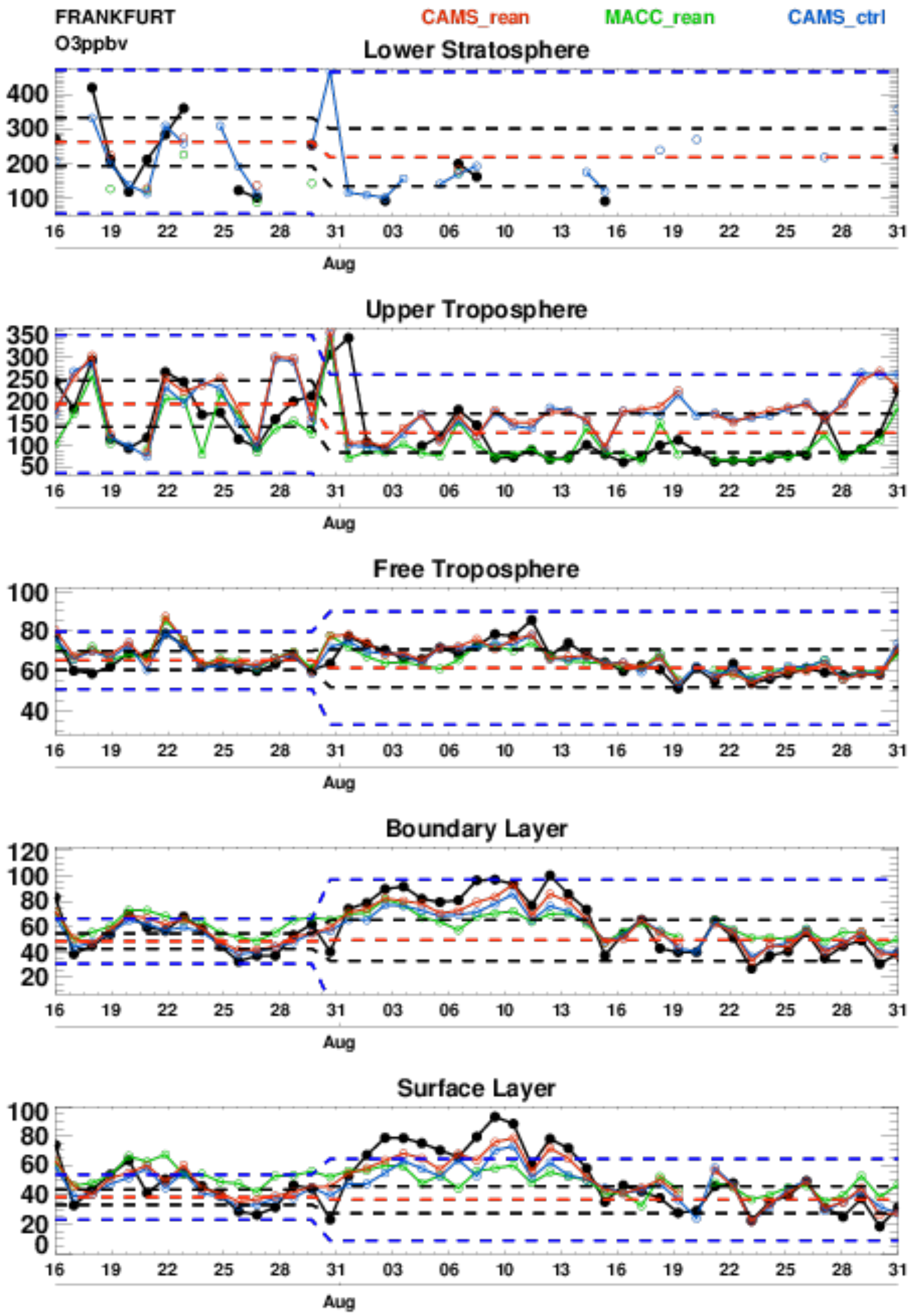

Figure 3.2.4.5. Time series of ozone over Frankfurt for the period of the intense heat wave over Europe 16 July- 31 August. Observations are in black, the CAMS reanalysis is in red, the CAMS control in blue and the MACC reanalysis in green. The red dashed line is the mean of the observations from 2003-2012 the black dashed line is 1 sigma from the mean, and the blue dashed line is 3 sigma from the mean.

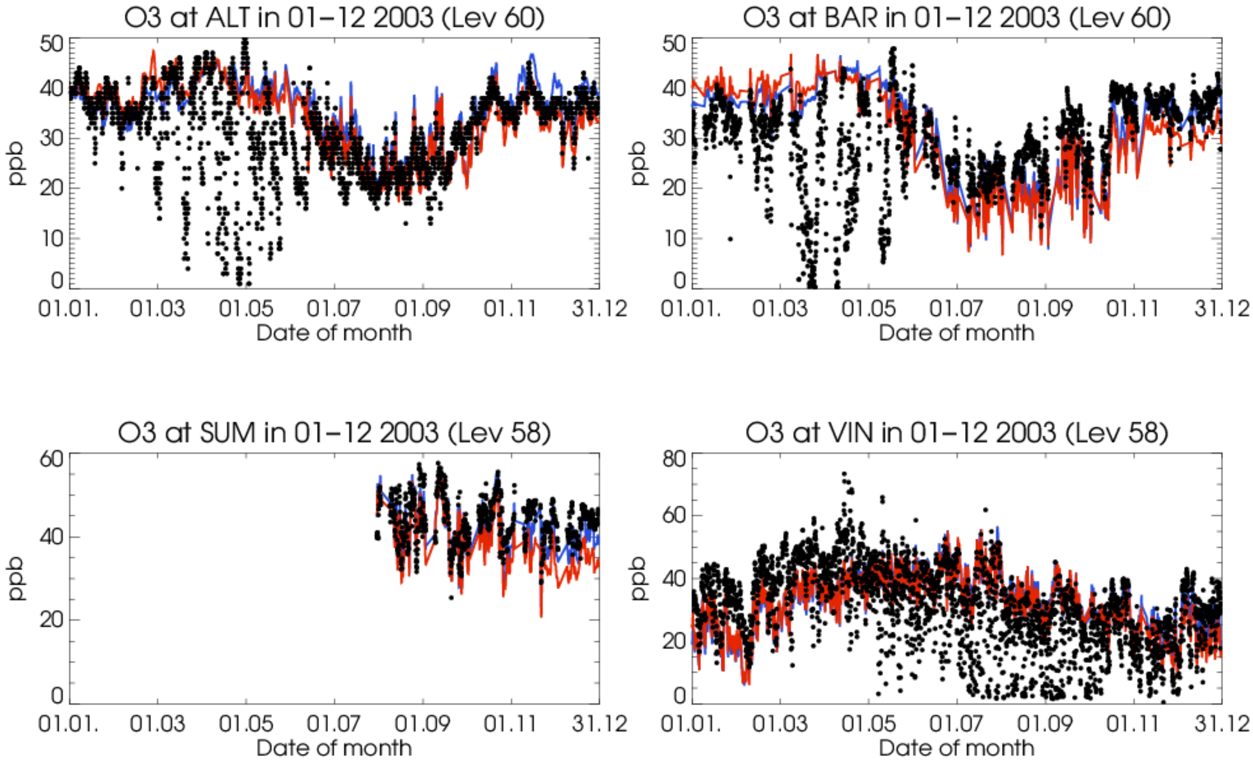

Fig 3.2.5.1: Time series for O_3 in the period 01-12 2003 for GAW stations in the Arctic.

3.2.5 Verification with observations in the Arctic

In the Arctic, O_3 mixing ratios are mostly slightly overestimated between -13 and 3% (calculated over the whole period). This overestimation appears mostly during spring when ozone depletion events are not captured by the model, see Fig.3.2.5.1. During the rest of the season, the model tends to underestimate O_3. The model shows good correlation during the winter period, whereas during spring and summer, correlation is low. The overall correlation is relatively low, due to the ozone depletion events, between 0.16 and 0.69.

The simulated surface O_3 mixing ratios in the Arctic are on average in good agreement with the observations apart from spring ozone depletion events related to halogen chemistry reactions that are not represented in the model simulations. This results in an overestimation during spring while the model tends to underestimate O_3 during fall and winter. Annually the O_3 mixing ratios are slightly overestimated (up to 3%), but at Summit, central Greenland the bias is negative (-13%) since there are only measurements for fall and winter. The model shows good correlation during the winter period, whereas the correlation is low during spring and summer. The overall correlation is relatively low (between 0.16 and 0.69) due to the ozone depletion events. The reanalysis and the control simulations are very similar.

Table 3.3.1.1: List of GAW stations used for the validation of reanalysis CO.

Station	Name	Latitude	Longitude	Altitude
Alert	ALT	82.45	-62.52	210
Cape Point	CPT	-34.35	18.48	230
Fraserdale	FRA	49.88	-81.57	210
Hohenpeissenberg	HPB	47.8	11.02	985
Jungfraujoch	JFJ	46.55	7.98	3578
Kollumerwaard	KOW	53.33	6.28	0
Minamitorishima	MNM	24.28	153.98	8
Payerne	PAY	46.82	6.95	490
Rigi	RIG	46.07	8.45	1031
Ryori	RYO	39.03	141.82	260
Sable Island	SAB	43.93	-60.02	5
Schauinsland	SCH	47.92	7.92	1205
Sonnblick	SNB	47.05	12.95	3106
Yonagunijima	YON	24.47	123.02	30

3.3 Carbon monoxide

3.3.1 Validation with Global Atmosphere Watch (GAW) Surface Observations

In the following, an evaluation of model performance of the CAMS reanalysis and control run has been carried out for the period January to December 2003. GAW hourly data from 14 stations from the World Data Centre for Greenhouse Gases (WDCGG) has been used for model verification, see Table 3.3.1.1.

Surface CO for GAW stations is mostly slightly underestimated (with MNMBs between -30% and 12%) by the reanalysis, see Fig 3.3.1.1 and Fig 3.3.1.3. MNMBs for the control are larger (between -17 and 18%) especially for Cape Point in the Southern Hemisphere.

For most stations the variability of modelled CO mixing ratios is slightly lower in the model than in the observations, see Fig.3.3.1.5. Single stations (RYO, FRA) show large modelled CO spikes (presumably fire signals) that are lacking in the observations, see Fig 3.3.1.8 and 3.3.1.9.

Correlation coefficients (see Fig. 3.3.1.2) are between 0.37 and 0.93 (on average 0.66).

The calculation of MNMBs for each month (Fig. 3.3.1.6) shows that MNMBs are more negative during the northern winter months (Jan, Feb, Nov, Dec) than during the summer. Correlation coefficients (Figs 3.3.1.4 and 3.3.1.7), however, are higher during the winter months. The control run shows very similar results (see time series in Figs 3.3.1.8 to 3.3.1.11), except for Cape Point station in the Southern Hemisphere, Figs. 3.3.1.3 and 3.3.1.11.

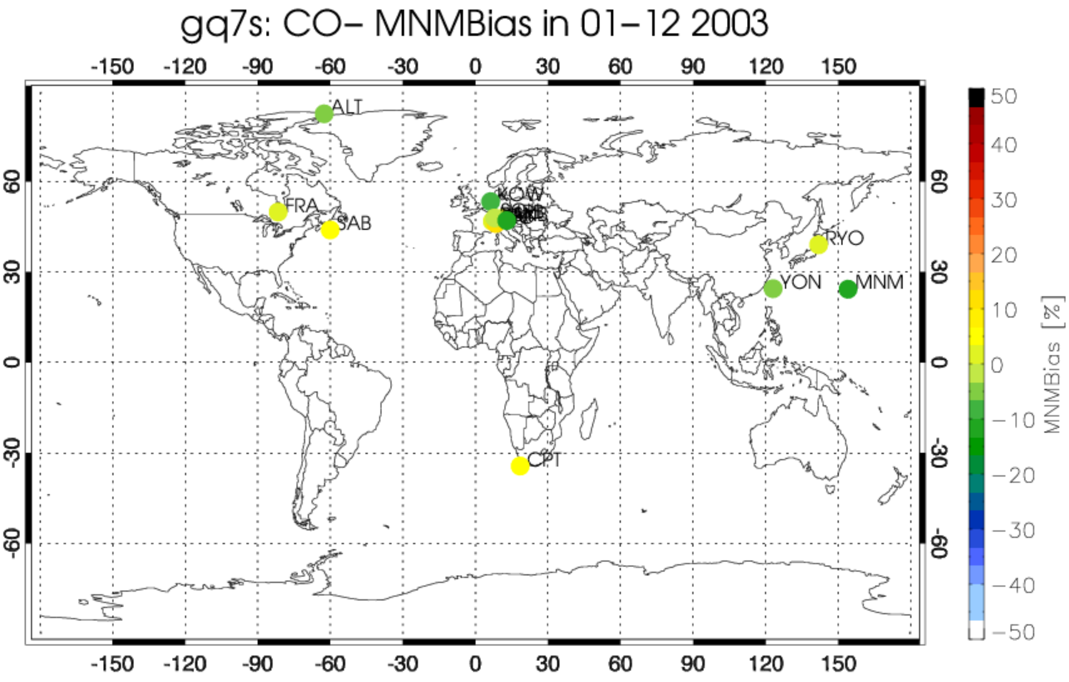

Fig 3.3.1.1: Distribution of overall MNMBs for CO for 2003 for GAW stations

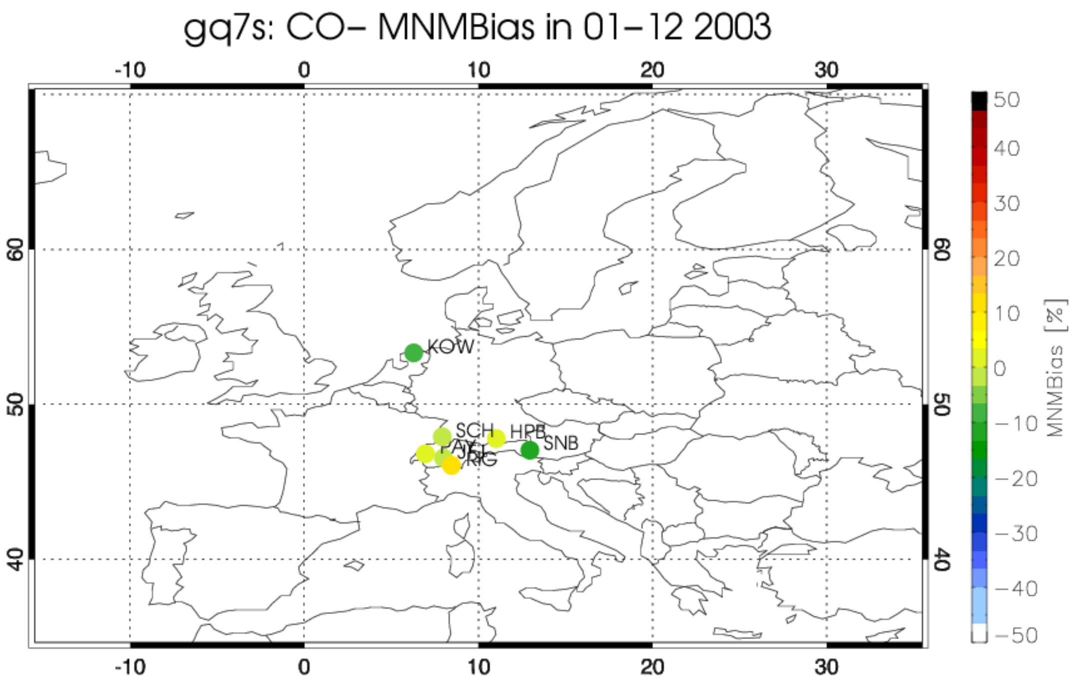

Fig 3.3.1.2: Distribution of overall MNMBs for CO for 2003 for GAW stations in Europe

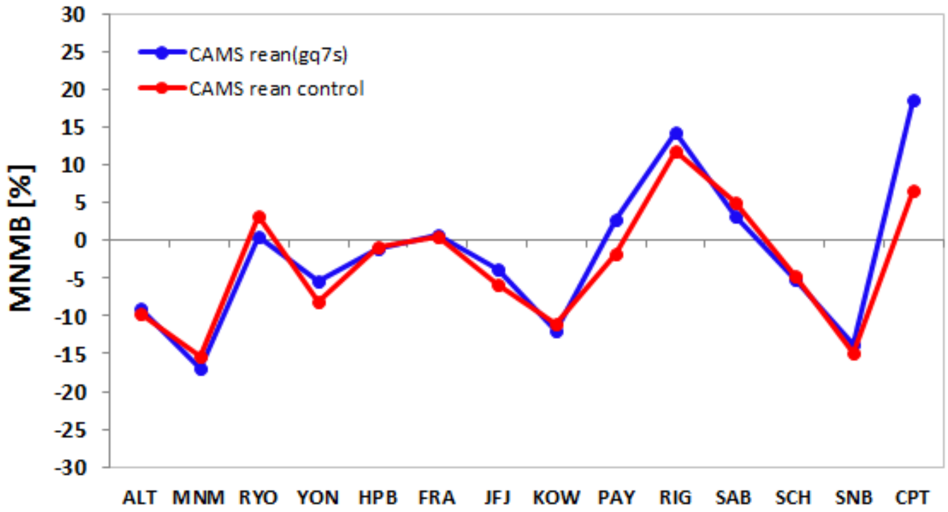

Fig 3.3.1.3: MNMBs for CO for GAW stations

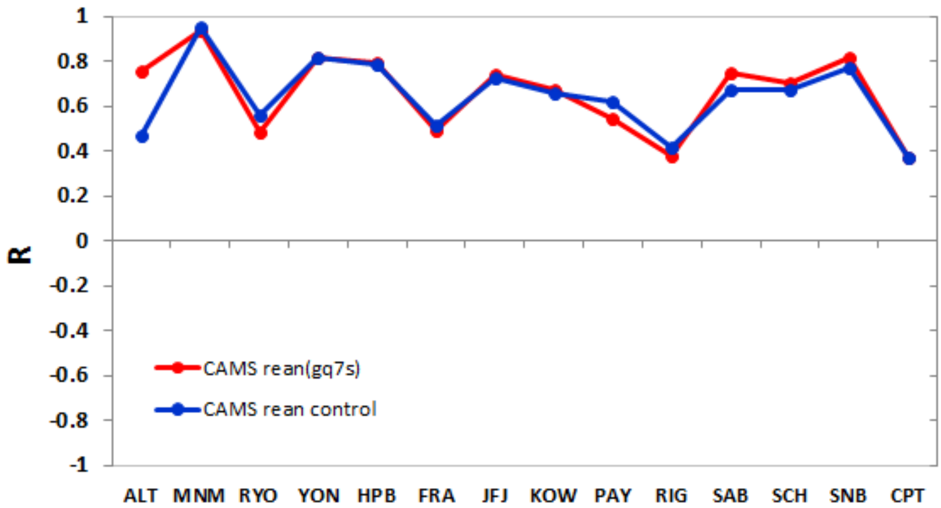

Fig 3.3.1.4: Correlation for CO for GAW stations

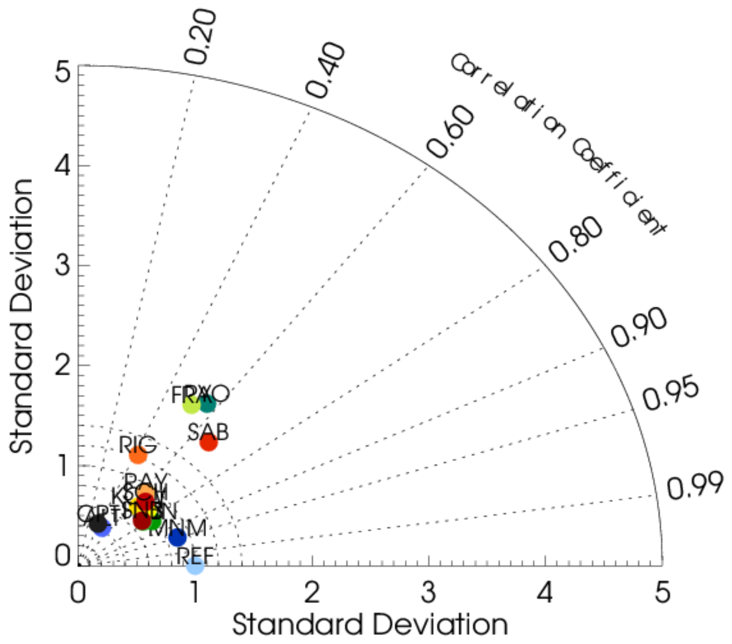

Fig 3.3.1.5: Taylor diagram for CO for GAW stations in the period 01-12 2003

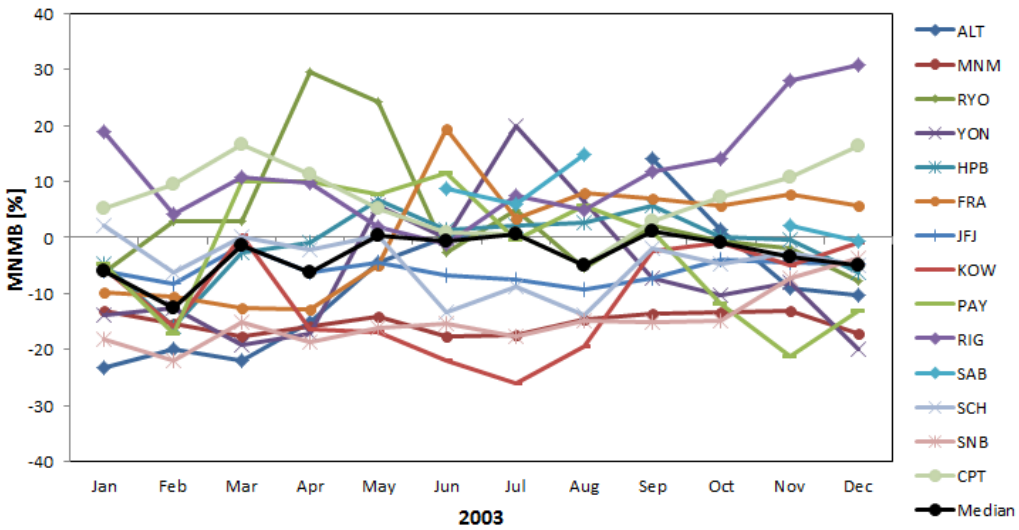

Fig 3.3.1.6: MNMBs calculated for each month for CO for GAW stations

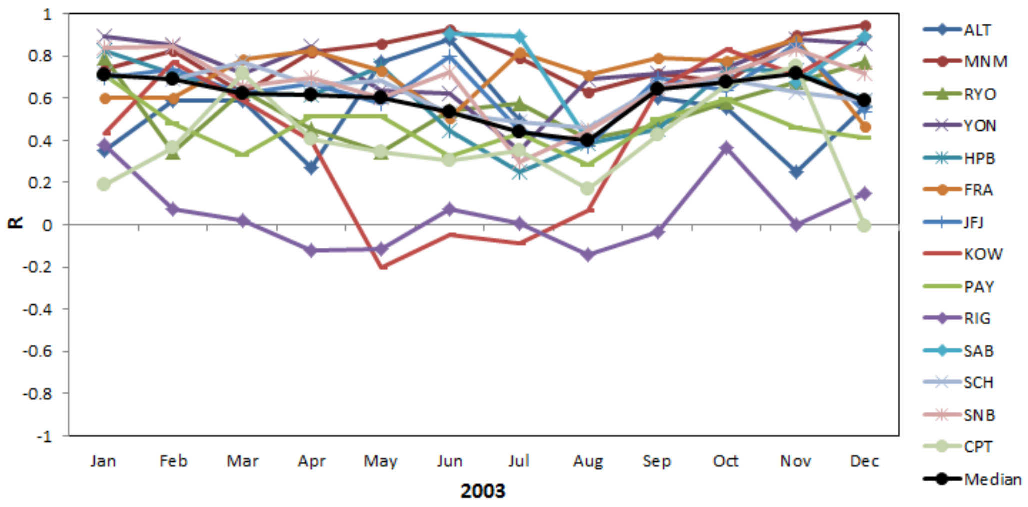

Fig 3.3.1.7: Correlation calculated for each month for CO for GAW stations

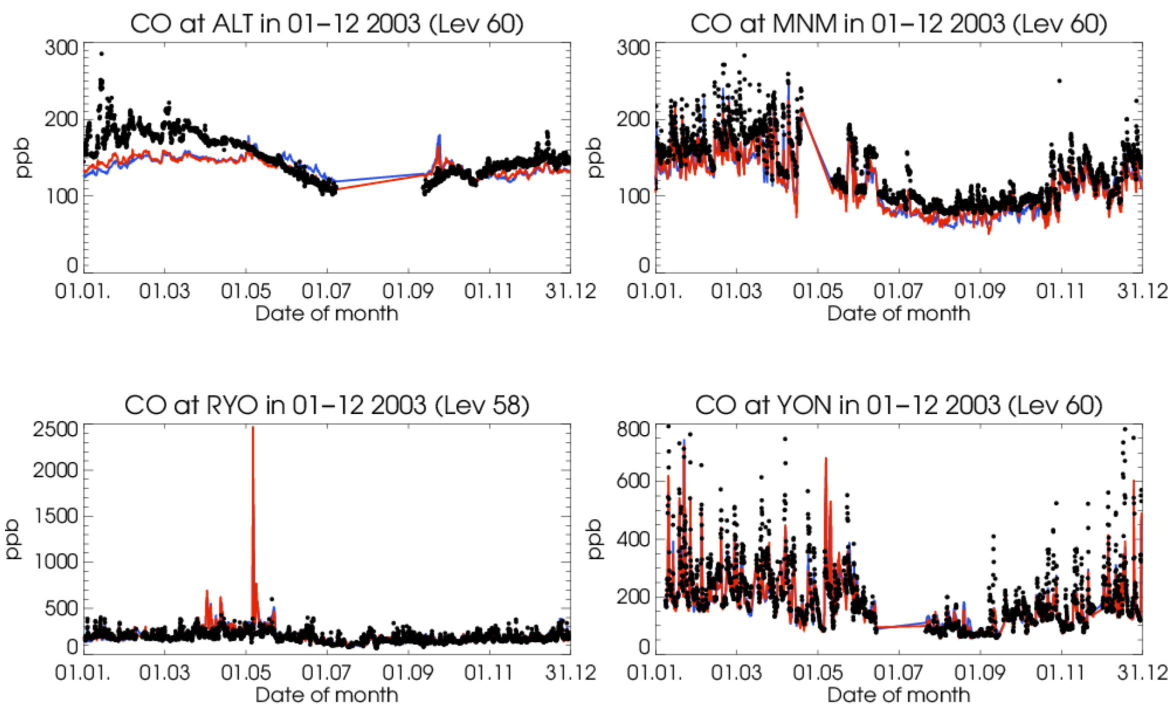

Fig 3.3.1.8: Time series plots for CO for GAW stations Alert (upper left panel), Minamitroshima (upper right panel), Ryori (lower left panel), and Yonagunijima (lower right panel) in the period 01-12 2003 (red: CAMS reanalysis, blue: control)

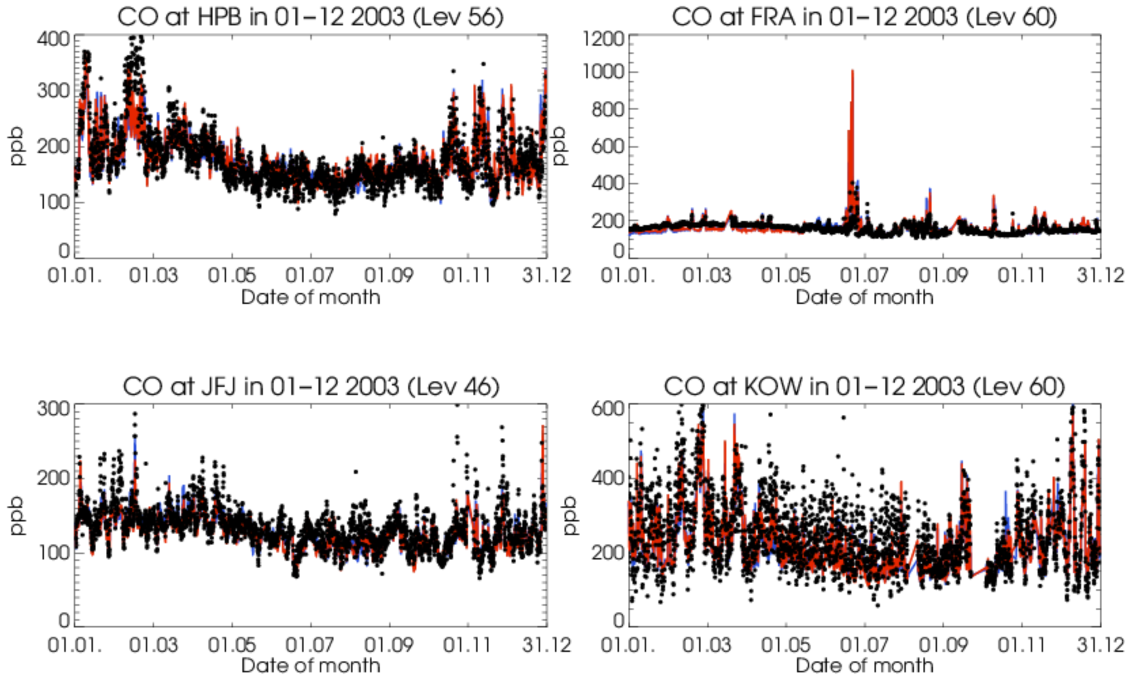

Fig 3.3.1.9: Time series plots for CO for GAW stations Hohenpeissenberg (upper left panel), Fraserdale (upper right panel), Jungfraujoch (lower left panel), and Kollumerwaard (lower right panel) in the period 01-12 2003 (red: CAMS reanalysis, blue: control)

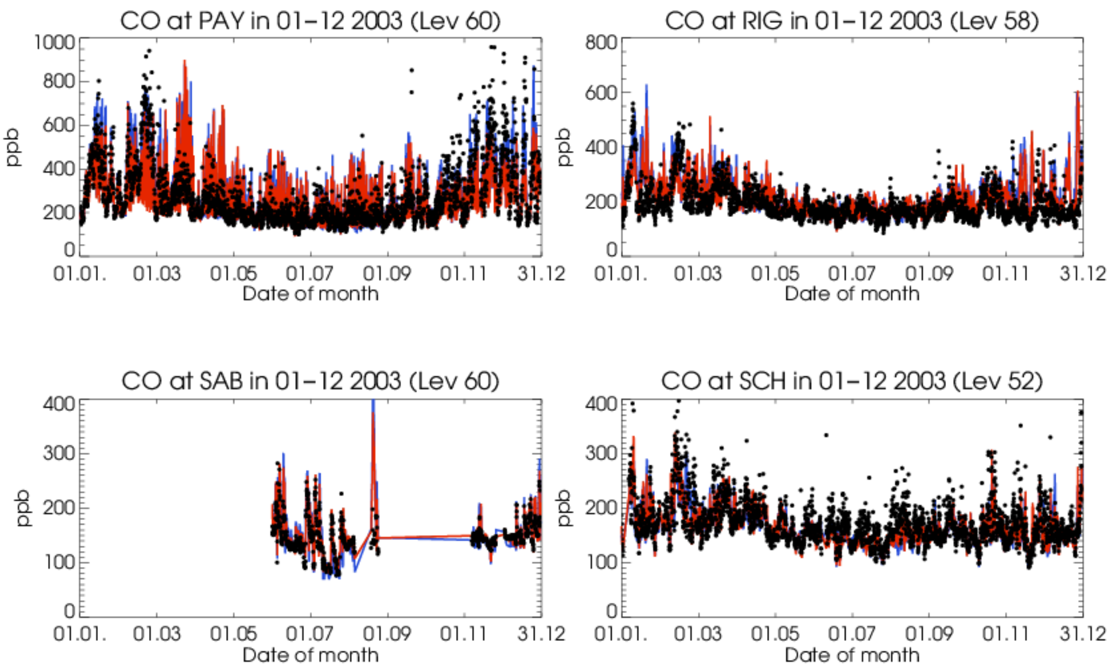

Fig 3.3.1.10: Time series plots for CO for GAW stations Payern (upper left panel), Rigi (upper right panel), and Sable Island (lower left panel), and Schauinsland (lower right panel) in the period 01-12 2003 (red: CAMS reanalysis, blue: control)

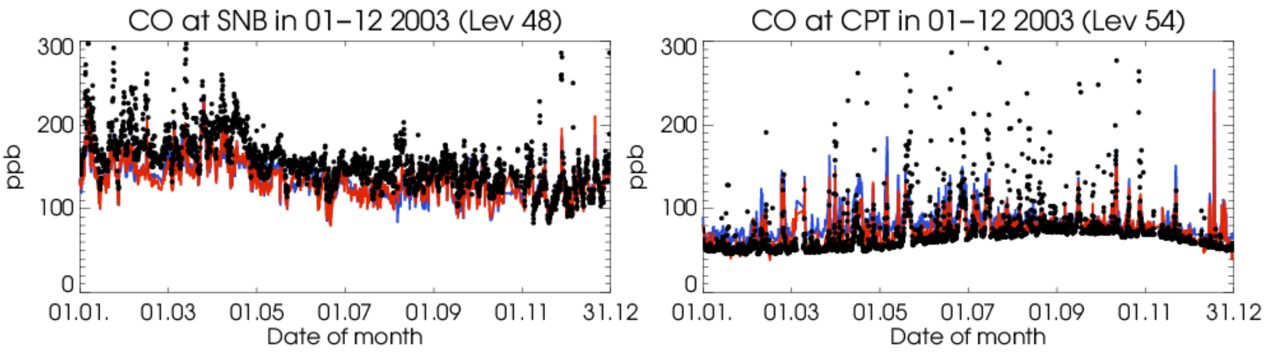

Fig 3.3.1.11: Time series plots for CO for GAW stations Sonnblick (left panel), and Cape Point (right panel) in the period 01-12 2003 (red: CAMS reanalysis, blue: control)

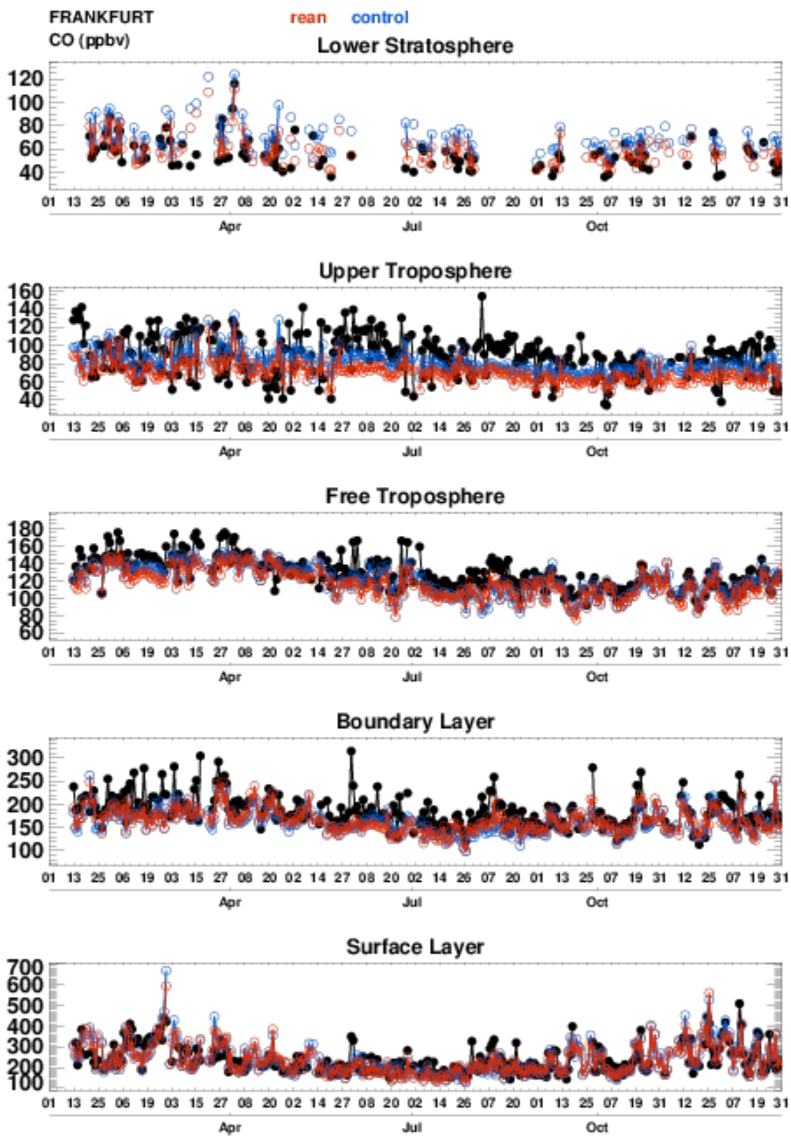

Figure 3.3.2.1. Time series for 2003 of CO at Frankfurt from IAGOS (MOZAIC) observations in black and for the control run (orange) and reanalysis in red.

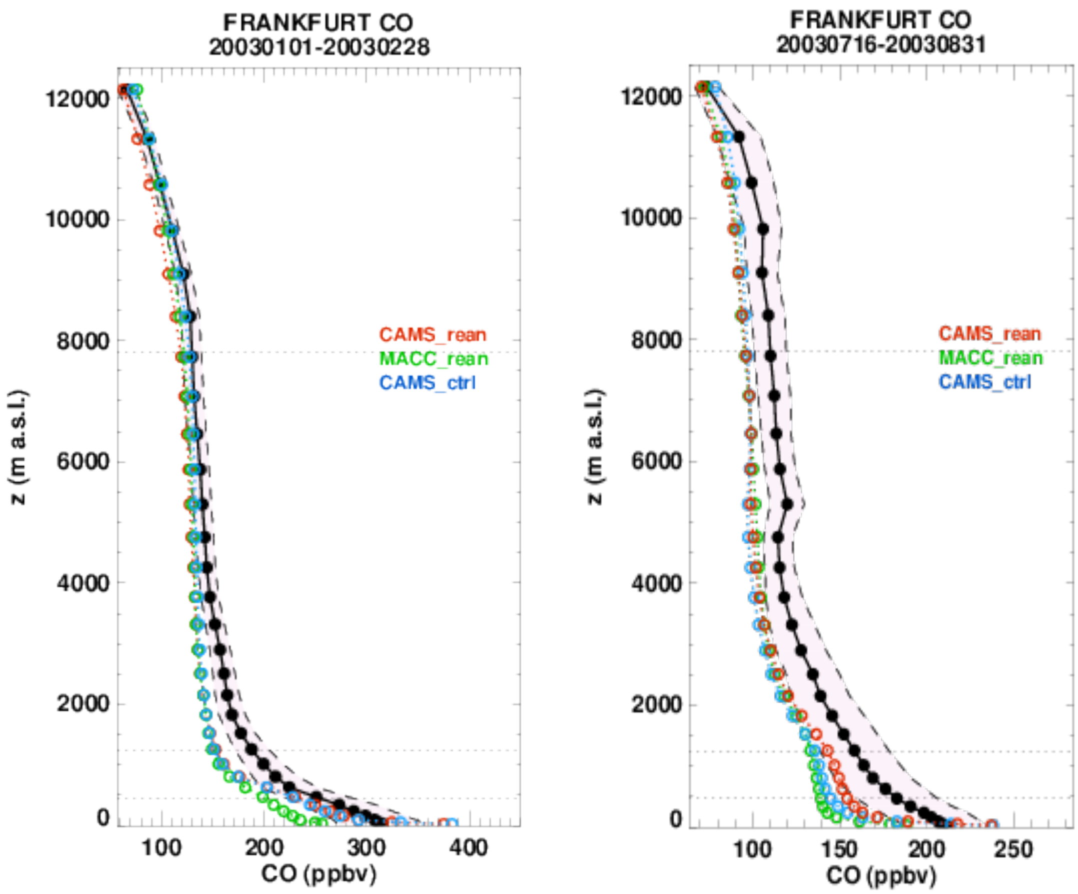

Figure 3.3.2.2. CO over Frankfurt during January and February (left) and July-August (right). The CAMS reanalysis is in red, the MACC reanalysis in green and the CAMS control in orange. The solid black line if the observations and the dashed black line shows the standard deviation of the observations.

3.3.2 IAGOS Aircraft observations

Figure 3.3.2.1 shows the time series for Frankfurt for 2003. In the surface layer, boundary layer and free troposphere the models slightly underestimate CO, with this underestimation being more pronounced in the upper troposphere. The MACC reanalysis systematically underestimated CO in the surface layer, particularly in the northern hemisphere in winter. Stein et al., (2014) attributed this to an underestimation of traffic emissions. The CAMS reanalysis appears to be better at capturing the high concentrations of CO in the surface layer over European airports (Frankfurt, Paris, Vienna, Munich) during winter 2003. (Fig. 3.3.2.3 shows profiles at Frankfurt, Paris, Munich and Vienna). Fig. 3.3.2.2 shows the profile of CO for Frankfurt averaged for January and February. In the surface and boundary layers, there is a clear improvement of the CAMS reanalysis compared with the old MACC reanalysis. In the upper troposphere the three runs behave similarly.

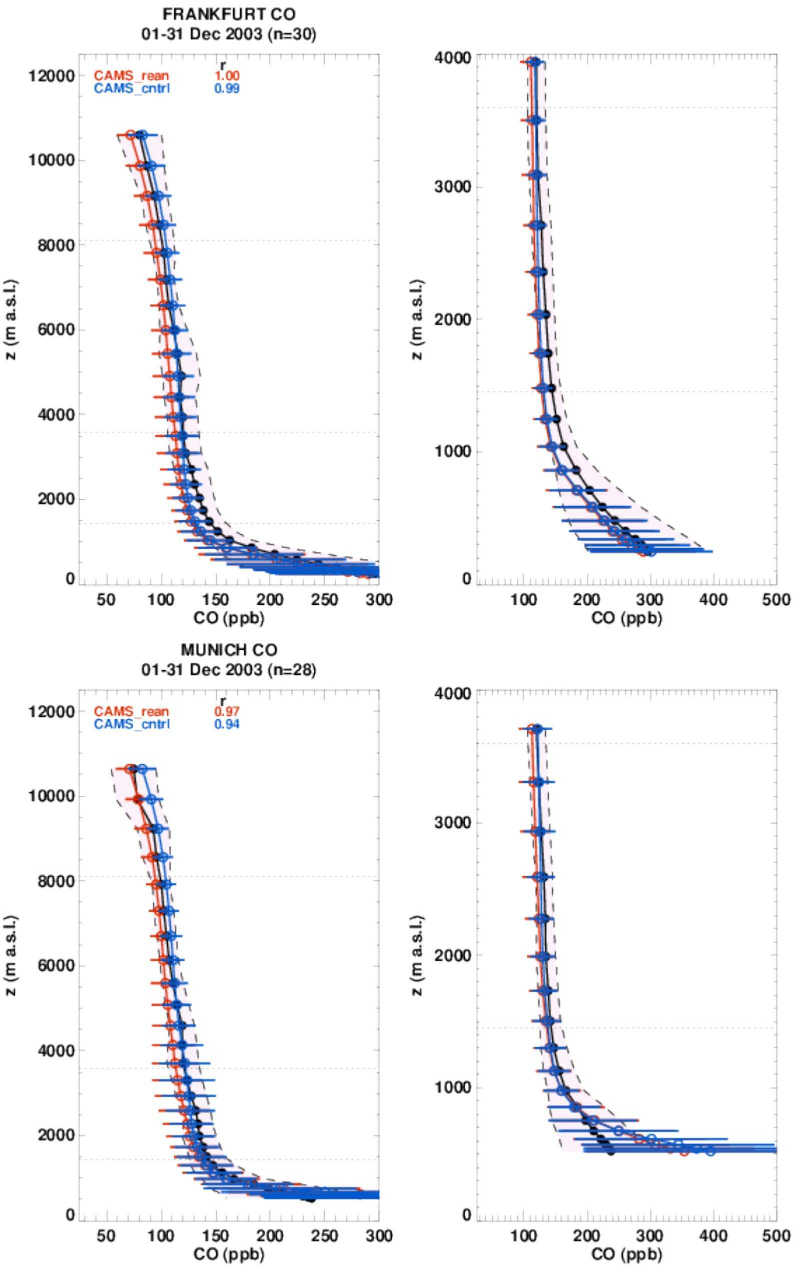

Figure 3.3.2.3-a. Monthly averaged ozone over Frankfurt, and Munich for December 2003. The solid black line if the observations and the dashed black line shows the standard deviation of the observations.

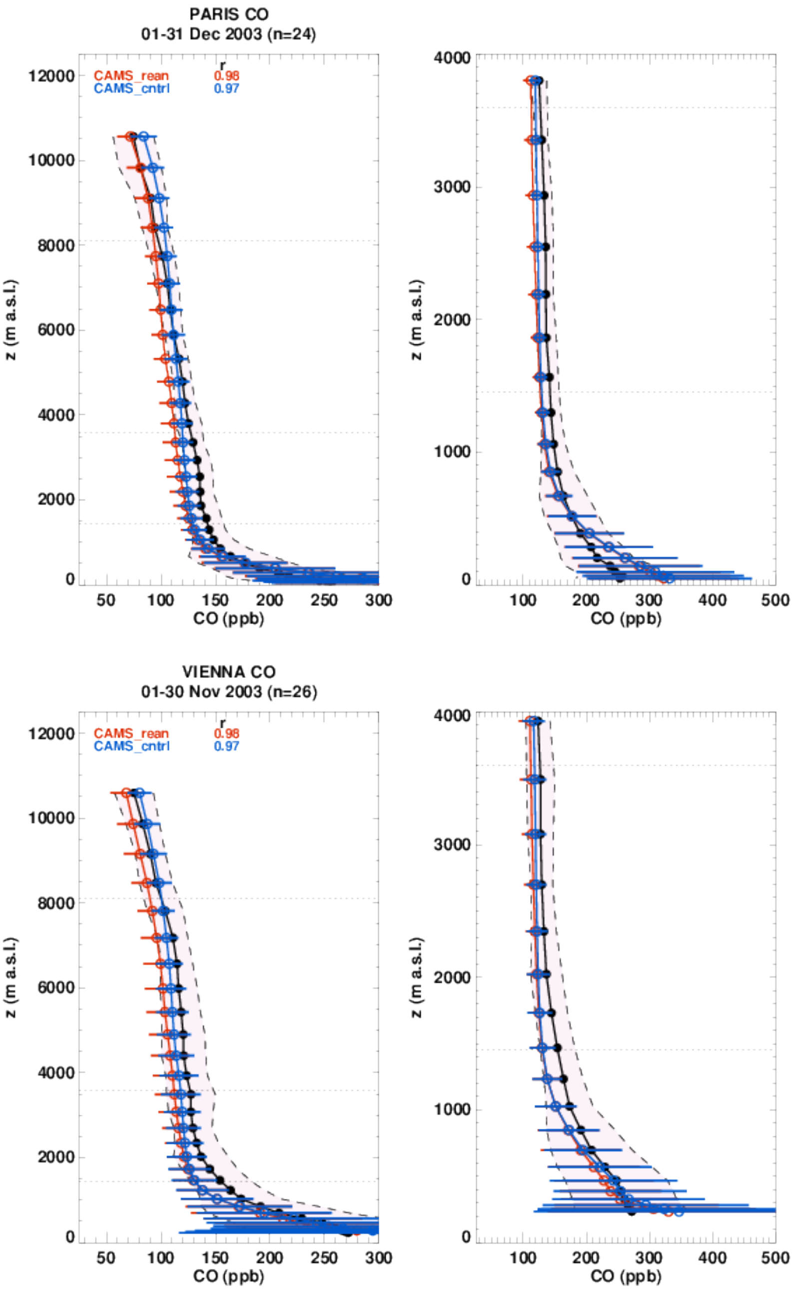

Figure 3.3.2.3-b. Monthly averaged ozone over Paris for December 2003 and Vienna for November 2003. The solid black line if the observations and the dashed black line shows the standard deviation of the observations.

Table 3.3.3.1: Seasonal relative mean bias (MB, %), standard deviation (STD, %) and number of observations used (NOBS) for 2003, compared to NDACC FTIR observations at Kiruna, Zugspitze and Izaña (mean bias and standard deviation in %). The overall uncertainty for the CO measurements is approximately 5%. The table compares the CAMS (rean17) and MACC (rean) reanalysis products.

		JF 2003			MAM			JJA			SON		
		MB	stddev	nobs	MB	stddev	nobs	MB	stddev	nobs	MB	stddev	nobs
rean	Kiruna	-4.93	2.54	21	-8.10	4.38	43	-15.88	4.25	46	-8.18	4.82	32
rean17		-7.14	2.08	21	-9.95	2.91	43	-10.08	2.71	45	-4.46	6.07	32
rean	Zugspitze	-4.20	4.43	237	-2.35	4.52	281	-9.25	4.39	199	-4.39	6.30	285
rean17		-6.52	4.01	237	-3.95	4.68	281	-9.41	6.22	190	-6.68	4.44	285
rean	Izana	-4.14	3.68	11	-8.20	4.46	54	-7.12	4.93	50	-4.22	4.77	36
rean17		-6.03	2.57	11	-8.20	4.26	54	-9.73	4.28	50	-7.27	4.43	36

3.3.3 FTIR tropospheric CO observations, Validation against FTIR observations from the NDACC network

In this section, we compare the CO profiles of the CAMS reanalysis model with FTIR measurements Kiruna (68°N) (left), Zugspitze (47°N) and Izaña (28°N). These ground-based, remote-sensing instruments are sensitive to the CO abundance in the troposphere and lower stratosphere, i.e. between the surface and up to 20 km altitude. Tropospheric CO profiles and columns are validated (up to 10km). A description of the instruments and applied methodologies can be found at http://nors.aeronomie.be. In the table and plots below the MACC-III reanalysis model (rean IFS MOZART) is indicated in green and the reanalysis, experiments gqm5+gq7s in red (rean17).

Table 3.3.3.1 and Fig. 3.3.3.1 show that the day to day variation of the tropospheric columns of CO agree well. All reanalysis models underestimate CO at all three sites with values between 5% to 10%, which is larger than the reported measurement uncertainty range (6%).

- The MACC reanalysis seems to perform better in terms of seasonal biases: only at KIRUNA the CAMS reanalysis agrees better to the observations than the MACC reanalysis.
- The CAMS reanalysis performs slightly better in terms of correlation coefficients calculated for 2003, with R > 0.9 at all three NDACC sites

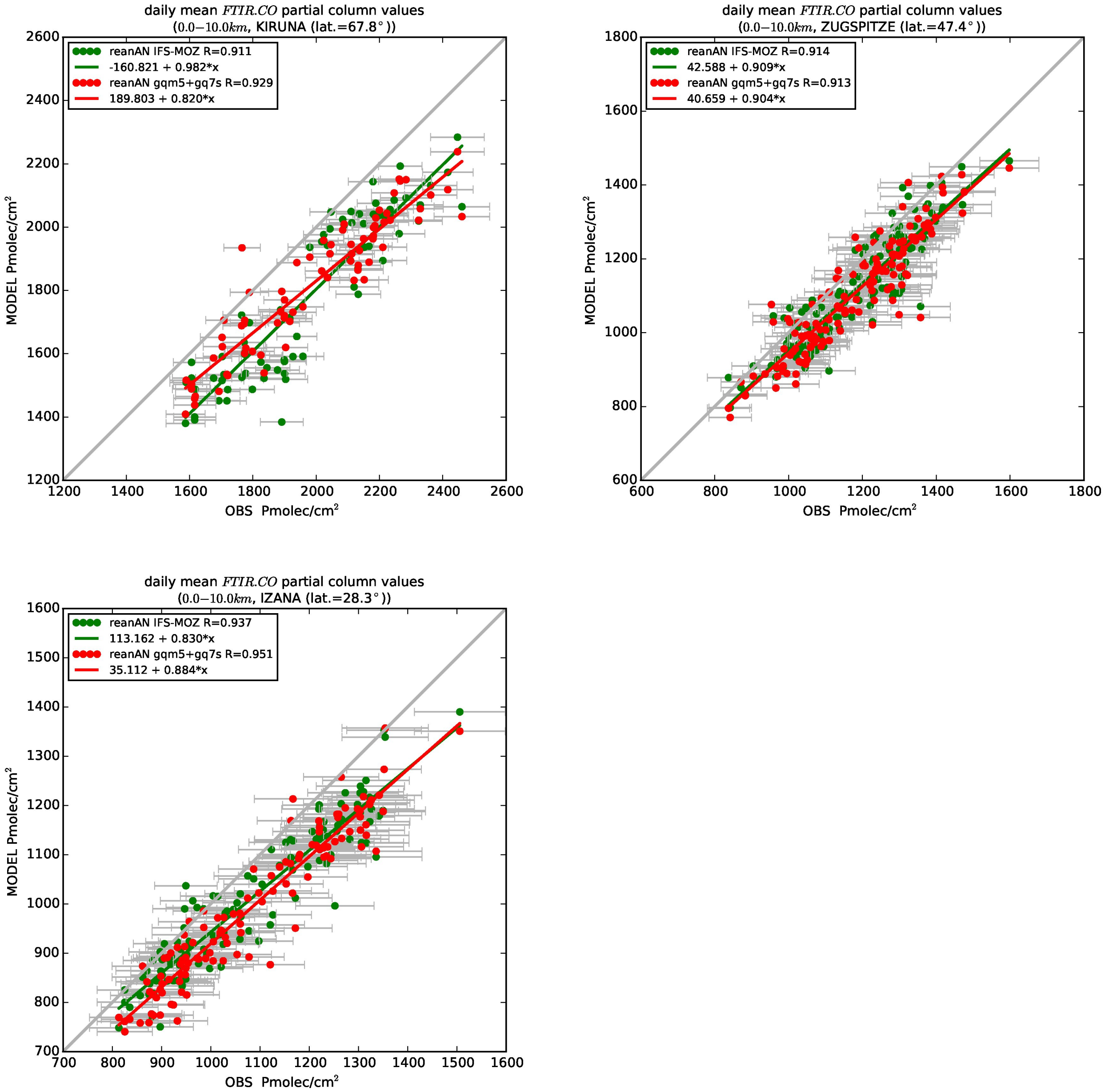

Figure 3.3.3.1: Correlation plots for tropospheric CO columns (till 10km) compared to NDACC FTIR data at Kiruna (68°N) (left), Zugspitze (47°N) and Izaña (28°N) for 2003, for the CAMS reanalysis (red) and MACC reanalysis (green). The correlation coefficients are slightly better compared to the MACC reanalysis (IFS MOZART).

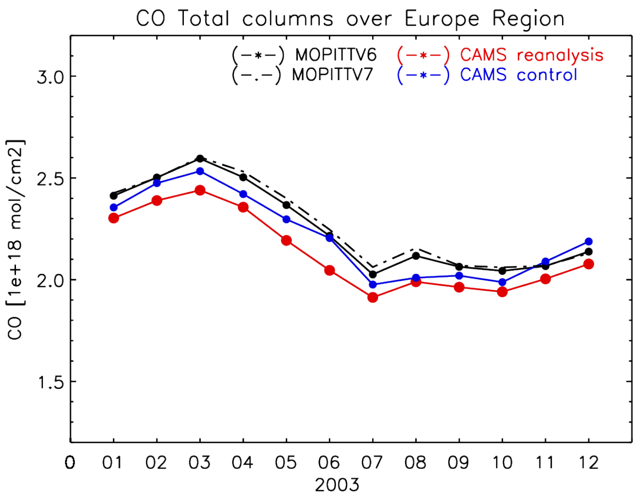
CO Total columns over Europe Region
(-*-) MOPITTV6
(-.-) MOPITTV7
(-*-) CAMS reanalysis
(-*-) CAMS control
CO [1e+18 mol/cm2]
2003

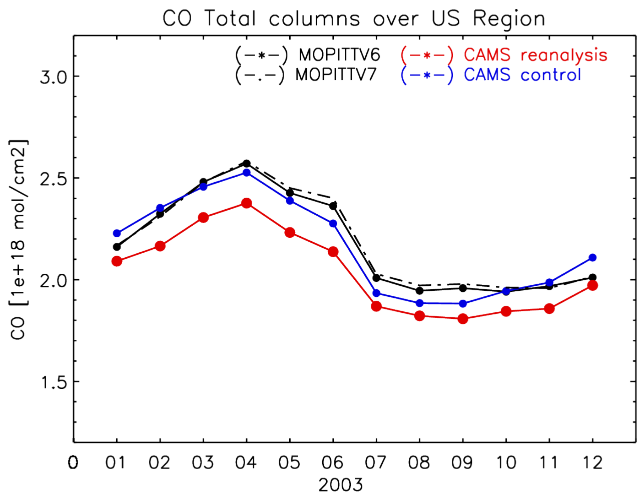
CO Total columns over US Region
(-*-) MOPITTV6
(-.-) MOPITTV7
(-*-) CAMS reanalysis
(-*-) CAMS control
CO [1e+18 mol/cm2]
2003

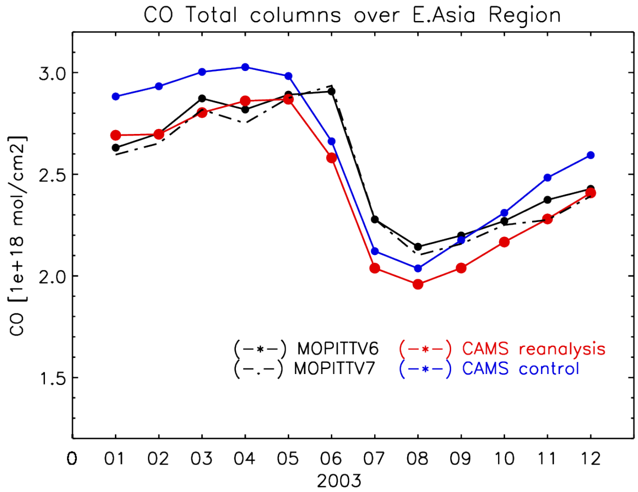
CO Total columns over E.Asia Region
(-*-) MOPITTV6
(-.-) MOPITTV7
(-*-) CAMS reanalysis
(-*-) CAMS control
CO [1e+18 mol/cm2]
2003

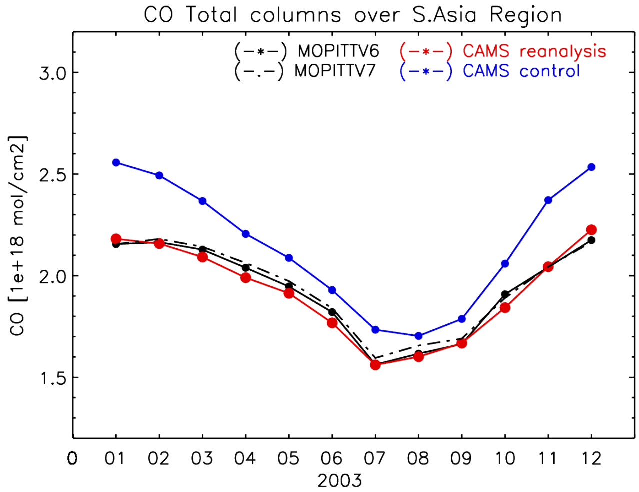
CO Total columns over S.Asia Region
(-*-) MOPITTV6
(-.-) MOPITTV7
(-*-) CAMS reanalysis
(-*-) CAMS control
CO [1e+18 mol/cm2]
2003

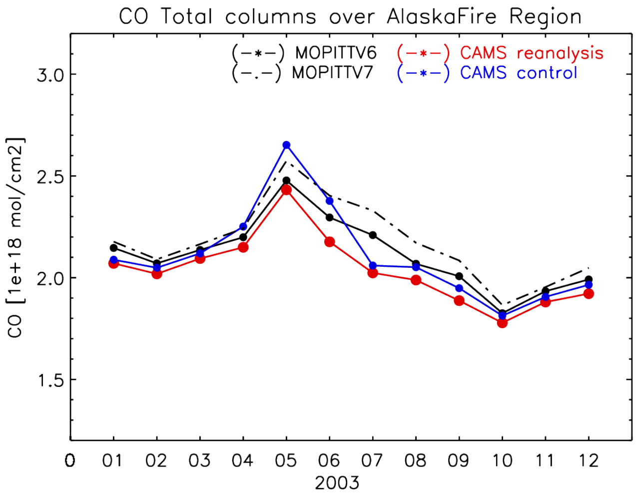
CO Total columns over AlaskaFire Region
(-*-) MOPITTV6
(-.-) MOPITTV7
(-*-) CAMS reanalysis
(-*-) CAMS control
CO [1e+18 mol/cm2]
2003

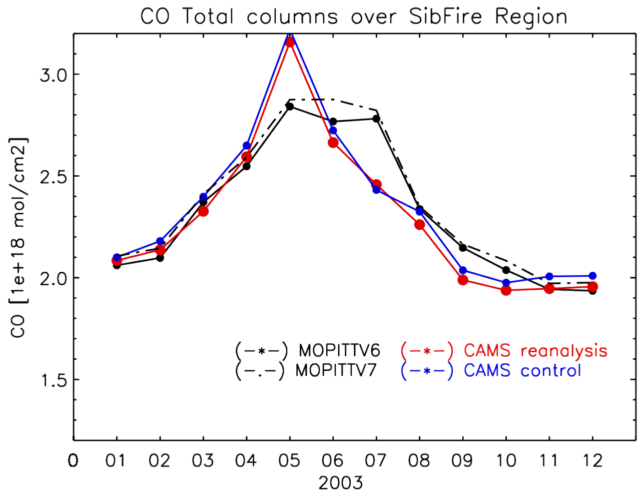
CO Total columns over SibFire Region
(-*-) MOPITTV6
(-.-) MOPITTV7
(-*-) CAMS reanalysis
(-*-) CAMS control
CO [1e+18 mol/cm2]
2003

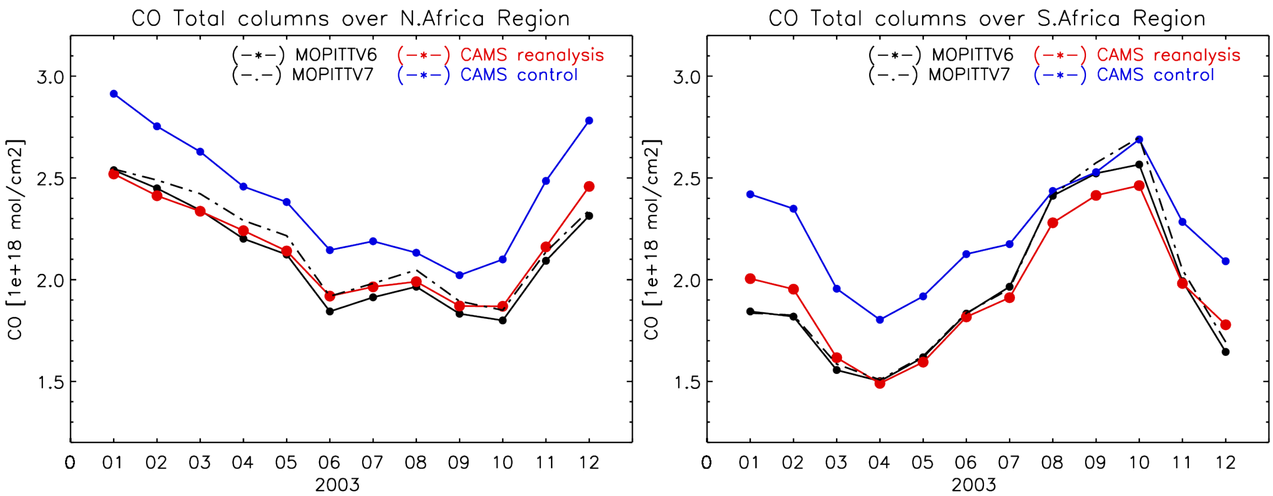

Fig. 3.3.4.1: CO total columns for satellite retrievals (black) MOPITT V6 and V7 and reanalysis data (red) and control run (blue) over selected regions for 2003.

3.3.4 Comparison CAMS reanalysis 2003 with MOPITT v6/v7 CO

Time series of CO total columns from the CAMS 2003 reanalysis and the control run are compared with CO total column retrievals from MOPITT version 6 and version 7 (thermal infrared radiances) (Emmons et. al., 2009) over eight selected regions. For the comparison with MOPITT, the modelled CO concentrations were transformed using MOPITT v6 averaging kernels.

The CO total column seasonality in different regions is well reproduced by the model runs (figure 3.3.4.1). CO total columns are slightly underestimated by the reanalysis model compared to the satellite retrievals in Europe and the US (up to 10%), while the control run is closer to the satellite observations than the reanalysis in these two regions. In East Asia, Alaskan and Siberian fire regions, the CO total columns are slightly underestimated by the reanalysis during June to October (5-10%). One exception is the Siberian fire region, where in May 2003 the CAMS reanalysis is higher than the satellite retrievals by ~15%, while in July 2003 both model runs underestimate the CO total columns by ~15% compared to the MOPITT observations. In both the North and South African Regions, the reanalysis run is in very good agreement with the MOPITT observations, while the control run shows a bias to the reanalysis and observations of ~10%, with the exception of Sep/Oct 2003 in the South African Region, where the reanalysis is slightly underestimating the satellite observations.

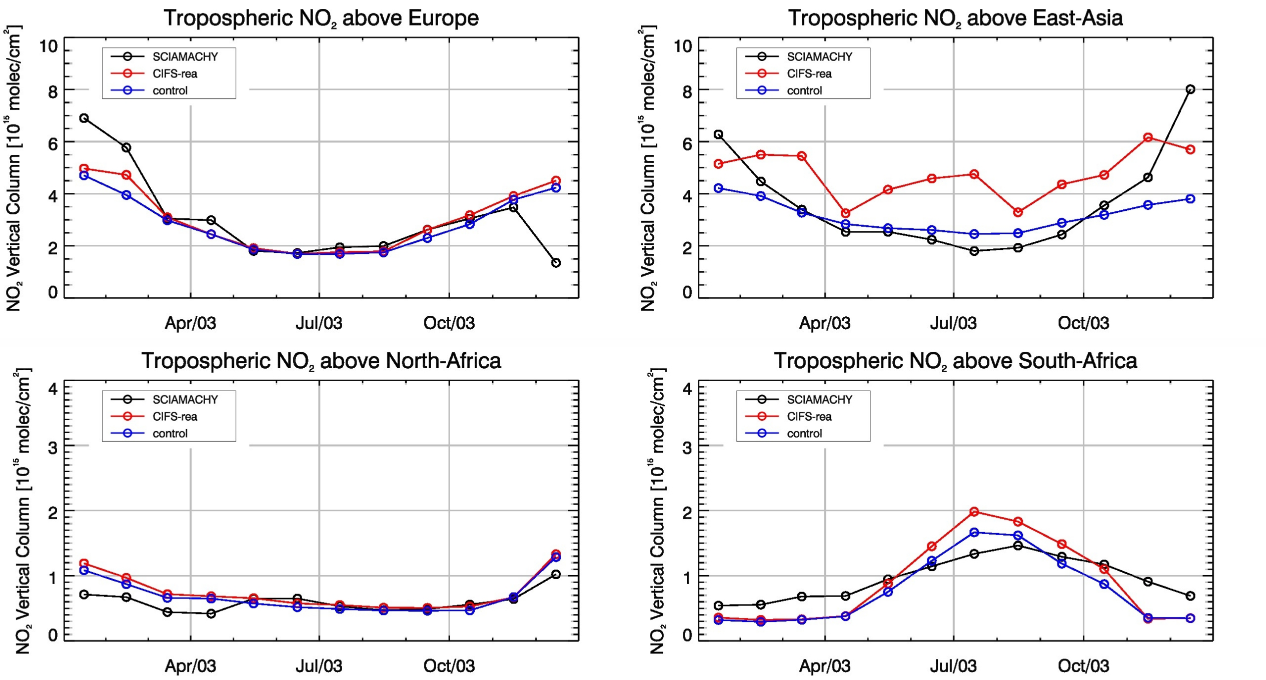

Figure 3.4.1.1. Comparison of time series of tropospheric NO_2 columns from SCIAMACHY to model results over selected regions. Upper panels represent regions dominated by anthropogenic emissions; lower panels represent those dominated by biomass burning.

3.4 Tropospheric nitrogen dioxide

3.4.1 Evaluation against SCIAMACHY NO2 retrievals

In this section, model columns of tropospheric NO_2 are compared to SCIAMACHY/Envisat NO_2 satellite retrievals (IUP-UB v0.7) [Richter et al., 2005]. This satellite data provides excellent coverage in space and time and very good statistics. However, only integrated tropospheric columns are available and the satellite data is always taken at the same local time, roughly 10:00 LT for SCIAMACHY, and at clear sky only. Therefore, model data are vertically integrated, interpolated in time and then sampled to match the satellite data. Specifically, SCIAMACHY data were gridded to model resolution (i.e. 0.75° x 0.75°). Model data were treated with the same reference sector subtraction approach as the satellite data. Uncertainties in NO_2 satellite retrievals are large and depend on the region and season. Winter values in mid and high latitudes are usually associated with larger error margins. As a rough estimate, systematic uncertainties in regions with significant pollution are on the order of 20% – 30%.

The seasonal variation of tropospheric NO_2 in some selected regions is shown in Fig. 3.4.1.1. Apart from East Asia, the seasonality and magnitude of satellite values is reasonably well represented by the CAMS reanalysis for the regions investigated. Over East Asia, the control agrees much better with SCIAMACHY, but underestimates wintertime values leading to an underestimation of the seasonal cycle. The CAMS reanalysis shows a strong variation of values from one month to another over East Asia and completely fails to reproduce the observed seasonality. Satellite observations in winter have larger uncertainties, but inaccuracies in winter NOx emissions and NO_2 lifetime in the highly polluted atmosphere over China could lead to larger model uncertainties during winter. The control is a bit closer to SCIAMACHY over South Africa.

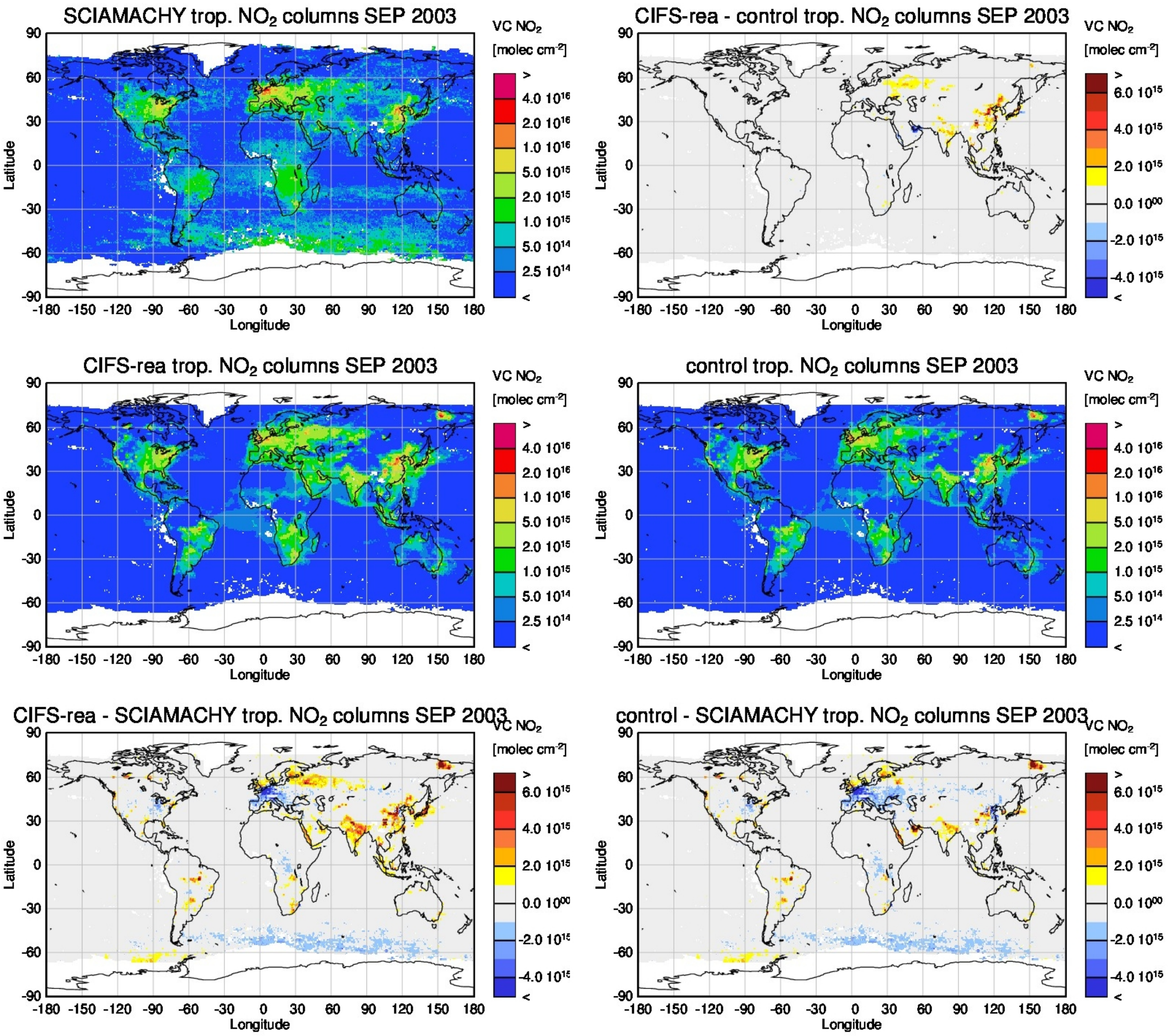

Figure 3.4.1.2. Global map comparisons of satellite retrieved and model simulated tropospheric NO_2 columns [molec. cm^{-2}] for September 2003. The top row shows monthly mean tropospheric NO_2 columns retrieved by SCIAMACHY as well as the difference between the CAMS reanalysis and control, the second row shows the corresponding tropospheric NO_2 columns for model simulated averages. The third row shows differences of monthly means between models and SCIAMACHY. SCIAMACHY data were gridded to model resolution (i.e. 0.75° x 0.75°). Model data were treated with the same reference sector subtraction approach as the satellite data.

Global monthly mean map comparisons (see Fig. 3.4.1.1 for an example for September 2003) show that the overall spatial distribution and magnitude of tropospheric NO_2 is well reproduced by both model runs, indicating that emission patterns and NO_x photochemistry are reasonably represented. Some differences are apparent between observations and simulations, with generally larger shipping signals simulated by the models. Boreal forest fire emissions are overestimated for example over Siberia in May (not shown) and September 2003. This overestimation also shows up for tropospheric HCHO for May 2003, but not for September 2003 (see section 3.6). This may point to uncertainties regarding fire emission factors, with the results indicating a different performance

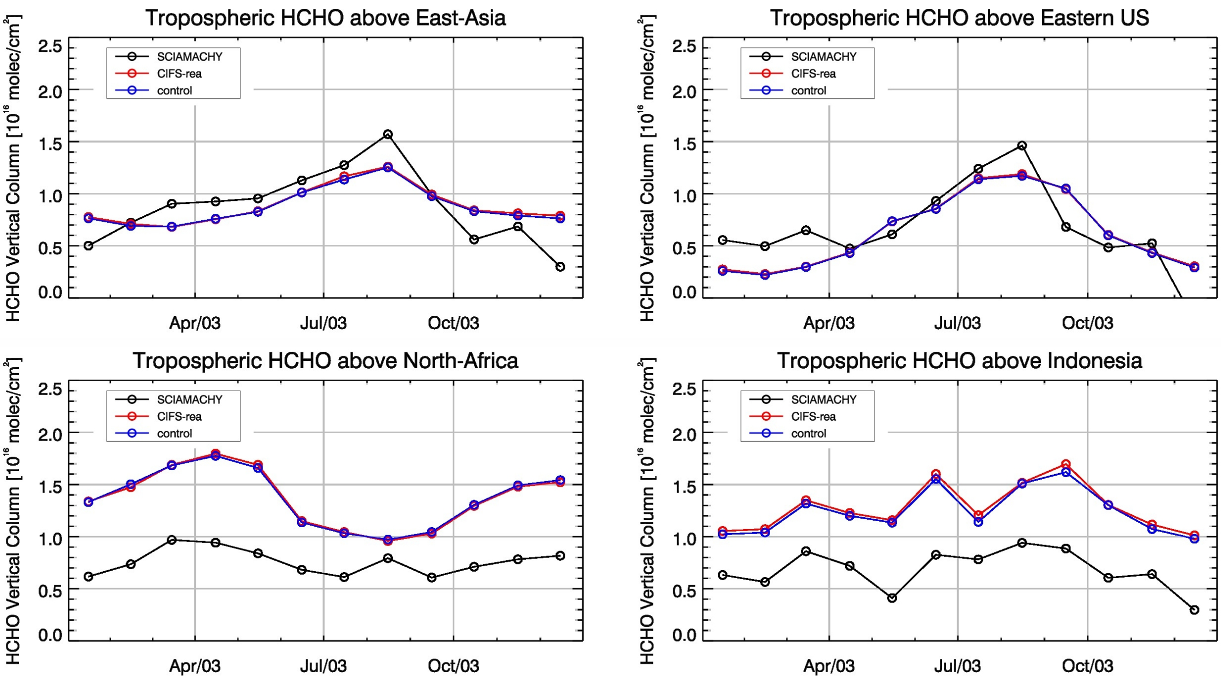

Figure 3.5.1.1. Comparison of time series of tropospheric HCHO columns from SCIAMACHY and model results over selected regions. The regions differ from those used for NO_2 to better focus on HCHO hotspots: East Asia (25-40°N, 110-125°E), Eastern US (30-40°N, 75-90°W), Northern Africa (0-15°N, 15°W-25°E) and Indonesia (5°S-5°N, 100-120°E). Negative satellite retrieved values over Eastern US are due to a lack of data during Northern Hemisphere winter months for this region.

depending on the trace gas, region and season. The reanalysis tends to show larger differences from SCIAMACHY than the control over India and East Asia during the whole season. Both model runs overestimate values over the Persian Gulf and the Red Sea from June to October. Values over anthropogenic pollution hotspots broadly around the Benelux countries and the German Ruhr area tend to be underestimated, while others are overestimated (e.g. Moscow and Helsinki).

3.5 Formaldehyde

3.5.1 Validation against SCIAMACHY HCHO satellite data

In this section, simulations of tropospheric formaldehyde are compared to SCIAMACHY/Envisat HCHO satellite retrievals (IUP-UB v1.0) [Wittrock et al., 2006]. As the retrieval is performed in the UV part of the spectrum where less light is available and the HCHO absorption signal is smaller than that of NO_2, the uncertainty of monthly mean HCHO columns is relatively large (20% – 40%) and both noise and systematic offsets have an influence on the results. However, absolute values and seasonality are retrieved more accurately over HCHO hotspots.

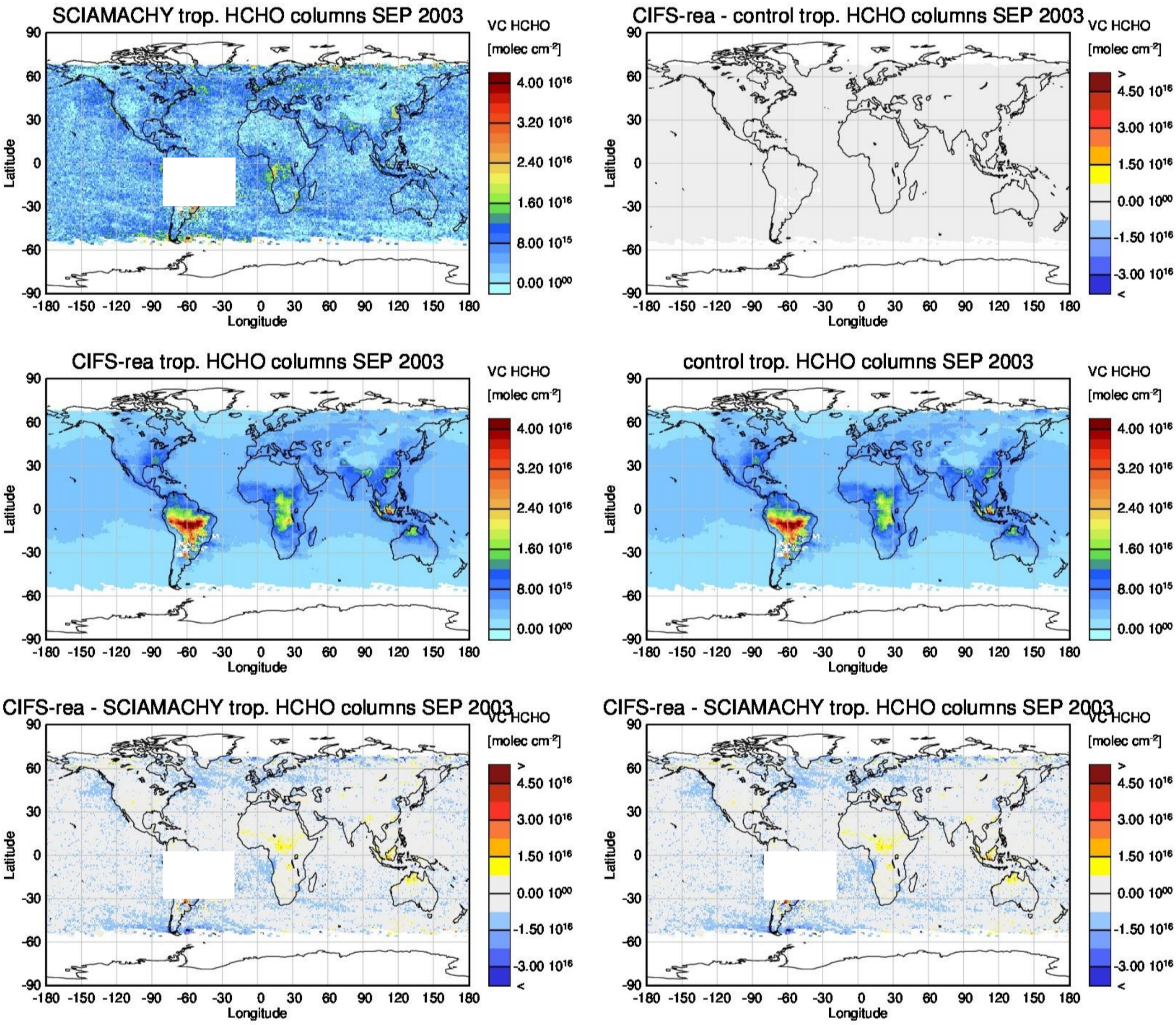

Figure 3.5.1.2. Global map comparisons of satellite retrieved and model simulated tropospheric HCHO columns [molec cm-2] for September 2003. The top row shows monthly mean tropospheric HCHO columns retrieved by SCIAMCHAY, the second row shows the same but for model simulated averages. The third row shows differences of monthly means between models and SCIAMACHY. SCIAMACHY data were gridded to model resolution (i.e. 0.75° x 0.75°). Model data were treated with the same reference sector subtraction approach as the satellite data. Satellite retrieved values in the region of the South Atlantic anomaly are not valid and therefore masked out (white boxes in all images except those which show model results only).

The time series in Fig. 3.5.1.1 show different cases for HCHO: regions dominated by biogenic emissions with some anthropogenic input (East Asia, Eastern US) and regions with both biogenic and pyrogenic sources (North-Africa and Indonesia). The CAMS reanalysis reproduces satellite observations for East Asia and Eastern US with respect to absolute values and seasonality. The reanalysis shows a positive offset compared to satellite retrievals for North Africa and Indonesia, while the seasonality is in agreement with the retrievals. It is not clear if this is due to a low bias in the satellite data or to a model overestimation of HCHO in these regions. There is almost no

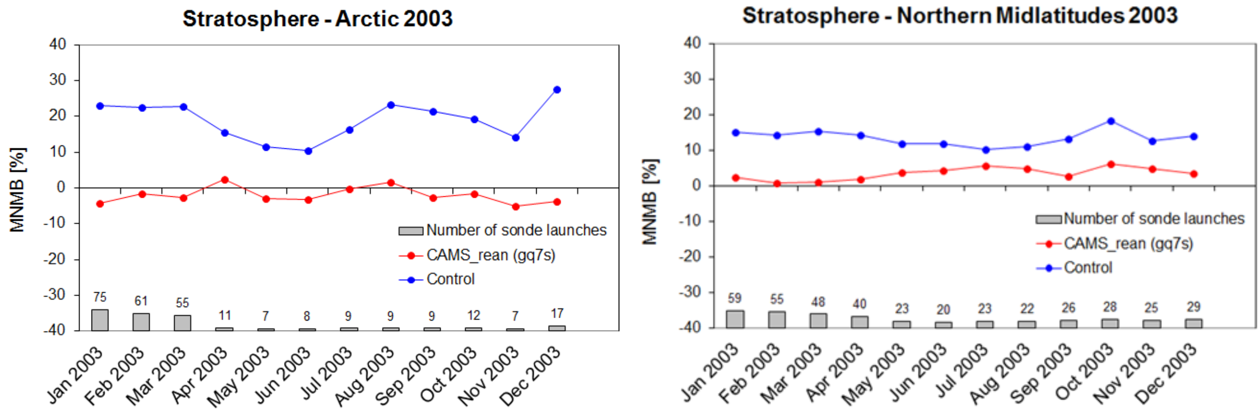

Figure 3.6.1.1: Comparisons with ozone sondes: MNMBs over the Arctic and Northern midlatitudes

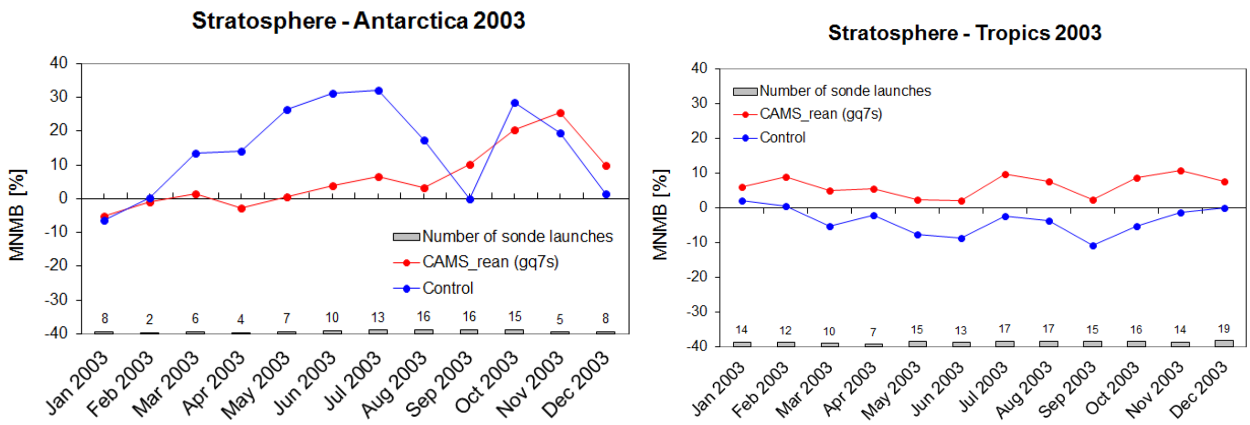

Figure 3.6.1.2: Comparisons with ozone sondes: MNMBs over Antarctica and the Tropics

difference between the reanalysis and the control for all regions, except for Indonesia where the control shows slightly lower values compared to the reanalysis.

Global monthly mean map comparisons (see Fig. 3.5.1.2 example for September 2003) show that the magnitude of oceanic and continental background values and the overall spatial distribution are well represented by the reanalysis and control. Compared to SCIAMACHY satellite retrievals, there is an overestimation of values for Central Africa during the whole season as well as Northern Australia during autumn and winter. Values over Europe are underestimated during spring, and there is an overestimation of values for boreal forest fires e.g. for May 2003 over Siberia (not shown). While values over boreal forest fires over Siberia are overestimated for tropospheric NO_2 for September 2003 (see section 3.5), this overestimation does not show up for HCHO for this month. This may point to uncertainties regarding fire emission factors, with the results indicating a different performance depending on the trace gas, region and season.

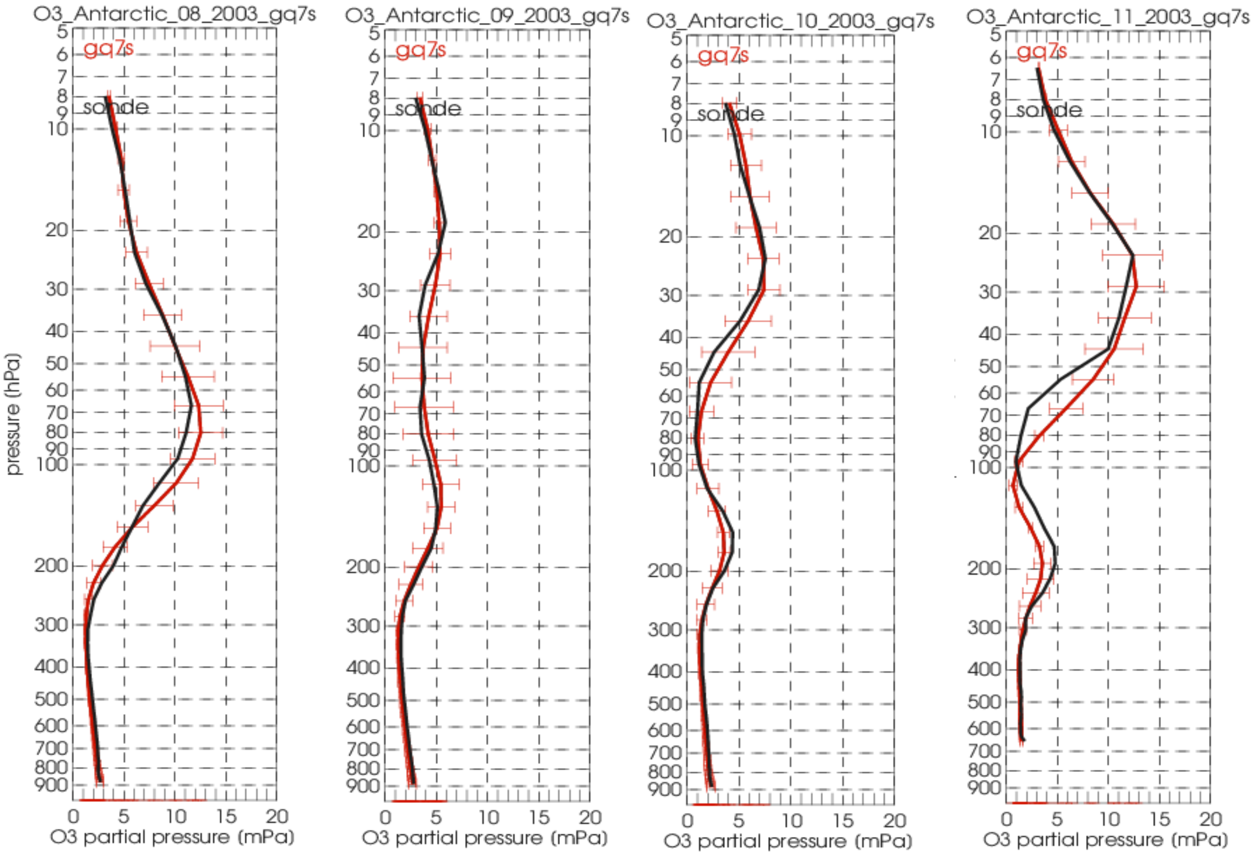

Figure 3.6.1.3: Mean profiles for Aug, Sep, Oct and Nov 2003 over Antarctica (monthly mean of soundings of the stations Neumayer and South Pole)

3.6 Stratospheric ozone

3.6.1 Validation against ozone sondes

In what follows, we present the results of the stratospheric ozone evaluation against ozone soundings from the NDACC, WOUDC, NILU and SHADOZ databases. The sondes have a precision of 3-5% (~10% in the troposphere for Brewer Mast) and an uncertainty of 5-10%. For further details see Cammas et al. (2009), Deshler et al. (2008) and Smit et al (2007). Model profiles of the reanalysis are compared to balloon sondes measurement data of 44 stations for the period January-December 2003. The validation covers the vertical range between 90 and 10hPa, (for the Tropics 60 and 10hPa). A description of the applied methodologies and a map with the sounding stations can be found in Eskes et al. (2016).

Over the over the **Northern Midlatitudes** O_3 partial pressures are reproduced correctly with MNMBs between 1 and 6%, see Fig.3.6.1.1. Over the **Arctic**, O_3 partial pressures are mostly slightly underestimated (MNMBs are between -5 and 2%). Over the **Tropics**, stratospheric Ozone is slightly overestimated throughout 2003 (MNMBs between 2 and 11%). Over **Antarctica**, MNMBs are ±6%, except during the ozone hole season, where MNMBs reach up to 25%. Stratospheric ozone is overestimated especially during October/November between 90-30 hPa, see Fig. 3.6.1.2 (left panel) and Fig. 3.6.1.3.

Table 3.6.2.1: Seasonal relative mean bias (MB, %, (M-O)/O), standard deviation (STD, %) of the partial (upper stratospheric 25km – 65km) ozone column for the considered period and number of observations used (NOBS), compared to NDACC microwave observations at Bern, Mauna Loa and Lauder (mean bias and standard deviation in %). Numbers are provided for both the CAMS and MACC reanalyses. The smallest bias is indicated in colour.

		JF 2003			MAM			JJA			SON		
		MB	stddev	nobs	MB	stddev	nobs	MB	stddev	nobs	MB	stddev	nobs
MACC	Bern	4.88	3.47	23	14.22	8.85	16	8.51	4.69	62	8.15	4.66	54
CAMS		-0.94	4.55	23	11.36	7.78	16	6.81	4.62	60	5.85	4.23	54
MACC	Mauna	0.17	4.39	5	-0.79	3.22	7	2.78	1.55	4	1.50	4.34	7
CAMS		-8.26	2.64	5	-6.69	3.22	7	-4.24	1.46	4	-6.23	3.89	7
MACC	Lauder	-8.14	3.71	17	0.22	4.54	4	2.30	3.13	8	3.92	4.25	7
CAMS		-0.21	3.45	17	4.01	5.55	4	1.47	4.59	8	-0.40	4.40	7

3.6.2 Validation against ozone observations from the NDACC network (MWR, LIDAR)

In this section we present a comparison between the MACC and CAMS reanalysis models against MWR and LIDAR observations from the NDACC network. A detailed description of the instruments and applied methodologies for all NDACC instruments can be found in the Annex 2 and at http://nors.aeronomie.be. MWR (microwave) at Mauna Loa (19.5°N, mountain station) and Bern (47°N, 7°E, northern midlatitude station). LIDAR at Lauder, New Zeeland (46°S, 169.7°E, altitude 370m) and Mauna Loa (Hawaii, 19°N, 155°W, altitude 3.3km). In the table and plots below the MACCIII reanalysis model (IFS MOZART) is indicated in green, the CAMS reanalysis in red (CAMSra).

From Table 3.6.2.1, the upper stratospheric partial column bias at Bern during MAM 2003 is highest and significant (bias=11%) compared to the 6% uncertainty on the partial column. However, note that during MAM only limited measurements are available at Bern and that the bias is determined by measurements only during the first week of April 2003. For the reanalysis, the typical bias at Bern is below 1%. At Lauder the reanalysis seems to perform best (note that the number of measurements is limited).

At Mauna Loa, the observed bias during the first half of 2003 in the CAMS reanalysis is significant and compared to the MACC reanalysis, the bias has increased. This is also confirmed by the LIDAR measurements at Mauna Loa: a strong underestimation (up to 20%) between 20-25km during MAM-2003 (see Figure 3.6.2.1).

The uncertainty on the LIDAR concentration increases with altitude and above 35km the observed differences are comparable to the measurement uncertainty (>10%, see http://nors.aeronomie.be/projectdir/PDF/NORS_D4.2_DUG.pdf)

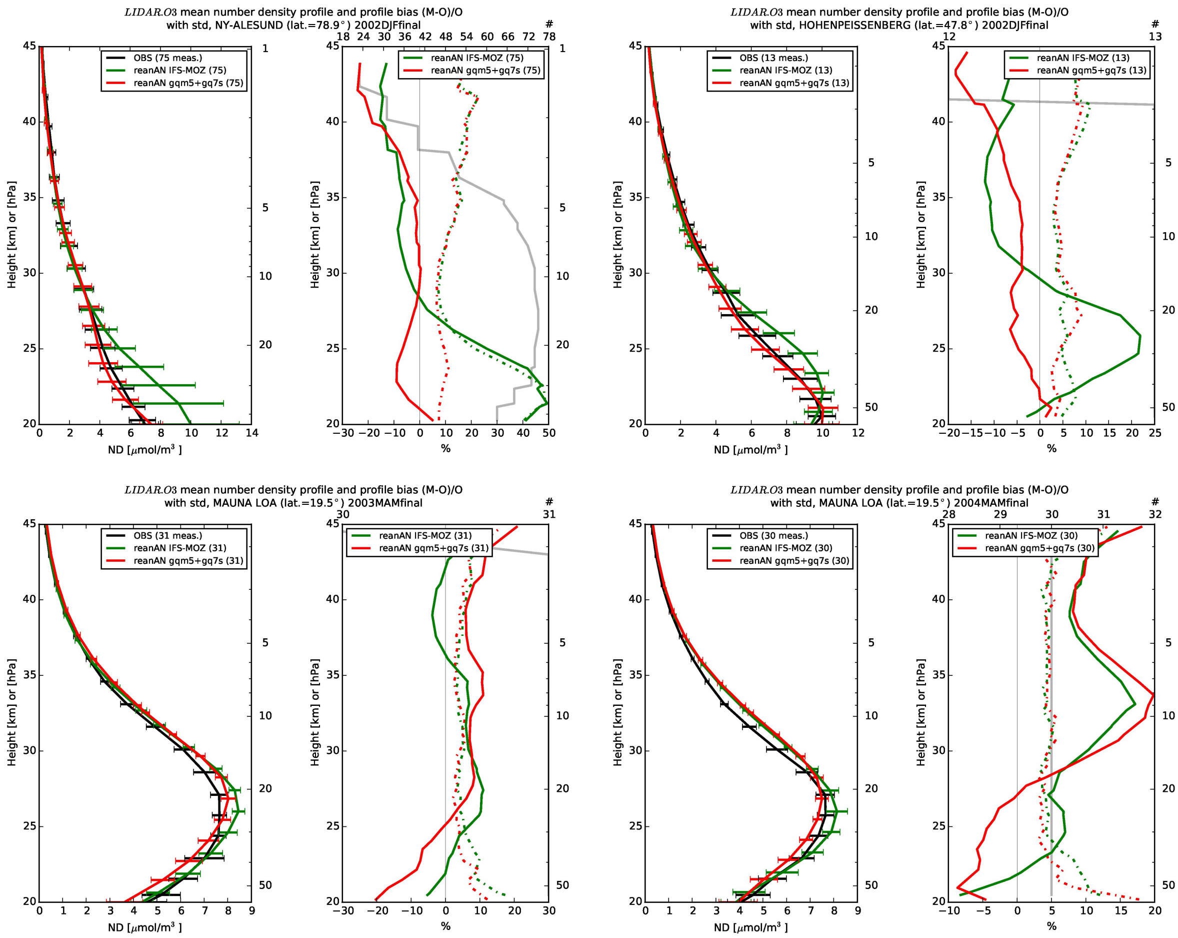

Figure 3.6.2.1: Comparison of the seasonally mean profile bias between the O_3 mixing ratios of the reanalyses and the LIDAR NDACC instruments at Ny Alesund, Mauna Loa, and Hohenpeissenberg. The first row shows the winter months JF 2003, the second row shows MAM 2003 and MAM 2004. The CAMS reanalysis performs best in the stratosphere around 20km altitude (biases are within profile uncertainty). The next row shows the performance at the tropical site at Mauna Loa: in 2003 strong underestimates are found (up to 20% at 20km altitude) while the reanalysis performs better during these months in 2004.

3.6.3 Comparison with observations by limb-scanning satellites

This section compares the model output with observations by limb scanning satellite instruments: MIPAS, HALOE, GOMOS, OSIRIS and SCIAMACHY. In order to keep the processing uniform, the ESA CCI harmonized dataset of ozone profiles from satellite limb and occultation measurements was chosen, see Sofieva et al. (2013). The only exception is MIPAS where we use the MIPAS-ESA v6 dataset.

All datasets are averaged over all longitudes and over the three most interesting latitude bands for stratospheric ozone: Antarctic (90°S-60°S), Tropics (30°S-30°N) and Arctic (60°N-90°N).

For reference, we also include the MACC reanalysis, which has been validated during the preoperational phase of CAMS, see Benediktow et al. (2014).

The satellite observations are affected by biases which depend on latitude range and altitude, and may have also long-term stability problem, see Hubert et al. (2016). In the following figures, we present the mean bias against the instruments.

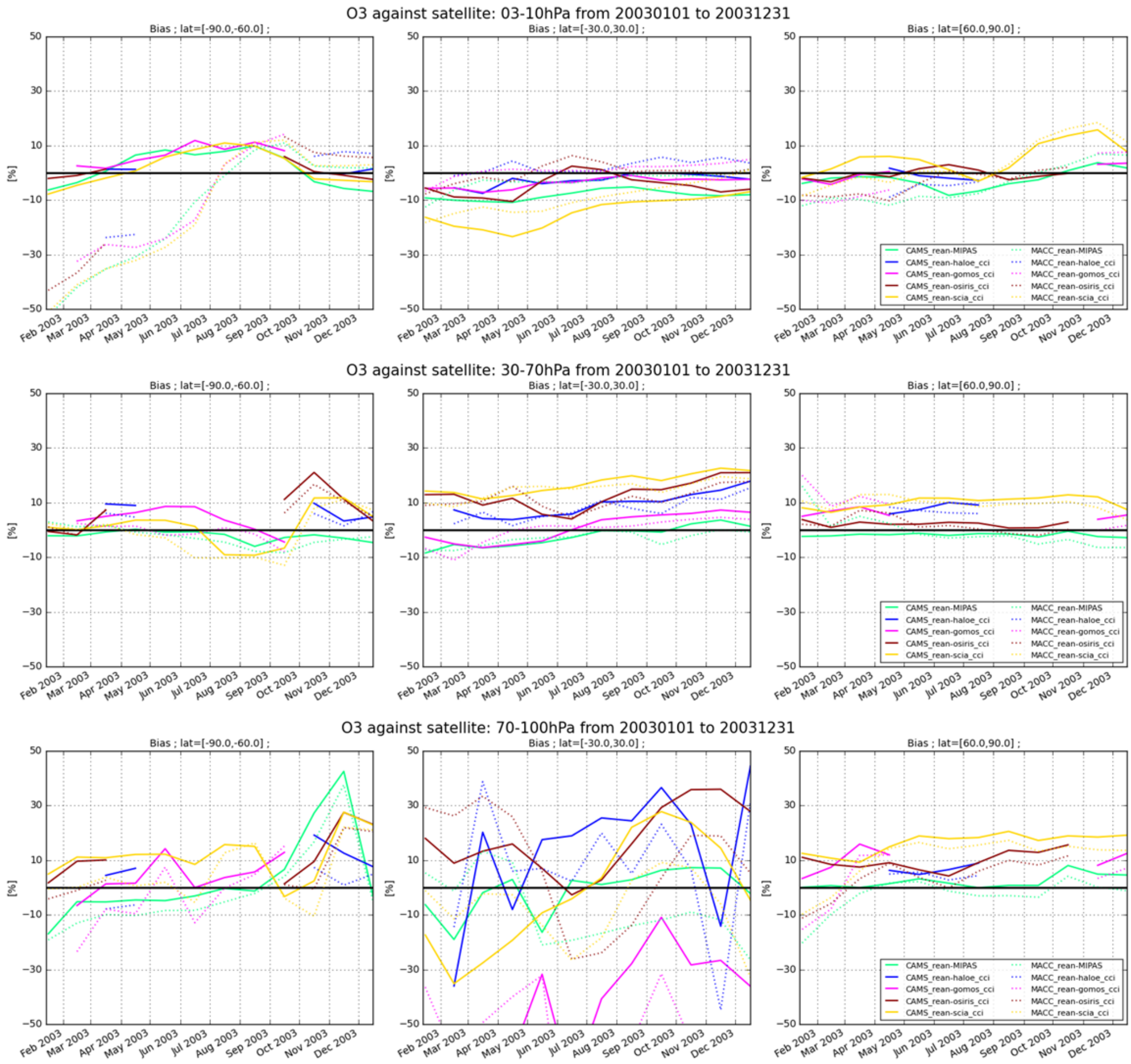

Figure 3.6.3.1: Time series comparing the normalized mean bias (model-obs)/obs (%) of ozone in the CAMS reanalyses and MACC reanalysis by comparison with observations from MIPAS, HALOE, GOMOS, OSIRIS and SCIAMACHY for the period 2003-01-01 to 2003-12-31 in the in the upper stratosphere (3-10hPa averages, top row), lower stratosphere (30-70hPa averages, middle row) and UTLS (70-100hPa averages, bottom row).

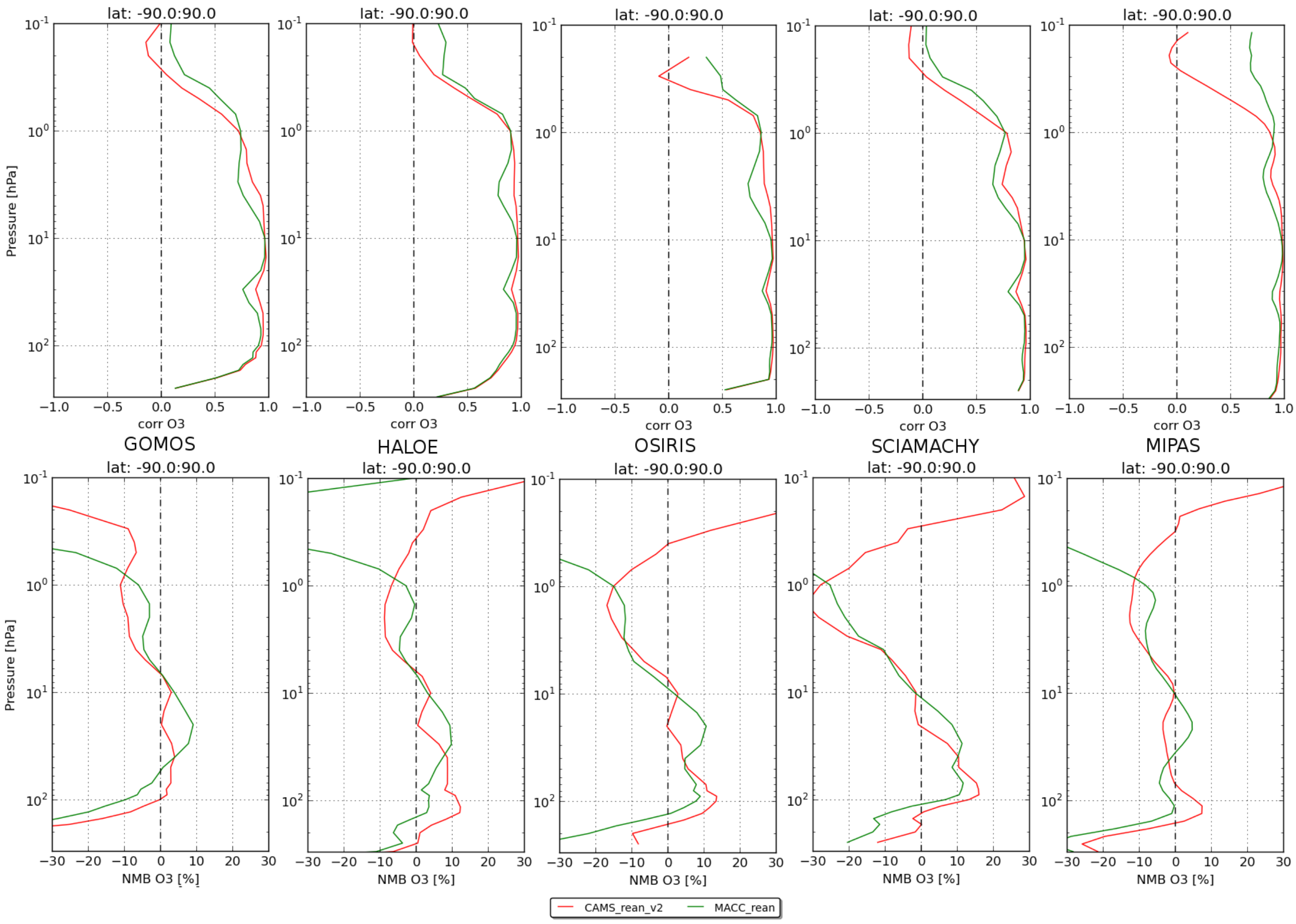

Figure 3.6.3.2: Correlation coefficient (top row) and normalized mean biases (bottom row) globally averaged over the year 2003: CAMS reanalysis (red) and MACC reanalysis (green) versus satellite observations, from left to right: GOMOS, HALOE, OSIRIS, SCIAMACHY and MIPAS.

In the upper stratosphere (3-10hPa, see Fig. 3.6.3.1 top row), except for the SCIAMACHY instrument, the absolute value of the bias is less than 12%; in the tropics, it is generally negative, while in the polar regions its sign depends on the period and instrument. Compared to the MACC reanalysis, there is a clear improvement in the polar regions; in the tropics, the values are generally 5% to 10% lower than the MACC reanalysis

In the middle lower stratosphere (30-70hPa, see Fig. 3.6.3.1 middle row), in the south polar region, the October overestimation with respect to ozone sondes is confirmed by OSIRIS, SCIAMACHY and HALOE, but it is not as severe (20%, 12% and 10% respectively). The low bias (about -2%) against MIPAS can be interpreted by the fact that the ozone profiles by this instrument were assimilated.

Globally the absolute value of the mean bias is comprised between -10% and +10% in the south polar region (except during the ozone hole period), between -3% and +12% in the north polar region, while the tropics are affected by a larger spread depending on the instruments.

In the lower stratosphere and UTLS (70-100hPa, see Fig. 3.6.3.1 bottom row), only the measurement in the polar regions can be used, as the biases relative to the instruments in the tropics are totally inconsistent.

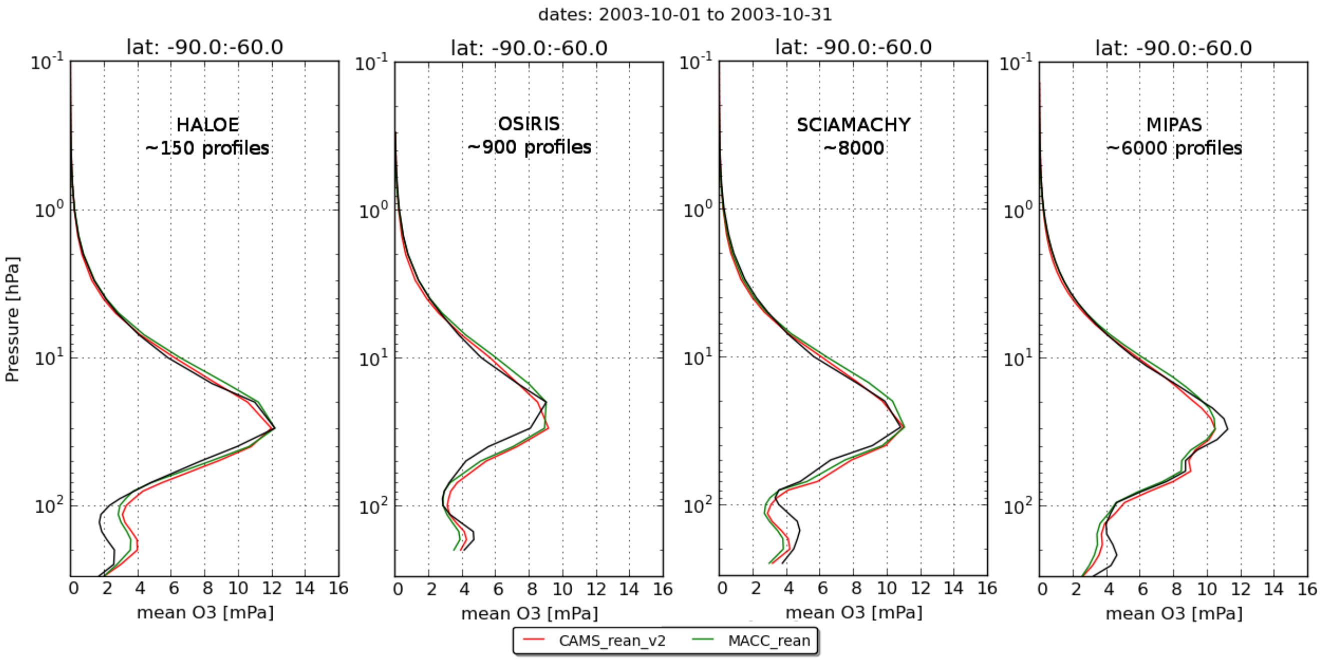

Figure 3.6.3.3: Mean profiles for October 2003 over the South Pole latitude band (90°S-60°S): CAMS reanalysis (red) and MACC (green) versus satellite observations (black) using, from left to right: HALOE, OSIRIS, SCIAMACHY and MIPAS.

Except for the ozone hole episode, globally the absolute value of the bias is <20%.

Figure 3.6.3.2 gives a global overview of the agreement between the reanalysis and the observations by the limb-scanning instruments, averaged over the whole year. The correlation coefficients are >0.7 for the pressure range 1-200hPa, but degrade rapidly above; they are generally better in the CAMS reanalysis than in the MACC reanalysis. Please note that no increments are applied by the data assimilation in the top 5 model levels (above about 1 hPa).

While the NMBs have different shapes, common features are apparent: there is an ozone deficit in the upper stratosphere (1-3 hPa) and it is more severe than with the MACC reanalysis. In the mid-lower stratosphere the biases are very small resulting in a better performance than the MACC reanalysis.

The ozone hole episode was studied with profiles of partial pressures averaged over October 2003 for 90°S-60°S, separately for each available instrument (see Fig. 3.6.3.3). The correlations between the reanalysis and each dataset observations are very good for this month (> 0.9), hence the differences between the 4 are due to different sampling in time and space.

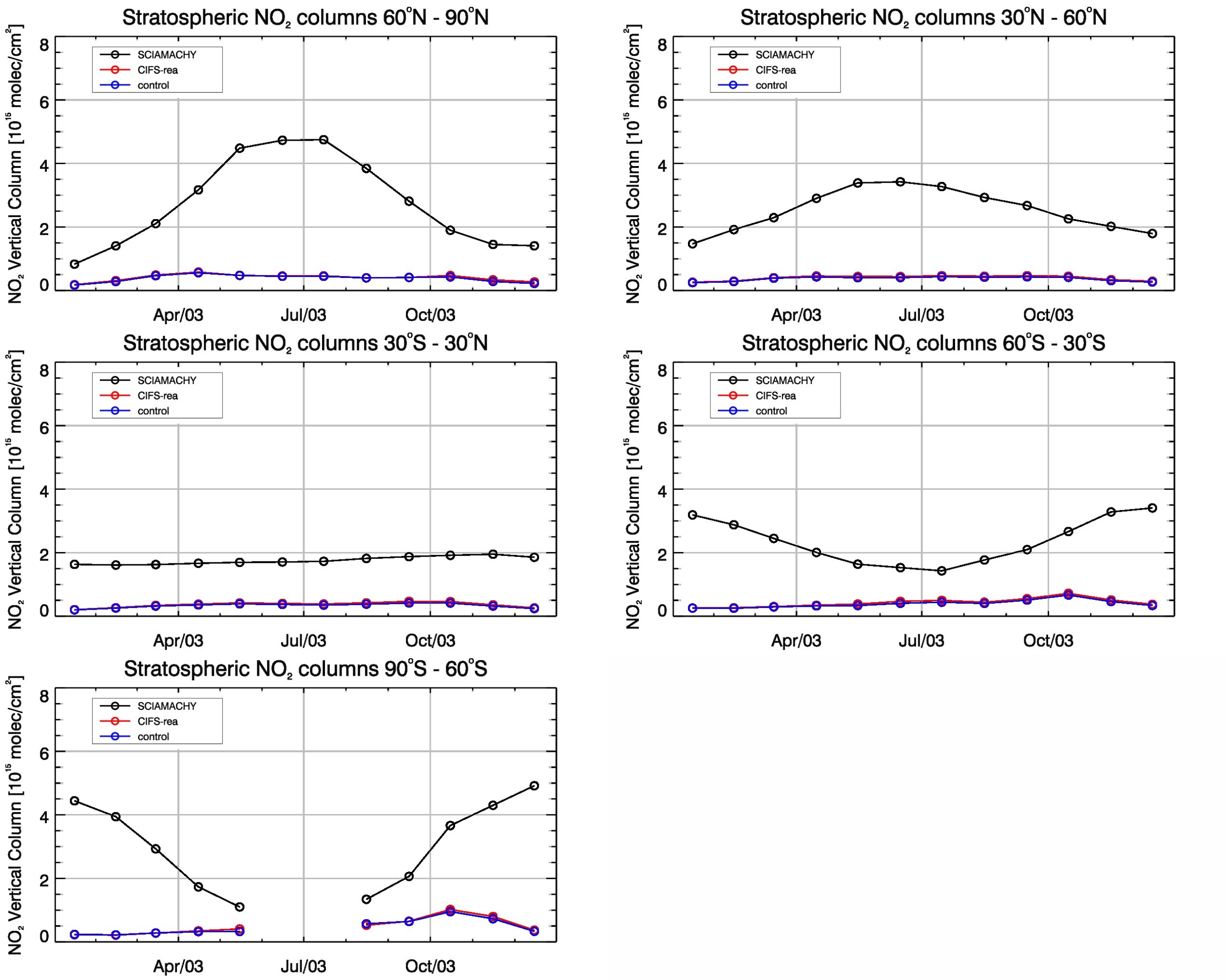

Figure 3.7.2.1. Time series of average stratospheric NO_2 columns [10^{15} molec cm^{-2}] from SCIAMACHY compared to model results for different latitude bands.

3.7 Stratospheric NO_2

3.7.1 Comparison with observation from the NDACC network (FTIR)

All NDACC FTIR stations (Ny Alesund 79N, Kiruna 68N, Jungfraujoch 47N, Izaña 28N and Reunion 21S) show a strong underestimation of the stratospheric NO_2 column with biases between 70 and 80%.

3.7.2 Comparison with SCIAMACHY satellite observations

Nitrogen dioxide from SCIAMACHY/Envisat satellite retrievals (IUP-UB v0.7) were compared to simulated stratospheric NO_2 columns. As expected, time series for different latitude bands (Fig. 3.7.2.1) show that the reanalysis and control fail to reproduce observed stratospheric NO_2 columns, due to the missing stratospheric chemistry in IFS.

4. References

Agustí-Panareda, A., Massart, S., Chevallier, F., Boussetta, S., Balsamo, G., Beljaars, A., Ciais, P., Deutscher, N. M., Engelen, R., Jones, L., Kivi, R., Paris, J.-D., Peuch, V.-H., Sherlock, V., Vermeulen, A. T., Wennberg, P. O., and Wunch, D.: Forecasting global atmospheric CO_2, Atmos. Chem. Phys., 14, 11959-11983, doi:10.5194/acp-14-11959-2014, 2014.

Agustí-Panareda, A., Massart, S., Chevallier, F., Balsamo, G., Boussetta, S., Dutra, E., and Beljaars, A.: A biogenic CO_2 flux adjustment scheme for the mitigation of large-scale biases in global atmospheric CO_2 analyses and forecasts, Atmos. Chem. Phys., 16, 10399-10418, doi:10.5194/acp-16-10399-2016, 2016.

Agusti-Panareda, A., Diamantakis, M., Bayona, V., Klappenbach, F., and Butz, A.: Improving the inter-hemispheric gradient of total column atmospheric CO_2 and CH_4 in simulations with the ECMWF semi-Lagrangian atmospheric global model, Geosci. Model Dev., 10, 1-18, doi:10.5194/gmd-10-1-2017, 2017.

Benedetti, A., J.-J. Morcrette, O. Boucher, A. Dethof, R. J. Engelen, M. Fisher, H. Flentjes, N. Huneeus, L. Jones, J. W. Kaiser, S. Kinne, A. Mangold, M. Razinger, A. J. Simmons, M. Suttie, and the GEMS-AER team: Aerosol analysis and forecast in the ECMWF Integrated Forecast System. Part II : Data assimilation, J. Geophys. Res., 114, D13205, doi:10.1029/2008JD011115, 2009.

Benedictow, A., A.M. Blechschmidt, I. Bouarar, E. Botek, S. Chabrillat, Y. Christophe, E. Cuevas, H. Clark, H. Flentje, A. Gaudel, J. Griesfeller, V. Huijnen, N. Huneeus, L. Jones, J. Kapsomenakis, S. Kinne, B. Langerock, K. Lefever, M. Razinger, A. Richter, M. Schulz, W. Thomas, V. Thouret, M. Vrekoussis, A. Wagner, C. Zerefos: Validation report of the MACC reanalysis of global atmospheric composition, MACC-II Deliverable D_83.6 (available from http://macc.copernicus-atmosphere.eu/services/aqac/global_verification/validation_reports)

Bergamaschi, P., et al. (2013), Atmospheric CH_4 in the first decade of the 21st century: Inverse modeling analysis using SCIAMACHY satellite retrievals and NOAA surface measurements, J. Geophys. Res. Atmos., 118, 7350–7369, doi:10.1002/jgrd.50480.

Cammas, J.P., Brioude J., Chaboureau J.-P., Duron J., Mari C., Mascart P., Nédélec P., Smit H., Pätz H.-W., Volz-Thomas A., Stohl A., and Fromm M., Injection in the lower stratosphere of biomass fire emissions followed by long-range transport: a MOZAIC case study. Atmos. Chem. Phys., 9, 5829-5846, 2009

Cariolle, D. and Teyssèdre, H.: A revised linear ozone photochemistry parameterization for use in transport and general circulation models: multi-annual simulations, Atmos. Chem. Phys., 7, 2183-2196, doi:10.5194/acp-7-2183-2007, 2007.

Ciais, P., M. Reichstein, N. Viovy, A. Granier, J. Ogee, V. Allard, M. Aubinet, N. Buchmann, C. Bernhofer, A. Carrara, F. Chevallier, N. De Noblet, A.D. Friend, P. Friedlingstein, T. Grunwald, B. Heinesch, P. Keronen, A. Knohl, G. Krinner, D. Loustau, G. Manca, G. Matteucci, F. Miglietta, J.M. Ourcival, D. Papale, K. Pilegaard, S. Rambal, G. Seufert, J.F. Soussana, M.J. Sanz, E.D. Schulze, T. Vesala, and R. Valentini, Europe-wide reduction in primary productivity caused by the heat and drought in 2003, Nature, 437 (7058), 529-533, 2005.

Dee, D. P. and S. Uppala, Variational bias correction of satellite radiance data in the ERA-Interim reanalysis. Quart. J. Roy. Meteor. Soc.,135, 1830-1841, 2009.

Deshler, T., J.L. Mercer, H.G.J. Smit, R. Stubi, G. Levrat, B.J. Johnson, S.J. Oltmans, R. Kivi, A.M. Thompson, J. Witte, J. Davies, F.J. Schmidlin, G. Brothers, T. Sasaki (2008) Atmospheric comparison of electrochemical cell ozonesondes from different maufacturers, and with different cathode solution strengths: The Balloon Experiment on Standards for Ozonsondes. J. Geophys. Res.113, D04307, doi:10.1029/2007JD008975

Emmons, L. K., D. P. Edwards, M. N. Deeter, J. C. Gille, T. Campos, P. Nédélec, P. Novelli, and G. Sachse, Measurements of Pollution In The Troposphere (MOPITT) validation through 2006 Atmos. Chem. Phys., 9, 1795-1803, 2009

Errera, Q., Daerden, F., Chabrillat, S., Lambert, J. C., Lahoz, W. A., Viscardy, S., Bonjean, S., and Fonteyn, D., 4D-Var Assimilation of MIPAS chemical observations: ozone and nitrogen dioxide analyses, Atmos. Chem. Phys., 8, 6169-6187, 2008.

Eskes, H., Huijnen, V., Arola, A., Benedictow, A., Blechschmidt, A.-M., Botek, E., Boucher, O., Bouarar, I., Chabrillat, S., Cuevas, E., Engelen, R., Flentje, H., Gaudel, A., Griesfeller, J., Jones, L., Kapsomenakis, J., Katragkou, E., Kinne, S., Langerock, B., Razinger, M., Richter, A., Schultz, M., Schulz, M., Sudarchikova, N., Thouret, V., Vrekoussis, M., Wagner, A., and Zerefos, C.: Validation of reactive gases and aerosols in the MACC global analysis and forecast system, Geosci. Model Dev., 8, 3523-3543, doi:10.5194/gmd-8-3523-2015, 2015.

Eskes, H.J., V. Huijnen, S, Basart, A. Benedictow, A.-M. Blechschmidt, S. Chabrillat, H. Clark, Y. Christophe, E. Cuevas, H. Flentje, K. M. Hansen, J. Kapsomenakis, B. Langerock, M. Ramonet, A. Richter, M. Schulz, A. Wagner, T. Warneke, C. Zerefos: Observations characterisation and validation methods document. Copernicus Atmosphere Monitoring Service (CAMS) report, CAMS84_2015SC1_D84.8.1_2016Q2_201603, March 2016. Available from: http://atmosphere.copernicus.eu/user-support/validation/verification-global-services

Flemming, J., Huijnen, V., Arteta, J., Bechtold, P., Beljaars, A., Blechschmidt, A.-M., Diamantakis, M., Engelen, R. J., Gaudel, A., Inness, A., Jones, L., Josse, B., Katragkou, E., Marecal, V., Peuch, V.-H., Richter, A., Schultz, M. G., Stein, O., and Tsikerdekis, A.: Tropospheric chemistry in the Integrated Forecasting System of ECMWF, Geosci. Model Dev., 8, 975-1003, doi:10.5194/gmd-8-975-2015, 2015.

Flemming, J., Benedetti, A., Inness, A., Engelen, R. J., Jones, L., Huijnen, V., Remy, S., Parrington, M., Suttie, M., Bozzo, A., Peuch, V.-H., Akritidis, D., and Katragkou, E.: The CAMS interim Reanalysis of Carbon Monoxide, Ozone and Aerosol for 2003–2015, Atmos. Chem. Phys., 17, 1945-1983, doi:10.5194/acp-17-1945-2017, 2017.

Granier, C. et al.: Evolution of anthropogenic and biomass burning emissions of air pollutants at global and regional scales during the 1980–2010 period. Climatic Change (109), 2011

Hubert, D., Lambert, J.-C., Verhoelst, T., Granville, J., Keppens, A., Baray, J.-L., Bourassa, A. E., Cortesi, U., Degenstein, D. A., Froidevaux, L., Godin-Beekmann, S., Hoppel, K. W., Johnson, B. J., Kyrölä, E., Leblanc, T., Lichtenberg, G., Marchand, M., McElroy, C. T., Murtagh, D., Nakane, H., Portafaix, T., Querel, R., Russell III, J. M., Salvador, J., Smit, H. G. J., Stebel, K., Steinbrecht, W., Strawbridge, K. B., Stübi, R., Swart, D. P. J., Taha, G., Tarasick, D. W., Thompson, A. M., Urban, J., van Gijsel, J. A. E., Van Malderen, R., von der Gathen, P., Walker, K. A., Wolfram, E., and Zawodny, J. M.: Ground-based assessment of the bias and long-term stability of 14 limb and occultation ozone profile data records, Atmos. Meas. Tech., 9, 2497-2534, doi:10.5194/amt-9-2497-2016, 2016.

Huijnen, V., et al.: The global chemistry transport model TM5: description and evaluation of the tropospheric chemistry version 3.0, Geosci. Model Dev., 3, 445-473, doi:10.5194/gmd-3-445-2010, 2010.

Huijnen, V., H.J. Eskes, A. Wagner, M. Schulz, Y. Christophe, M. Ramonet, S. Basart, A. Benedictow, A.-M. Blechschmidt, S. Chabrillat, H. Clark, E. Cuevas, H. Flentje, K.M. Hansen, U. Im, J. Kapsomenakis, B. Langerock, A. Richter, N. Sudarchikova, V. Thouret, T. Warneke, C. Zerefos, Validation report of the CAMS near-real-time global atmospheric composition service. System evolution and performance statistics; Status up to 1 June 2016, Copernicus Atmosphere Monitoring Service (CAMS) report, CAMS84_2015SC1_D.84.1.4_2016Q3_201609, September 2016.

Inness, A., Blechschmidt, A.-M., Bouarar, I., Chabrillat, S., Crepulja, M., Engelen, R. J., Eskes, H., Flemming, J., Gaudel, A., Hendrick, F., Huijnen, V., Jones, L., Kapsomenakis, J., Katragkou, E., Keppens, A., Langerock, B., de Mazière, M., Melas, D., Parrington, M., Peuch, V. H., Razinger, M., Richter, A., Schultz, M. G., Suttie, M., Thouret, V., Vrekoussis, M., Wagner, A., and Zerefos, C.: Data assimilation of satellite-retrieved ozone, carbon monoxide and nitrogen dioxide with ECMWF's Composition-IFS, Atmos. Chem. Phys., 15, 5275-5303, doi:10.5194/acp-15-5275-2015, 2015.

Kaiser, J. W., Heil, A., Andreae, M. O., Benedetti, A., Chubarova, N., Jones, L., Morcrette, J.-J., Razinger, M., Schultz, M. G., Suttie, M., and van der Werf, G. R.: Biomass burning emissions estimated with a global fire assimilation system based on observed fire radiative power, Biogeosciences, 9, 527-554, doi:10.5194/bg-9-527-2012, 2012.

Lefever, K., van der A, R., Baier, F., Christophe, Y., Errera, Q., Eskes, H., Flemming, J., Inness, A., Jones, L., Lambert, J.-C., Langerock, B., Schultz, M. G., Stein, O., Wagner, A., and Chabrillat, S.: Copernicus stratospheric ozone service, 2009–2012: validation, system intercomparison and roles of input data sets, Atmos. Chem. Phys., 15, 2269-2293, doi:10.5194/acp-15-2269-2015, 2015.

Le Quere, C., C. Rodenbeck, E.T. Buitenhuis, T.J. Conway, R. Langenfelds, A. Gomez, C. Labuschagne, M. Ramonet, T. Nakazawa, N. Metzl, N. Gillett, and M. Heimann, Saturation of the Southern Ocean CO2 sink due to recent climate change, Science, 316 (5832), 1735-1738, 2007.

Lopez, M., M. Schmidt, M. Ramonet, J.L. Bonne, A. Colomb, V. Kazan, P. Laj, and J.M. Pichon, Three years of semicontinuous greenhouse gas measurements at the Puy de Dome station (central France), Atmospheric Measurement Techniques, 8 (9), 3941-3958, 2015.

Massart, S., Agusti-Panareda, A., Aben, I., Butz, A., Chevallier, F., Crevoisier, C., Engelen, R., Frankenberg, C., and Hasekamp, O.: Assimilation of atmospheric methane products into the MACC-II system: from SCIAMACHY to TANSO and IASI, Atmos. Chem. Phys., 14, 6139-6158, doi:10.5194/acp-14-6139-2014, 2014.

Massart, S., Agustí-Panareda, A., Heymann, J., Buchwitz, M., Chevallier, F., Reuter, M., Hilker, M., Burrows, J. P., Deutscher, N. M., Feist, D. G., Hase, F., Sussmann, R., Desmet, F., Dubey, M. K., Griffith, D. W. T., Kivi, R., Petri, C., Schneider, M., and Velazco, V. A.: Ability of the 4-D-Var analysis of the GOSAT BESD XCO_2 *retrievals to characterize atmospheric* CO_2 *at large and synoptic scales, Atmos. Chem. Phys., 16, 1653-1671, doi:10.5194/acp-16-1653-2016, 2016.*

Morcrette, J.-J., O. Boucher, L. Jones, D. Salmond, P. Bechtold, A. Beljaars, A. Benedetti, A. Bonet, J. W. Kaiser, M. Razinger, M. Schulz, S. Serrar, A. J. Simmons, M. Sofiev, M. Suttie, A. M. Tompkins, and A. Untch: Aerosol analysis and forecast in the ECMWF Integrated Forecast System. Part I: Forward modelling, J. Geophys. Res., 114, D06206, doi:10.1029/2008JD011235, 2009.

Obspack, 2016, Cooperative Global Atmospheric Data Integration Project; (2016):Multi-laboratory compilation of atmospheric carbon dioxide data for the period 1957-2015; obspack_co2_1_GLOBALVIEWplus_v2.1_2016_09_02; NOAA Earth System Research Laboratory, Global Monitoring Division.http://dx.doi.org/10.15138/G3059Z.

Ramonet, M., P. Ciais, T. Aalto, C. Aulagnier, F. Chevallier, D. Cipriano, T.J. Conway, L. Haszpra, V. Kazan, F. Meinhardt, J.-D. Paris, M. Schmidt, P. Simmonds, I. Xueref-Remy, and J. Necki, A recent build-up of atmospheric CO2 over Europe. Part 1: observed signals and possible explanations, Tellus B, DOI: 10.1111/j.1600-0889.2009.00442, 2010.

Richter, A., Burrows, J. P., Nüß, H., Granier, C, Niemeier, U.: Increase in tropospheric nitrogen dioxide over China observed from space, Nature, 437, 129-132, doi: 10.1038/nature04092, 2005

Sindelarova, K., Granier, C., Bouarar, I., Guenther, A., Tilmes, S., Stavrakou, T., Müller, J.-F., Kuhn, U., Stefani, P., and Knorr, W.: Global data set of biogenic VOC emissions calculated by the MEGAN model over the last 30 years, Atmos. Chem. Phys., 14, 9317-9341, doi:10.5194/acp-14-9317-2014, 2014.

Smit, H.G.J., W. Straeter, B.J. Johnson, S.J. Oltmans, J. Davies, D.W. Tarasick, B. Hoegger, R. Stubi, F.J. Schmidlin, T. Northam, A.M. Thompson, J.C. Witte, I. Boyd: Assessment of the performance of ECC-ozonesondes under quasi-flight conditions in the environmental simulation chamber: Insights from the Juelich Ozone Sonde Intercomparison Experiment (JOSIE), J. Geophys. Res. 112, D19306, doi:10.1029/2006JD007308, 2007.

Sofieva, V. F., Rahpoe, N., Tamminen, J., Kyrölä, E., Kalakoski, N., Weber, M., Rozanov, A., von Savigny, C., Laeng, A., von Clarmann, T., Stiller, G., Lossow, S., Degenstein, D., Bourassa, A., Adams, C., Roth, C., Lloyd, N., Bernath, P., Hargreaves, R. J., Urban, J., Murtagh, D., Hauchecorne, A., Dalaudier, F., van Roozendael, M., Kalb, N., and Zehner, C.: Harmonized dataset of ozone profiles from satellite limb and occultation measurements, Earth Syst. Sci. Data, 5, 349-363, doi:10.5194/essd-5-349-2013, 2013, http://www.earth-syst-sci-data.net/5/349/2013/.

Stein, O., Schultz, M. G., Bouarar, I., Clark, H., Huijnen, V., Gaudel, A., George, M., and Clerbaux, C.: On the wintertime low bias of Northern Hemisphere carbon monoxide found in global model simulations, Atmos. Chem. Phys., 14, 9295-9316, doi:10.5194/acp-14-9295-2014, 2014.

Tressol, M., C. Ordonez, R. Zbinden, J. Brioude, V. Thouret, C. Mari, P. Nedelec, J.-P. Cammas, H. Smit, H.-W. Patz, and A. Volz-Thomas, Air pollution during the 2003 European heat wave as seen by MOZAIC airliners,Atmos. Chem. Phys., 8, 2133-2150, doi:10.5194/acp-8-2133-2008, 2008.

van der A, R. J. , M. A. F. Allaart, and H. J. Eskes, Multi sensor reanalysis of total ozone, Atmos. Chem. Phys., 10, 11277–11294, doi:10.5194/acp-10-11277-2010, www.atmos- chem-phys.net/10/11277/2010/, 2010

van der A, R. J., Allaart, M. A. F., and Eskes, H. J.: Extended and refined multi sensor reanalysis of total ozone for the period 1970–2012, Atmos. Meas. Tech., 8, 3021-3035, doi:10.5194/amt-8-3021-2015, 2015.

Wittrock, F., A. Richter, H. Oetjen, J. P. Burrows, M. Kanakidou, S. Myriokefalitakis, R. Volkamer, S. Beirle, U. Platt, and T. Wagner, Simultaneous global observations of glyoxal and formaldehyde from space, Geophys. Res. Lett., 33, L16804, doi:10.1029/2006GL026310, 2006

Annex 1: Acknowledgements

Listed below are the authors contributing to the sections in this report. The authors contributing to the model description are also provided, as well as acknowledgements to the validation datasets.

Tropospheric reactive gases reactive gases

Hannah Clark, Valerie Thouret, CNRS-LA (editor, MOZAIC, IAGOS)
Annette Wagner, MPG (O_3 sondes, GAW data)
Harald Flentje, DWD (O_3 sondes, GAW data)
Anne Blechschmidt and Andreas Richter, IUB Bremen (GOME-2 NO2, HCHO)
John Kapsomenakis, Christos Zerefos, AA (ESRL)
Katinka Petersen and Natalia Sudarchikova, satellite IR observations (MPG)
Kaj Hansen, Ulas Im, AU (Arctic theme)
Bavo Langerock, BIRA (NDACC)

Tropospheric aerosol

Michael Schulz, MetNo (editor, Aerocom, Aeronet)
Anna Benedictow, Jan Griesfeller, MetNo (Aerocom, Aeronet)
Sara Basart, M. Teresa Pay, Oriol Jorba, BSC-CNS (Aeronet, MODIS, AirBase, SDS-WAS NAMEE RC)
Emilio Cuevas, AEMET (Aeronet, MODIS, AirBase, SDS-WAS NAMEE RC)

Stratospheric reactive gases

Yves Christophe, Simon Chabrillat, BIRA (satellite observations)
Annette Wagner, MPI-M (O3 sondes)
Bavo Langerock, BIRA (NDACC FTIR, MWR, UVVIS DOAS, LIDAR)
Anne Blechschmidt and Andreas Richter, IUB-UB Bremen (SCIAMACHY NO_2)

Greenhouse gases

Michel Ramonet, IPSL (ICOS)
Olivier Jossoud and Leonard Rivier, LSCE (ICOS)
Thorsten Warneke, UBC (TCCON)
Bavo Langerock, BIRA (TCCON)

Reactive gases and aerosol modeling

Antje Inness, Johannes Flemming, Richard Engelen (ECMWF)
Vincent Huijnen (KNMI)

Acknowledgements for the validation datasets used

We are grateful to the numerous operators of the Aeronet network and to the central data processing facility at NASA Goddard Space Flight Center for providing the NRT sun photometer data, especially Ilya Slutker, David Giles and Brent Holben for sending the data.

The authors thank to all researchers, data providers and collaborators of the World Meteorological Organization's Sand and Dust Storm Warning Advisory and Assessment System (WMO SDS-WAS) for Northern Africa, Middle East and Europe (NAMEE) Regional Node. Also special thank to Canary Government as well as AERONET, MODIS, U.K. Met Office MSG, MSG Eumetsat and EOSDIS World Viewer principal investigators and scientists for establishing and maintaining data used in the activities of the WMO SDS-WAS NAMEE Regional Center (http://sds-was.aemet.es/).

We acknowledge the European Environment Information and Observation Network (Eionet) Air Quality portal which provides details relevant for the reporting of air quality information from EU Member States and other EEA member and co-operating countries. This information is submitted according to Directives 2004/107/EC and 2008/50/EC of the European Parliament and of the Council.

Also, we want to acknowledge the PM10 observations obtained from the openair project (http://www.openair-project.org/) which is a Natural Environment Research Council (NERC) knowledge exchange project that aims to provide a collection of open-source tools for the analysis of air pollution data.

We wish to acknowledge the provision of ozone sonde data by the World Ozone and Ultraviolet Radiation Data Centre established at EC in Toronto (http://woudc.org), by the Data Host Facility of the Network for the Detection of Atmospheric Composition Change established at NOAA (http://ndacc.org), by the Norwegian Institute for Air Research and by the National Aeronautics and Space Administration (NASA).

We wish to thank the NDACC investigators for the provision of observations at Ny Alesund, Bern, Jungfraujoch, Izaña, Reunion Maido, Hohenpeissen, Mauna Loa, Lauder.

We wish to thank ESA for providing the HARMonized dataset of Ozone profiles (HARMOZ).

We acknowledge the strong support of the European Commission, Airbus, and the airlines (Lufthansa, Air France, Austrian, Air Namibia, Cathay Pacific, Iberia and China Airlines so far) which have carried the MOZAIC or IAGOS equipment and undertaken maintenance since 1994. In its last 10 years of operation, MOZAIC has been funded by INSU-CNRS (France), Météo-France, Université Paul Sabatier (Toulouse, France) and Research Center Jülich (FZJ, Jülich, Germany). IAGOS has been additionally funded by the EU projects IAGOS-DS and IAGOS-ERI. The MOZAIC–IAGOS database is supported by AERIS (CNES and INSU-CNRS).

The authors acknowledge the provision of Global Atmosphere Watch (GAW) data by the World Data Centre for Greenhouse Gases (WDCGG).

We wish to acknowledge the provision of ozone sonde data by the World Ozone and Ultraviolet Radiation Data Centre established at EC in Toronto (https//woudc.org), by the Data Host Facility of the Network for the Detection of Atmospheric Composition Change established at NOAA (http://ndacc.org), by the Norwegian Institute for Air Research (http://www.nilu.no/) and by the National Aeronautics and Space Administration NASA (https://tropo.gsfc.nasa.gov/shadoz/).

The authors acknowledge the European Monitoring and Evaluation Programme (EMEP; http://www.emep.int/) for the provision of ground based ozone concentrations.

The MOPITT CO data were obtained from the NASA Langley Research Center ASDC. We acknowledge the LATMOS IASI group for providing IASI CO data.

SCIAMACHY lv1 radiances were provided to IUP-UB by ESA through DLR/DFD.

We acknowledge the European Space Agency (ESA) for providing the consolidated and harmonized ozone datasets through its Chemistry-Climate Initiative (HARMOZ O3 CCI; http://www.esa-ozone-cci.org/). Besides the European instruments aboard Envisat (MIPAS, GOMOS, SCIAMACHY), this includes datasets by Third-Party Missions which were originally provided by NASA (HALOE, SAGE) and by the University of Saskatchewan, Canada (ODIN/OSIRIS; http://osirus.usas.ca/).

We acknowledge the provision of CO_2 data from SNO-RAMCES/ICOS network coordinated by LSCE/OVSQ (CEA-CNRS-UVSQ, Université Paris-Saclay), with support of C-CAPS/NUIG/EPA (Ireland), LaMP/OPGC, and IPEV.

We acknowledge all the contributors to the Obspack data packages.

Copernicus Atmosphere Monitoring Service

ECMWF - Shinfield Park, Reading RG2 9AX, UK

Contact: info@copernicus-atmosphere.eu

atmosphere.copernicus.eu copernicus.eu ecmwf.int